



HAL
open science

Problèmes inverses d'estimation de sources, applications à l'EEG et à la MEG

Paul Asensio

► **To cite this version:**

Paul Asensio. Problèmes inverses d'estimation de sources, applications à l'EEG et à la MEG. Mathématiques [math]. Université cote d'azur, 2023. Français. NNT : . tel-04366056

HAL Id: tel-04366056

<https://hal.science/tel-04366056>

Submitted on 28 Dec 2023

HAL is a multi-disciplinary open access archive for the deposit and dissemination of scientific research documents, whether they are published or not. The documents may come from teaching and research institutions in France or abroad, or from public or private research centers.

L'archive ouverte pluridisciplinaire **HAL**, est destinée au dépôt et à la diffusion de documents scientifiques de niveau recherche, publiés ou non, émanant des établissements d'enseignement et de recherche français ou étrangers, des laboratoires publics ou privés.

UNIVERSITÉ
CÔTE D'AZUR

ÉCOLE DOCTORALE
SCIENCES ET TECHNOLOGIES
DE L'INFORMATION ET
DE LA COMMUNICATION

THÈSE DE DOCTORAT

Problèmes inverses d'estimation de
sources, applications à l'EEG et à la
MEG

Paul Asensio

Centre Inria de l'Université Côte d'Azur

**Présentée en vue de l'obtention
du grade de docteur en Génie**

informatique, automatique et
traitement du signal

d'Université Côte d'Azur

Dirigée par : Juliette Leblond

Co-encadrée par : Laurent Baratchart

Soutenue le : 21/09/2023

Devant le jury, composé de :

Yannick Privat, Professeur,

Université de Strasbourg - Rapporteur

Bernhard Beckermann, Professeur, Université de Lille - Rapporteur

Stanislas Kupin, Professeur, Université de Bordeaux - Examineur

Jean-Yves Dauvignac, Professeur, Université Côte d'Azur –
Examineur

Juliette Leblond, Directrice de Recherche, Université Côte d'Azur –
Directrice de thèse

Laurent Baratchart, Directeur de Recherche émérite, Université Côte
d'Azur – Co-Directeur de thèse

informatiques mathématiques
Inria

Problèmes inverses d'estimation de sources, applications à l'EEG et à la MEG

Jury :

Rapporteurs

Yannick Privat, Professor, Université de Strasbourg

Bernhard Beckermann, Professor, Université de Lille

Examineurs

Stanislas Kupin, Professor, Université de Bordeaux

Jean-Yves Dauvignac, Professor, Université Côte d'Azur

Directrice de thèse

Juliette Leblond, Directrice de Recherche, Université Côte d'Azur

Co-Directeur de thèse

Laurent Baratchart, Directeur de Recherche émérite, Université Côte d'Azur

Inverse problems of source localization with applications to EEG and MEG

Jury:

Reviewers

Yannick Privat, Professor, Université de Strasbourg

Bernhard Beckermann, Professor, Université de Lille

Examiners

Stanislas Kupin, Professor, Université de Bordeaux

Jean-Yves Dauvignac, Professor, Université Côte d'Azur

Thesis Advisor

Juliette Leblond, Research Director, Université Côte d'Azur

Thesis Co-advisor

Laurent Baratchart, Emeritus Research Director, Université Côte d'Azur

Résumé

Dans cette thèse, nous étudions les problèmes d'approximation au sens des moindres carrés liés à des équations aux dérivées partielles elliptiques. Les problèmes inverses étudiés sont liés aux solutions des équations de Maxwell, soit sous l'approximation quasi-statique conduisant à une équation de Poisson, soit sous l'approximation harmonique en temps induisant une équation de Helmholtz. Ces problèmes concernent la localisation de sources en imagerie cérébrale, la localisation de charges à partir de mesures continues du champ électromagnétique qu'elles génèrent et la reconnaissance de formes à partir de mesures discrètes d'ondes électromagnétiques réfléchies.

Dans un premier chapitre, ces problèmes au sens des moindres carrés sont liés aux solutions des équations de Poisson issues des équations de Maxwell sous l'approximation quasi-statique. Nous étudions dans ce cas les problèmes inverses de localisation de sources en imagerie cérébrale ou de localisation de charges à partir de mesures continues du champ électromagnétique qu'elles induisent. Pour ces problèmes, nous étudions principalement les fonctions "objectif" associées et leur solvabilité numérique. En effet, ces fonctions n'étant pas convexes, nous étudions l'unicité des leurs points critiques et donc de leurs minima locaux afin d'assurer la convergence des méthodes de descente vers la solution désirée. Nous étudions différents problèmes : l'estimation du courant à partir de mesures du potentiel électrique ou de l'induction magnétique et l'estimation de charge électrique à partir de mesures du champ électrique ; l'étude est faite pour deux ensembles de mesures différents : une sphère et un plan infini. Des illustrations numériques sont fournies pour tous ces problèmes.

Dans un deuxième chapitre, nous étudions un problème de reconstruction de forme et d'estimation de propriétés électriques à partir de mesures discrètes d'ondes électromagnétiques réfléchies sur un objet. Pour ce problème, les champs sont des solutions de l'équation d'Helmholtz provenant des équations de Maxwell dans l'approximation harmonique en temps. La question de la reconstruction en elle-même peut être traitée par des techniques d'apprentissage automatique. Les paramètres choisis sont les pôles de la fonction qui exprime le champ électrique en fonction de la fréquence. Dans cette thèse, nous étudions des méthodes d'approximation rationnelle du champ afin de décrire comment ces pôles peuvent être estimés. Nous introduisons et étudions deux généralisations de l'approximation de Padé au sens des moindres carrés : l'approximation de Padé au sens des moindres carrés en 0 et l'approximation de Padé multipoints au sens des moindres carrés. Pour la première approximation, nous généralisons le théorème de Nuttall-Pommerenke, tandis que nous montrons un résultat plus faible pour la seconde et discutons une conjecture plus forte.

Mots clés : Problème inverse, Électroencéphalographie, Magnétoencéphalographie

Abstract

In this thesis, we study least-squares approximation problems linked to elliptic partial differential equations. The studied inverse problems are linked to solutions of Maxwell equations under either the quasi-static approximation leading to a Poisson equation or under the time-harmonic approximation leading to a Helmholtz equation. These problems arise from source localization in brain imaging, charge localization from continuous measurements of the electromagnetic field they induce and shape recognition from discrete measurements of scattered electromagnetic wave.

In a first chapter, these least-squares problems are linked to solutions of Poisson equations coming from Maxwell equations under the quasi-static approximation. We study in this case inverse problems of source localization in brain imaging or charge localization from continuous measurements of the electromagnetic field they induce. For these problems, we mainly study the associated least-squares criteria and their numerical solvability. Indeed, as the criteria are not convex, we study the uniqueness of critical points of the criteria hence of the local minima in order to ensure the convergence of descent methods to the desired solution. We study different problems: current recovery from measures of the electric potential or magnetic induction and charge recovery from measures of the electric field; the study is done for two different sets of measurements: a sphere and an infinite plane. Numerical illustrations are provided for all of these problems.

In a second chapter, we study a problem of shape reconstruction and electric properties recovery from discrete measurements of scattered electromagnetic waves on an object. In this case, the fields are solution of Helmholtz equation coming from Maxwell equations under the time-harmonic approximation. The reconstruction issue by itself can be achieved based on machine learning techniques. The chosen parameters are the poles of the function which express the field with respect to the frequency. In this thesis we study rational approximation methods of the field in order to describe how these poles can be recovered. We introduce and study two least-squares generalizations of Padé approximation: the least-squares Padé approximation at 0 and the least-square multipoint Padé approximation. For the first approximation we generalize the Nuttall-Pommerenke theorem while we showed a weaker result for the second one and only discuss a stronger conjecture.

Keywords: Inverse problem, Electroencephalography, Magnetoencephalography

Résumé		4
Abstract		5
General introduction		9
I Critical point for least-squares inverse potential problems		11
I.1 Introduction		11
I.1.1 General framework		11
I.1.2 Main Problems		12
I.1.3 Overview		14
I.2 A dipole localization electrical inverse problem		15
I.2.1 Main results		15
I.2.2 Preliminary computations		17
I.2.2.a Gradient in p		17
I.2.2.b Gradient in x		18
I.2.3 Planar case (Proof of Theorem I.2.2)		18
I.2.3.a Explicit computation of the criterion		19
I.2.3.b First step: use of homogeneity		21
I.2.3.c Second step: use of strict positivity		22
I.2.3.d Reciprocal		22
I.2.4 Spherical case (Proof of Proposition I.2.3)		23
I.2.4.a Explicit computation of the criterion		23
I.2.4.b Critical point computation		25
I.3 A charge localization electrical inverse problem		27
I.3.1 Main results		27
I.3.2 Planar case (Proof of Theorem I.3.2)		29
I.3.3 Spherical case (Proof of Theorem I.3.3)		30
I.4 A dipole localization magnetic inverse problem		32
I.4.1 Main result		32
I.4.2 Proof of Theorem I.4.1		32
I.4.2.a First step: use of homogeneity		33
I.4.2.b Second step: derivatives in the plane		33
I.4.2.c Reciprocal		35
I.5 Numerical illustration		38

I.5.1	Dipole and charge localization electric inverse problems	38
I.5.1.a	Planar case	38
I.5.1.b	Spherical case	39
I.5.2	Dipole localization magnetic inverse problem	41
I.6	Conclusion	45
II	Rational approximation of scattered electromagnetic waves	46
II.1	Introduction	46
II.1.1	Scattering	46
II.1.2	Rational approximation	49
II.1.2.a	Padé approximation at 0	49
II.1.2.b	Multipoint Padé approximation	50
II.1.3	Overview	51
II.2	High-frequency approximation	53
II.2.1	Luneburg-Kline series	53
II.2.1.a	Solving the eikonal equation	54
II.2.1.b	Solving the transport equation	55
II.2.2	Creeping Waves	59
II.2.3	Rational approximation using high-frequency behavior	64
II.3	Least-squares Padé approximant at 0	67
II.3.1	Existence and uniqueness	68
II.3.1.a	Existence	68
II.3.1.b	Strong uniqueness property	69
II.3.1.c	Functions for which the strong uniqueness property fails	70
II.3.1.d	Weak uniqueness property	70
II.3.1.e	Choice of the normalization	71
II.3.2	Proof of Theorem II.3.2	72
II.4	Least-squares multipoint Padé approximant	75
II.4.1	Proof of Theorem II.4.2	76
II.4.1.a	Definition of the polynomial \mathbf{a}_z	78
II.4.1.b	Upper bound of the polynomial \mathbf{a}_z	79
II.4.1.c	Upper bound of the error	80
II.4.2	Study of Conjecture II.4.1	81
II.4.3	Non-zero determinant	82
II.4.3.a	Case A	86
II.4.3.b	Case B	86
II.4.3.c	Case C	87
II.4.3.d	Case B-C	88
II.4.3.e	Case A-B	89
II.4.3.f	Case A-C	90
II.4.3.g	Case A-B-C	90
II.5	Conclusion	91
A	Clifford algebra	92
B	Logarithmic capacity	94
	List of Illustrations	96
	Figures	96
	Tables	97

List of Symbols	99
Bibliography	99

In this thesis, we study least-squares approximation problems linked to elliptic partial differential equations. Two questions are mainly considered in this work:

- Are the solutions to least-squares approximation problems numerically computable?
- How do these solutions compare with the approximated function when we increase simultaneously the amount of data and the complexity of the approximation set?

More precisely, the studied inverse problems are linked to solutions of Maxwell equations under either the quasi-static approximation leading to a Poisson equation, or under the time-harmonic approximation leading to a Helmholtz equation. These problems arise from applications like source localization in brain imaging, charge localization from continuous measurements of the electromagnetic field they induce, and shape recognition from discrete measurements of scattered electromagnetic wave.

In a first chapter, these least-squares problems are linked to solutions of Poisson equations coming from Maxwell equations under the quasi-static approximation. We study in this case inverse problems of source localization in brain imaging or charge localization, from continuous measurements of the electromagnetic fields they induce. For these problems, we mainly study the associated least-squares criteria for pointwise sources and their numerical solvability. Indeed, as the criteria are not convex, we study the uniqueness of critical points of the criteria hence of the local minima in order to ensure the convergence of descent methods to the desired source term. We study different problems: current recovery from measures of the electric potential or magnetic induction, and charge recovery from measures of the electric field; the study is done for two different sets of measure: a sphere and an infinite plane.

In a second chapter, we study a problem of shape reconstruction and electric properties recovery from discrete measurements of scattered electromagnetic waves. In this case, the fields are solution of Helmholtz equation coming from Maxwell equations under the time-harmonic approximation. The reconstruction issue by itself can be achieved based on machine learning techniques. The chosen parameters are the poles of the function which express the field with respect to the frequency. In this thesis, we study rational approximation methods of the field in order to describe how these poles can be recovered. We introduce and study two least-squares generalizations of Padé approximation: the least-squares Padé approximation at 0 and the least-square multipoint Padé approximation. For the first approximation, we generalize the Nuttall-Pommerenke theorem, while

we showed a weaker result for the second one and only discuss a stronger conjecture. Numerical illustrations are provided.

The first question is studied in both chapters. In the first chapter, we study the uniqueness of the local minimizer of some least-squares criteria in order to show the computability of the minimizer through numerical methods. In the second chapter, we also study the uniqueness of some least-squares approximants which is a desired property for numerical computations. The second question is also studied in both chapters. In the first chapter, we study the uniqueness of the global minimum of some least-squares criteria in order to show that solving these problems leads to a perfect reconstruction of the measured function. In the second chapter, we study the error done when considering some variations of Padé approximation and show some results linked to the Nuttall-Pommerenke theorem which control this error.

Publications

Participations in conferences

- Surface identification through rational approximation of the back-scattering of an electromagnetic planar wave. CMFT 2021, January 2021, Valparaíso, Chile [online].
- Surface identification through rational approximation of the back-scattering of an electromagnetic planar wave. ERNSI 2021, September 2021, Rennes, France [online].
- Critical points for least-square estimation of dipolar sources in inverse problems for Poisson equation. IPMS 2022, May 2022, Paradise bay, Malta.
- Surface identification through back-scattering of an electromagnetic planar wave, by rational approximation. Waves 2022, July 2022, Palaiseau, France.

Articles submitted for publication

- [1] P. Asensio and J. Leblond, “Critical points for least-squares estimation of dipolar sources in inverse problems for Poisson equation.” Accepted for publication in Computational Methods and Function Theory, 2023.
- [2] P. Asensio, J.-M. Badier, J. Leblond, J.-P. Marmorat, and M. Nemaire, “A layer potential approach to inverse problems in brain imaging.” Accepted for publication in Journal of Inverse and Ill-posed Problems, 2023.

Article in preparation

- [3] P. Asensio, L. Baratchart, and J. Leblond, “A Nuttall-Pommerenke theorem for least-square rational approximant of analytic functions.” Working paper, 2023.

I.1 Introduction

I.1.1 General framework

In this work, we study the inverse problem of recovering vector-valued pointwise sources in a domain $\Omega \subset \mathbb{R}^3$ from measurements of the emitted potential on its boundary $\partial\Omega$. In particular, we inquire the uniqueness of the critical points of the least-squares criterion linked to this source recovery inverse problem. As the criterion is not convex, uniqueness of local minimizer is needed to ensure the convergence of classical optimization scheme to a global minimizer.

Such inverse problems have applications in medical imaging (electroencephalography (EEG)) as in [4] and in geosciences (rock magnetization) as in [5]. In these applications the sources are either electric currents due to brain activity or magnetizations due to remanent rock magnetization. In both cases, the model comes from Maxwell equations in the quasi-static approximation [6, Sec. 5.3]. This approximation leads to a Poisson equation with a source term in divergence form:

$$\begin{cases} \Delta u = \nabla \cdot \mu \text{ in } \mathbb{R}^n, \\ \lim_{|z| \rightarrow \infty} |u(z)| = 0. \end{cases} \quad (\text{I.1})$$

for some measure μ with compact support included in a smooth domain $\Omega \subset \mathbb{R}^n$ and a solution u in the distributional sense.

In this work, we study the two settings. The first setting is such that Ω is the lower half-space and $\partial\Omega$ the horizontal plane. This configuration is more adapted to the geometry a Scanning Magnetic Microscopy used in particular paleontology studies about rock magnetization where we typically have data on a horizontal plane above the rock. The second setting is such that Ω is the unit ball and $\partial\Omega$ the unit sphere. This configuration is adapted for EEG in which the measurements are considered on the scalp of a patient usually modeled as a sphere.

I.1.2 Main Problems

We consider the inverse problem of source recovery:

Problem I.1.1. *Given $u_0 \in L^2(\partial\Omega)$ find $\mu_0 \in [\mathcal{M}(\mathbb{R}^n)]^n$ such that u_0 is the trace on $\partial\Omega$ of the solution of the Poisson equation (I.1) with $\mu = \mu_0$.*

This inverse problem of source recovery is strongly ill-posed. A classical possible regularization is to restrict the space of sources to finite sums of a fixed number $n_d \geq 1$ of dipoles:

$$\mathcal{S}_{n_d} = \left\{ \sum_{i=1}^{n_d} p_i \delta_{x_i}, x_i \in \Omega, p_i \in \mathbb{R}^n, \forall i \in \llbracket 1, n_d \rrbracket \right\},$$

where a dipole $p\delta_x$ is parameterized by its location $x \in \Omega$ and its moment $p \in \mathbb{R}^3$. The measure δ_x is the Dirac delta distribution supported at $x \in \Omega$ and $n_d \in \mathbb{N}$ plays the role of the regularization parameter. This model is well adapted for localized dipolar sources such as epileptic foci in EEG. This regularization is enough to guarantee the uniqueness of the solution to the inverse problem [7, Thm 1] when dealing with both Dirichlet and Neumann data. Indeed, there are no silent sources in the space of finite sum of dipoles (this subject was deeply discussed in [8]). Nevertheless, because of the non-convexity of the least-squares criterion, still exists the question of the multiple local minima of the objective function hence of the numerical solvability of the problem even when the data are noiseless and the original source term μ actually belongs to the approximation space \mathcal{S}_{n_d} .

In this work, we mainly deal with the dimension 3 ($n = 3$), with a single dipole $\mu = p_0\delta_{x_0}$ ($n_d = 1$) where $p_0 \in \mathbb{R}^3$ and $x_0 \in \Omega$. In this case, Equation (I.1) becomes:

$$\begin{cases} \Delta u_0 = 4\pi \nabla \cdot (p_0 \delta_{x_0}) \text{ in } \mathbb{R}^3, \\ \lim_{|z| \rightarrow \infty} |u_0(z)| = 0. \end{cases} \quad (\text{I.2})$$

As in Equation (I.1), the partial differential equation (I.2) is to be understood in the distributional sense, with the Dirac delta distribution δ_{x_0} supported at $x_0 \in \Omega$ and the divergence $\nabla \cdot (p_0 \delta_{x_0})$ being defined by:

$$\begin{aligned} \langle \delta_{x_0}, \varphi \rangle &= \varphi(x_0), \\ \langle \nabla \cdot (p_0 \delta_{x_0}), \varphi \rangle &= -p_0 \cdot \nabla \varphi(x_0), \end{aligned}$$

for all test functions $\varphi \in \mathcal{D}(\mathbb{R}^3)$ where $\mathcal{D}(\mathbb{R}^3)$ is the set of infinitely differentiable functions with compact support in \mathbb{R}^3 . The solution to Equation (I.2) in the dual $\mathcal{D}'(\mathbb{R}^3)$ of $\mathcal{D}(\mathbb{R}^3)$ is unique as the difference of two solutions would be a bounded harmonic function in \mathbb{R}^3 hence zero according to Liouville's Theorem (see [9, Thm 2.1]). This solution is given by:

$$u_0(z) = \frac{p_0 \cdot (x_0 - z)}{|x_0 - z|^3}, \forall z \in \mathbb{R}^3 \setminus \{x_0\}. \quad (\text{I.3})$$

From now on, we will consider sets $\Omega \subset \mathbb{R}^3$ which satisfy the following hypotheses:

- Ω is an open domain of \mathbb{R}^3 ,
 - $\Omega^c = \mathbb{R}^3 \setminus \Omega$ is unbounded,
 - its boundary $\partial\Omega$ is Lipschitz smooth.
- (I.4)

We will make use of the notation $0_{\mathbb{R}^3} = (0, 0, 0)^T$ for the null vector of \mathbb{R}^3 . We are interested in retrieving the location $x_0 \in \Omega$ and the moment $p_0 \in \mathbb{R}^3$ using measurements (assumed to be noiseless) of the solution u_0 on the boundary $\partial\Omega$ by minimizing the least-square criterion $J_{\partial\Omega}$:

$$J_{\partial\Omega} : \Omega \times \mathbb{R}^3 \longrightarrow \mathbb{R}_+$$

$$(x, p) \longmapsto \int_{\partial\Omega} \left(\frac{p \cdot (x - z)}{|x - z|^3} - u_0(z) \right)^2 d\sigma(z), \quad (\text{I.5})$$

with u_0 given for all $(x_0, p_0) \in \Omega \times \mathbb{R}^3$ by Equation I.3 and where σ is the Lebesgue measure on $\partial\Omega$. Hence, we considering solving the minimization problem:

Problem I.1.2. *Given $u_0|_{\partial\Omega} \in L^2(\partial\Omega)$, find $(x^*, p^*) \in \Omega \times \mathbb{R}^3$ such that:*

$$(x^*, p^*) \in \underset{(x, p) \in \Omega \times \mathbb{R}^3}{\text{Arg min}} J_{\partial\Omega}(x, p).$$

To ascertain that we actually find p_0 and x_0 when numerically solving Problem I.1.2, we will prove that the least-squares criterion I.5 has only one critical point $(x_c, p_c) = (x_0, p_0)$ when Ω is the lower half-space in \mathbb{R}^3 . Analogous results were given by [10] for similar problems in two-dimensional domains. Part of the results presented for this problem were submitted for publication in [1].

In a second part, we consider a similar inverse problem linked to an electric charge localization retrieval from the measure of the electric field it produces in the vacuum [6, Eq. 1.3]. In this case, the source is scalar hence there is no moment to consider. In this problem, we study the function:

$$E_0(z) = q_0 \frac{x_0 - z}{|x_0 - z|^3}, \quad \forall z \in \mathbb{R}^3 \setminus \{x_0\},$$

which is the solution in $[\mathcal{D}'(\mathbb{R}^3)]^3$ of:

$$\begin{cases} \Delta E_0 &= 4\pi q_0 \nabla \delta_{x_0} \text{ in } \mathbb{R}^3, \\ \lim_{|z| \rightarrow \infty} |E_0(z)| &= 0. \end{cases} \quad (\text{I.6})$$

As for Problem I.1.1, we are interested in retrieving the location $x_0 \in \Omega$ and the charge $q_0 \in \mathbb{R}$ using measurements (assumed to be noiseless) of the solution E_0 on the boundary $\partial\Omega$ by minimizing the least-square criterion $j_{\partial\Omega}$:

$$j_{\partial\Omega} : \Omega \times \mathbb{R} \longrightarrow \mathbb{R}_+$$

$$(x, q) \longmapsto \int_{\partial\Omega} \left| q \frac{x - z}{|x - z|^3} - E_0(z) \right|^2 d\sigma(z), \quad (\text{I.7})$$

with E_0 given for all $(x_0, q_0) \in \Omega \times \mathbb{R}$ by Equation I.6 and where σ is the Lebesgue measure on $\partial\Omega$. Hence, we considering solving the minimization problem:

Problem I.1.3. *Given $E_0|_{\partial\Omega} \in [L^2(\partial\Omega)]^3$, find $(x^*, q^*) \in \Omega \times \mathbb{R}$ such that:*

$$(x^*, q^*) \in \underset{(x, q) \in \Omega \times \mathbb{R}}{\text{Arg min}} j_{\partial\Omega}(x, q).$$

To ascertain that we actually find q_0 and x_0 when numerically solving Problem I.1.3, we will prove that the least-squares criterion (I.7) has only one critical point $(x_c, q_c) = (x_0, q_0)$ when Ω is the lower half-space \mathbb{R}_-^3 in \mathbb{R}^3 and when Ω is the unit ball \mathbb{B} in \mathbb{R}^3 .

In a third part, we consider a similar inverse problem linked to an electric dipolar source retrieval from the measure of the magnetic field it produces in the vacuum [11, Eq. 4]. In this problem, we study the function:

$$B_0(z) = \frac{p_0 \times (x_0 - z)}{|x_0 - z|^3}, \forall z \in \mathbb{R}^3 \setminus \{x_0\}, \quad (\text{I.8})$$

which is the solution in $[\mathcal{D}'(\mathbb{R}^3)]^3$ of:

$$\begin{cases} \Delta B_0 &= 4\pi \nabla \times (p_0 \delta_{x_0}) \text{ in } \mathbb{R}^3, \\ \lim_{|z| \rightarrow \infty} |B_0(z)| &= 0. \end{cases}$$

We are interested in retrieving the location $x_0 \in \Omega$ and the moment $p_0 \in \mathbb{R}^3$ using measurements (assumed to be noiseless) of the solution B_0 on the boundary $\partial\Omega$ by minimizing the least-square criterion $\tilde{J}_{\partial\Omega}$:

$$\begin{aligned} \tilde{J}_{\partial\Omega} : \Omega \times \mathbb{R}^3 &\longrightarrow \mathbb{R}_+ \\ (x, p) &\longmapsto \int_{\partial\Omega} \left| \frac{p \times (x - z)}{|x - z|^3} - B_0(z) \right|^2 d\sigma(z), \end{aligned} \quad (\text{I.9})$$

with B_0 given for all $(x_0, p_0) \in \Omega \times \mathbb{R}^3$ by Equation I.8 and where σ is the Lebesgue measure on $\partial\Omega$. Hence, we considering solving the minimization problem:

Problem I.1.4. *Given $B_0|_{\partial\Omega} \in [L^2(\partial\Omega)]^3$, find $(x^*, p^*) \in \Omega \times \mathbb{R}^3$ such that:*

$$(x^*, p^*) \in \underset{(x,p) \in \Omega \times \mathbb{R}^3}{\text{Arg min}} \tilde{J}_{\partial\Omega}(x, p).$$

To ascertain that we actually find p_0 and x_0 when numerically solving Problem I.1.4, we study the critical points of the criterion (I.9) when Ω is the lower half-space \mathbb{R}_-^3 in \mathbb{R}^3 and the moment p_0 is vertical. We show that contrarily to the previous criteria, this one admits multiple critical points.

I.1.3 Overview

In Section I.2, we study the dipole localization electric inverse problem of minimizing the criterion (I.5) from given measurements of u_0 . In Section I.2.1, we state our main results for two different geometries in Theorem I.2.2 and Proposition I.2.3 which are respectively proven in Subsection I.2.3 and Section I.2.4 for the planar and spherical geometries.

In Section I.3, we study the charge localization electric inverse problem of minimizing the criterion (I.7) from given measurements of E_0 . In Section I.3.1, we state our main results for two different geometries in Theorem I.3.2 and Theorem I.3.3 which are respectively proven in Section I.3.2 and Section I.3.3 for the planar and spherical geometries.

In Section I.4, we study the dipole localization magnetic inverse problem of minimizing the criterion (I.9) from given measurements of B_0 . In Section I.4.1, we state our main result in Theorem I.4.1 for the planar geometry which is proven in Section I.4.2.

In Section I.5, we provide numerical illustrations for both problems. We finally provide some concluding remarks and further possible developments of the present work in Section I.6.

I.2 A dipole localization electrical inverse problem

In this section, we study the critical points of the criterion $J_{\partial\Omega}$ given by Equation (I.5) for two different geometries, $\partial\Omega$ being the horizontal plane and the unit sphere in \mathbb{R}^3 both centered at $0_{\mathbb{R}^3}$. It can be noted that these cases are not restrictive as using rotations and homotheties the results can be extended to any plane and sphere.

I.2.1 Main results

A preliminary result is given by Proposition I.2.1 for general geometric situations following hypotheses (I.4).

Proposition I.2.1. *For each $(x_0, p_0) \in \Omega \times \mathbb{R}^3$ with $p_0 \neq 0_{\mathbb{R}^3}$, the criterion $J_{\partial\Omega}$ admits a unique global minimizer $(x^*, p^*) \in \Omega \times \mathbb{R}^3$. It coincides with the original source: $x^* = x_0$ and $p^* = p_0$.*

If $p_0 = 0_{\mathbb{R}^3}$, the minimizers of $J_{\partial\Omega}$ are all the $(x, 0_{\mathbb{R}^3})$ with $x \in \Omega$.

Proof. As $J_{\partial\Omega}$ is non-negative and $J_{\partial\Omega}(x_0, p_0) = 0$, $J_{\partial\Omega}$ admits 0 as a global minimum. Let $(x^*, p^*) \in \Omega \times \mathbb{R}^3$ be a global minimizer of $J_{\partial\Omega}$, we have $J_{\partial\Omega}(x^*, p^*) = 0$. Let us define on Ω^c the difference:

$$\forall z \in \Omega^c, h(z) = \frac{p^* \cdot (x^* - z)}{|x^* - z|^3} - \frac{p_0 \cdot (x_0 - z)}{|x_0 - z|^3},$$

such that:

$$\int_{\partial\Omega} h^2 d\sigma = J_{\partial\Omega}(x^*, p^*) = 0. \quad (\text{I.10})$$

Clearly, h is a continuous bounded function in Ω^c , is harmonic in $\Omega^c \setminus \partial\Omega$ and, if Ω^c is unbounded:

$$h(z) \xrightarrow{|z| \rightarrow \infty} 0.$$

The function h is equal to 0 on $\partial\Omega$ according to the strict positivity of the integral (I.10). Therefore, the function h is equal to 0 on Ω^c according to the uniqueness result [12, Vol. 1, Chap. II, Par. 4, Prop. 1 and 9]. Hence, we have:

$$\forall z \in \Omega^c, Q(z) = (p^* \cdot (x^* - z))^2 |x_0 - z|^6 - (p_0 \cdot (x_0 - z))^2 |x^* - z|^6 = 0.$$

As Q is a polynomial of the variables (z_1, z_2, z_3) that is null on Ω^c which contains a non-empty open set in \mathbb{R}^3 , it is null in \mathbb{R}^3 . However, as $|z|$ goes to infinity, we have the following asymptotic expansion for Q :

$$\begin{aligned} \frac{Q(z)}{|z|^6} &\underset{|z| \rightarrow \infty}{=} - [(p_0 \cdot z)^2 - (p^* \cdot z)^2] \\ &+ 2 \left[(p_0 \cdot x_0)(p_0 \cdot z) - (p^* \cdot x^*)(p^* \cdot z) + 3(x^* \cdot z) \frac{(p_0 \cdot z)^2}{|z|^2} - 3(x_0 \cdot z) \frac{(p^* \cdot z)^2}{|z|^2} \right] \\ &+ O(1). \end{aligned}$$

By identifying the first coefficient with 0 we see that $p^* = \pm p_0$. Then if $p_0 \neq 0_{\mathbb{R}^3}$, by identifying the second term with 0, we sequentially find that $p_0 \cdot x^* = p_0 \cdot x_0$ by looking in the direction p_0 and finally $x^* = x_0$. Furthermore, because h is null on $\partial\Omega$, we have $p^* = p_0$. Hence, if $p_0 \neq 0_{\mathbb{R}^3}$, there is a unique global minimizer to $J_{\partial\Omega}$: $(x^*, p^*) = (x_0, p_0)$. If $p_0 = 0_{\mathbb{R}^3}$, then for all $x \in \Omega$, $(x, 0_{\mathbb{R}^3})$ is a global minimizer of $J_{\partial\Omega}$. \square

Remark 1. This proof could have been done in any dimension $n \geq 3$ with minimal changes. Hence, the Proposition I.2.1 remains true for all $n \geq 3$.

The main result of this work is given by Theorem I.2.2 and deals only with the half-space geometry. Let $\Omega = \mathbb{R}_-^3$ be the lower half-space, \mathbb{R}_+^3 be the upper half-space and $\partial\Omega = \Pi$ be the horizontal plane of constant height $z_3 = 0$ in \mathbb{R}^3 . Let $x_0 = (x_{01}, x_{02}, x_{03})^T$ be a point in \mathbb{R}_-^3 and p_0 a vector in \mathbb{R}^3 (the situation is summarized on Figure I.1). We are interested in estimating x_0 and p_0 using measurements of u_0 on Π by solving the least-squares inverse problem:

$$(x^*, p^*) = \arg \min_{(x,p) \in \mathbb{R}_-^3 \times \mathbb{R}^3} J_\Pi(x, p),$$

with the criterion J_Π being given by:

$$J_\Pi : \mathbb{R}_-^3 \times \mathbb{R}^3 \longrightarrow \mathbb{R}_+$$

$$(x, p) \longmapsto \int_\Pi \left(\frac{p \cdot (x - z)}{|x - z|^3} - \frac{p_0 \cdot (x_0 - z)}{|x_0 - z|^3} \right)^2 d\sigma(z), \quad (\text{I.11})$$

where σ is now the Lebesgue measure on Π : $d\sigma(z) = dz_1 dz_2$, $z = (z_1, z_2, 0) \in \Pi$.

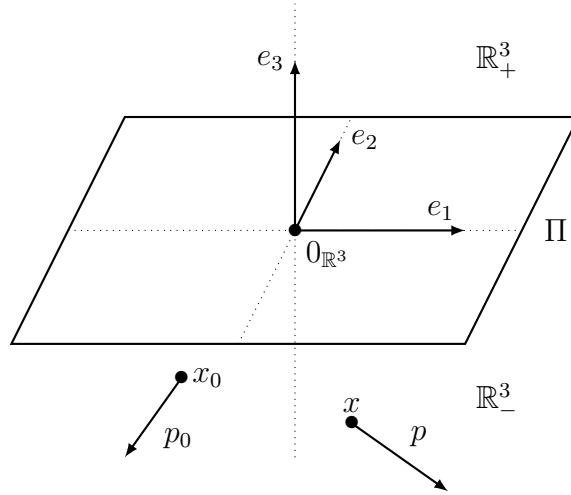


Figure I.1: Setting of this study in the half-space ($\Omega = \mathbb{R}_-^3$).

Our main result is the following:

Theorem I.2.2. *For each $(x_0, p_0) \in \mathbb{R}_-^3 \times \mathbb{R}^3$ with $p_0 \neq 0_{\mathbb{R}^3}$, the criterion J_Π admits a unique critical point $(x_c, p_c) \in \mathbb{R}_-^3 \times \mathbb{R}^3$ such that $\nabla_x J_\Pi(x_c, p_c) = \nabla_p J_\Pi(x_c, p_c) = 0_{\mathbb{R}^3}$. It coincides with the global minimizer: $x_c = x_0$ and $p_c = p_0$.*

If $p_0 = 0_{\mathbb{R}^3}$, the critical points are all the $(x, 0_{\mathbb{R}^3})$ with $x \in \mathbb{R}_-^3$.

Section I.2.3 is devoted to the proof of Theorem I.2.2.

We also showed a weaker result for the spherical situation. Let $\mathbb{B} \subset \mathbb{R}^3$ be the open ball of radius 1 and center $0_{\mathbb{R}^3}$ and $\mathbb{S} \subset \mathbb{R}^3$ the sphere of same radius and center. Let $x_0 = (x_{01}, x_{02}, x_{03})^T$ be a point in \mathbb{B} and p_0 a vector in \mathbb{R}^3 (the situation is summarized on Figure I.2). In this setting, we want, for all $p_0 \in \mathbb{R}^3$ and $x_0 = 0_{\mathbb{R}^3}$, to compute the critical points of the criterion on \mathbb{S} :

$$J_\mathbb{S} : \mathbb{B} \times \mathbb{R}^3 \longrightarrow \mathbb{R}_+$$

$$(x, p) \longmapsto \int_\mathbb{S} \left(\frac{p \cdot (x - z)}{|x - z|^3} - \frac{p_0 \cdot (x_0 - z)}{|x_0 - z|^3} \right)^2 d\sigma(z). \quad (\text{I.12})$$

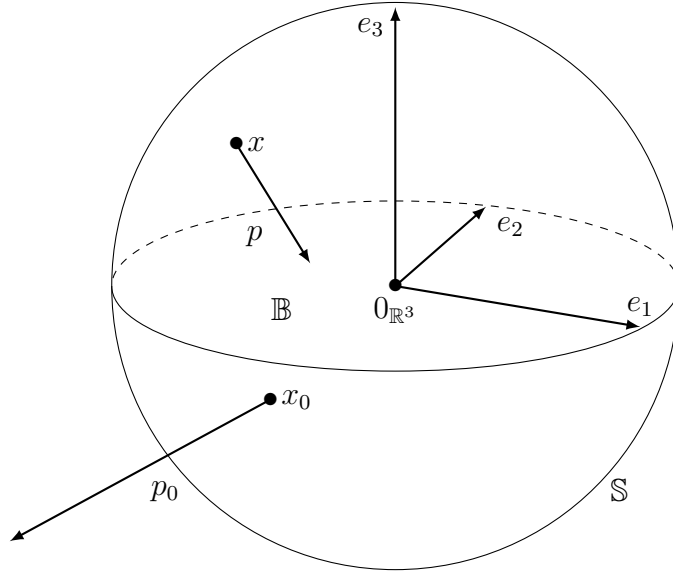


Figure I.2: Setting of this study in the spherical case ($\Omega = \mathbb{B}$).

Proposition I.2.3. *For $x_0 = 0_{\mathbb{R}^3}$ and each $p_0 \in \mathbb{R}^3$ with $p_0 \neq 0_{\mathbb{R}^3}$, the criterion $J_{\mathbb{S}}$ admits a unique critical point $(x_c, p_c) \in \mathbb{B} \times \mathbb{R}^3$ such that $\nabla_x J_{\mathbb{S}}(x_c, p_c) = \nabla_p J_{\mathbb{S}}(x_c, p_c) = 0_{\mathbb{R}^3}$. It coincides with the global minimizer: $x_c = x_0 = 0_{\mathbb{R}^3}$ and $p_c = p_0$.*

If $p_0 = 0_{\mathbb{R}^3}$, the critical points are all the $(x, 0_{\mathbb{R}^3})$ with $x \in \mathbb{B}$.

Section I.2.4 is devoted to the proof of Proposition I.2.3.

I.2.2 Preliminary computations

In this section, we make general considerations that apply to any configuration for which Ω satisfy the hypothesis (I.4).

I.2.2.a Gradient in p

By expanding the square in Equation (I.5), we have for all $(x, p) \in \Omega \times \mathbb{R}^3$:

$$J_{\partial\Omega}(x, p) = p^T M_{\partial\Omega}(x, x)p + p_0^T M_{\partial\Omega}(x_0, x_0)p_0 - 2p_0^T M_{\partial\Omega}(x, x_0)p, \quad (\text{I.13})$$

where the 3×3 matrix $M_{\partial\Omega}(x, x_0)$ is defined by:

$$M_{\partial\Omega}(x, x_0) = \int_{\partial\Omega} \left(\frac{x_0 - z}{|x_0 - z|^3} \right) \left(\frac{x - z}{|x - z|^3} \right)^T d\sigma(z). \quad (\text{I.14})$$

Therefore, the gradient of $J_{\partial\Omega}$ with respect to p is given by:

$$\nabla_p J_{\partial\Omega}(x, p) = 2M_{\partial\Omega}(x, x)p - 2M_{\partial\Omega}(x, x_0)^T p_0.$$

One can see that the matrix $M_{\partial\Omega}(x, x)$ is symmetric and positive definite for each $x \in \Omega$, as for all $v \in \mathbb{R}^3$, $v \neq 0_{\mathbb{R}^3}$:

$$v^T M_{\partial\Omega}(x, x)v = \int_{\partial\Omega} \left(\frac{v \cdot (x - z)}{|x - z|^3} \right)^2 d\sigma(z) > 0,$$

which leads to $M_{\partial\Omega}(x, x)$ being invertible. Therefore, if $(x_c, p_c) \in \Omega \times \mathbb{R}^3$ is a critical point then necessarily:

$$p_c = M_{\partial\Omega}(x_c, x_c)^{-1} M_{\partial\Omega}(x_c, x_0)^T p_0 \stackrel{\text{def}}{=} p(x_c). \quad (\text{I.15})$$

One can see from Equation (I.15) that in this case:

$$p_c^T M_{\partial\Omega}(x_c, x_c) p_c - p_0^T M_{\partial\Omega}(x_c, x_0) p_c = 0. \quad (\text{I.16})$$

Furthermore, if $p_0 = 0_{\mathbb{R}^3}$ then the critical points of $J_{\partial\Omega}$ are the $(x, 0_{\mathbb{R}^3})$ for any $x \in \Omega$. Indeed, for all $(x_c, p_c) \in \Omega \times \mathbb{R}^3$ critical point of $J_{\partial\Omega}$, Equation (I.15) leads to $p_c = 0_{\mathbb{R}^3}$ and as $J_{\partial\Omega}(\cdot, 0_{\mathbb{R}^3})$ is in this case uniformly null, for all $x \in \Omega$, $(x, 0_{\mathbb{R}^3})$ is a critical point of $J_{\partial\Omega}$. So, we will suppose in the following that:

$$p_0 \neq 0_{\mathbb{R}^3}. \quad (\text{I.17})$$

In order not to carry heavy notation, we will drop the dependency in x , x_0 and $\partial\Omega$ of $M = M_{\partial\Omega}(x, x_0)$ and all its derived quantities when there is no ambiguity.

I.2.2.b Gradient in x

For all $x \in \Omega$, let $p = p(x)$ be defined as in Equation (I.15) and $I_{\partial\Omega}(x) = J_{\partial\Omega}(x, p(x))$. Then, by definition of $p(x)$, the critical points of $J_{\partial\Omega}$ are all the $(x_c, p(x_c))$ where $x_c \in \Omega$ is a critical point of $I_{\partial\Omega}$. For all $x \in \Omega$, in view of Equations (I.13) and (I.15) and because of Equation (I.16), we have:

$$\begin{aligned} I_{\partial\Omega}(x) &= p(x)^T M(x, x) p(x) + p_0^T M(x_0, x_0) p_0 - 2p_0^T M(x, x_0) p(x) \\ &= -p_0^T M(x, x_0) p(x) + p_0^T M(x_0, x_0) p_0, \end{aligned}$$

So, computing the gradient of $I_{\partial\Omega}$, we get for all $x \in \Omega$:

$$\begin{aligned} \nabla I_{\partial\Omega}(x) &= -\nabla (p_0^T M(x, x_0) p(x)) \\ &= -\nabla (p_0^T M(x, x_0) M(x, x)^{-1} M(x, x_0)^T p_0), \end{aligned}$$

in view of Equation (I.15). Therefore, upon defining the matrix:

$$K = K(x, x_0) \stackrel{\text{def}}{=} M(x, x_0) M(x, x)^{-1} M(x, x_0)^T, \quad (\text{I.18})$$

we obtain that $(x_c, p(x_c)) \in \Omega \times \mathbb{R}^3$ is a critical point of $J_{\partial\Omega}$ if and only if, for all $i \in \{1, 2, 3\}$:

$$p_0^T \left(\frac{\partial K}{\partial x_i}(x_c, x_0) \right) p_0 = 0. \quad (\text{I.19})$$

I.2.3 Planar case (Proof of Theorem I.2.2)

Let us fix $(x_0, p_0) \in \mathbb{R}_-^3 \times \mathbb{R}^3$. In this section, we want to compute the critical points of the criterion J_{Π} . To do so, in Section I.2.3.a, we express Equation (I.11) by computing certain integrals. In Sections I.2.3.b and I.2.3.c, we characterize (x_0, p_0) as being the unique critical point of (I.11) by first proving that any critical point $(x_c, p_c) \in \mathbb{R}_-^3 \times \mathbb{R}^3$ is such that x_c and x_0 belong to the same horizontal plane using the homogeneity of the criterion; then, we appropriately combine derivatives to show uniqueness of a critical point with positivity arguments and conclude the proof in Section I.2.3.d.

I.2.3.a Explicit computation of the criterion

Our goal in this section is to compute the matrices $M(x, x)$ and $M(x, x_0)$ defined by Equation (I.14) with $\partial\Omega = \Pi$. The elements of these matrices are given for x and x_0 in \mathbb{R}_-^3 by:

$$M(x, x_0)_{i,j} = \int_{\Pi} \frac{x_j - z_j}{|x - z|^3} \frac{x_{0i} - z_i}{|x_0 - z|^3} d\sigma(z), \quad (\text{I.20})$$

for all $(i, j) \in \{1, 2, 3\}^2$.

In order to compute the integrals (I.20), we make use of Clifford analytic calculus presented in Appendix A. Let us call M_1 , M_2 and M_3 the columns of M and identify them with their corresponding vectors in $\mathcal{Cl}_{0,3}(\mathbb{R})$:

$$\begin{aligned} M_1 &= M_{1,1} e_1 + M_{2,1} e_2 + M_{3,1} e_3, \\ M_2 &= M_{1,2} e_1 + M_{2,2} e_2 + M_{3,2} e_3, \\ M_3 &= M_{1,3} e_1 + M_{2,3} e_2 + M_{3,3} e_3. \end{aligned}$$

Upon defining $x^+ \in \mathbb{R}_+^3$ as the symmetric of x with respect to Π and identifying x , x^+ , x_0 and all $z \in \Pi$ with their corresponding vectors in $\mathcal{Cl}_{0,3}(\mathbb{R})$, we have:

$$\begin{aligned} M_1 \odot e_1 + M_2 \odot e_2 + M_3 \odot e_3 &= \int_{\Pi} \frac{x_0 - z}{|x_0 - z|^3} \odot \frac{x - z}{|x - z|^3} d\sigma(z) \\ &= - \int_{\Pi} \frac{x_0 - z}{|x_0 - z|^3} \odot e_3 \odot e_3 \odot \frac{x - z}{|x - z|^3} d\sigma(z) \\ &= \int_{\Pi} \frac{x_0 - z}{|x_0 - z|^3} \odot e_3 \odot \frac{x^+ - z}{|x^+ - z|^3} d\sigma(z) \odot e_3 \\ &= 4\pi \frac{x^+ - x_0}{|x^+ - x_0|^3} \odot e_3, \end{aligned} \quad (\text{I.21})$$

where we used the relations:

$$\begin{aligned} e_3 \odot e_3 &= -\mathbf{1}, \\ e_3 \odot (x - z) &= -(x^+ - z) \odot e_3, \end{aligned}$$

and Lemma A.0.1 (Appendix A) as $z \mapsto \frac{x^+ - z}{|x^+ - z|^3}$ is left Clifford analytic in \mathbb{R}_-^3 since $x^+ \in \mathbb{R}_+^3$. Using Lemma A.0.1, we also have:

$$\begin{aligned} (-M_1 \odot e_1 - M_2 \odot e_2 + M_3 \odot e_3) \odot e_3 &= \int_{\Pi} \frac{x_0 - z}{|x_0 - z|^3} \odot e_3 \odot \frac{x - z}{|x - z|^3} d\sigma(z) \\ &= 0, \end{aligned} \quad (\text{I.22})$$

because $z \mapsto \frac{x - z}{|x - z|^3}$ is left Clifford analytic in \mathbb{R}_+^3 since $x \in \mathbb{R}_-^3$. Using these equations, we get the following relations between terms:

$$M_{1,1} + M_{2,2} = M_{3,3} = -2\pi \frac{x_3 + x_{03}}{|x^+ - x_0|^3} = -2\pi \frac{x_{a3}}{|x_a|^3}, \quad (\text{I.23})$$

$$M_{3,1} = -M_{1,3} = -2\pi \frac{x_1 - x_{01}}{|x^+ - x_0|^3} = 2\pi \frac{x_{a1}}{|x_a|^3}, \quad (\text{I.24})$$

$$M_{3,2} = -M_{2,3} = -2\pi \frac{x_2 - x_{02}}{|x^+ - x_0|^3} = 2\pi \frac{x_{a2}}{|x_a|^3}, \quad (\text{I.25})$$

$$M_{2,1} = M_{1,2}, \quad (\text{I.26})$$

where we defined $x_a \in \mathbb{R}_-^3$ by $x_a = x_0 - x^+$. Indeed:

- Equation (I.23) comes from the $\mathbf{1}$ coordinate of Equation (I.21) and the e_3 coordinate of Equation (I.22).
- Equation (I.24) comes from the $e_3 \odot e_1$ coordinate of Equation (I.21) and the e_1 coordinate of Equation (I.22).
- Equation (I.25) comes from the $e_2 \odot e_3$ coordinate of Equation (I.21) and the e_2 coordinate of Equation (I.22).
- Equation (I.26) comes from the $e_1 \odot e_2$ coordinate of Equation (I.21) or the $e_1 \odot e_2 \odot e_3$ coordinate of Equation (I.22).

We are left to compute:

$$\begin{aligned} M_{1,1} &= \int_{\Pi} \frac{x_1 - z_1}{|x - z|^3} \frac{x_{01} - z_1}{|x_0 - z|^3} d\sigma(z), \\ M_{2,2} &= \int_{\Pi} \frac{x_2 - z_2}{|x - z|^3} \frac{x_{02} - z_2}{|x_0 - z|^3} d\sigma(z), \\ M_{2,1} = M_{1,2} &= \int_{\Pi} \frac{x_1 - z_1}{|x - z|^3} \frac{x_{02} - z_2}{|x_0 - z|^3} d\sigma(z). \end{aligned}$$

To do so, we use the previously computed $M_{3,3}$ in Equation (I.23) and define:

$$\begin{aligned} m_{3,3}(x_{a1}, x_{a2}, x_{a3}) &= M_{3,3}(x, x_0) \\ &= \int_{\Pi} \frac{x_3}{|x - z|^3} \frac{x_{03}}{|x_0 - z|^3} d\sigma(z) \\ &= -2\pi \frac{x_{a3}}{[x_{a1}^2 + x_{a2}^2 + x_{a3}^2]^{\frac{3}{2}}}. \end{aligned}$$

By integration and differentiation, we can transform the integrand of $M_{3,3}$ into those of $M_{1,1}$, $M_{2,2}$, $M_{2,1}$ and $M_{1,2}$. Indeed it is easily checked that for $i \in \{1, 2\}$:

$$\begin{aligned} \frac{x_i - z_i}{|x - z|^3} &= \int_{-\infty}^{x_3} \partial_{x_i} \frac{y}{[(x_1 - z_1)^2 + (x_2 - z_2)^2 + y^2]^{\frac{3}{2}}} dy, \\ \frac{x_{0i} - z_i}{|x_0 - z|^3} &= \int_{-\infty}^{x_{03}} \partial_{x_{0i}} \frac{y}{[(x_{01} - z_1)^2 + (x_{02} - z_2)^2 + y^2]^{\frac{3}{2}}} dy. \end{aligned}$$

So, by applying Fubini's theorem then differentiating under the integral sign, we get for $i \in \{1, 2\}$:

$$\begin{aligned} \int_{-\infty}^{x_{03}} \int_{-\infty}^{x_3} \partial_{x_i} \partial_{x_{0i}} m_{3,3}(x_{a1}, x_{a2}, y_1 + y_2) dy_1 dy_2 &= M_{i,i}, \\ \int_{-\infty}^{x_{03}} \int_{-\infty}^{x_3} \partial_{x_1} \partial_{x_{02}} m_{3,3}(x_{a1}, x_{a2}, y_1 + y_2) dy_1 dy_2 &= M_{2,1} = M_{1,2}. \end{aligned}$$

Since $m_{3,3}$ is a function of $x_{a1} = x_{01} - x_1$, $x_{a2} = x_{02} - x_2$ and $x_{a3} = x_{03} + x_3$, we can simplify the differentiations and for $i, j \in \{1, 2\}$:

$$\partial_{x_i} \partial_{x_{0j}} m_{3,3} = -\partial_{x_{ai}} \partial_{x_{aj}} m_{3,3}.$$

Then, using known antiderivatives, we compute $M_{1,1}$, $M_{2,2}$, $M_{2,1}$ and $M_{1,2}$, for all $i, j \in \{1, 2\}$:

$$\begin{aligned}
M_{i,j} &= 2\pi \int_{y_1=-\infty}^{x_3} \partial_{x_{ai}} \partial_{x_{aj}} \int_{y_2=-\infty}^{x_{03}} \frac{y_1 + y_2}{[x_{a1}^2 + x_{a2}^2 + (y_1 + y_2)^2]^{\frac{3}{2}}} dy_1 dy_2 \\
&= -2\pi \int_{-\infty}^{x_{a3}} \partial_{x_{ai}} \partial_{x_{aj}} \frac{1}{[x_{a1}^2 + x_{a2}^2 + y^2]^{\frac{1}{2}}} dy \\
&= -2\pi \int_{-\infty}^{x_{a3}} \left[-\frac{\delta_{i,j}}{[x_{a1}^2 + x_{a2}^2 + y^2]^{3/2}} + 3 \frac{x_{ai} x_{aj}}{[x_{a1}^2 + x_{a2}^2 + y^2]^{5/2}} \right] dy \\
&= \frac{2\pi}{(x_{a1}^2 + x_{a2}^2)} \left[\delta_{ij} \frac{|x_a| + x_{a3}}{|x_a|} - x_{ai} x_{aj} \frac{2|x_a|^3 + 3x_{a3}|x_a|^2 - x_{a3}^3}{|x_a|^3 (x_{a1}^2 + x_{a2}^2)} \right]. \tag{I.27}
\end{aligned}$$

Remark 2. We can see that all the expressions $M_{i,j}$ for $(i, j) \in \{1, 2, 3\}^2$ are homogeneous of degree -2 in all their variables $x_1, x_{01}, x_2, x_{02}, x_3$ and x_{03} .

By taking the limits of the previously computed terms as x_0 goes to x , we find for that all $x \in \mathbb{R}_-^3$:

$$M(x, x) = \frac{\pi}{4x_3^2} \begin{bmatrix} 1 & 0 & 0 \\ 0 & 1 & 0 \\ 0 & 0 & 2 \end{bmatrix}.$$

One can see that $M(x, x_0)$ is also invertible for $x \neq x_0$ as for $(x_{a1}, x_{a2}) \neq (0, 0)$:

$$\det(M(x, x_0)) = \frac{8\pi^3}{(x_{a1}^2 + x_{a2}^2)^2 |x_a|^4} (|x_a| + x_{a3})^2 > 0.$$

I.2.3.b First step: use of homogeneity

One can see that for all $x \in \mathbb{R}_-^3$, the matrix $K = K(x, x_0)$ defined by Equation (I.18) is symmetric positive definite as:

$$K = \left((M(x, x)^{-1})^{1/2} M(x, x_0)^T \right)^T \left((M(x, x)^{-1})^{1/2} M(x, x_0)^T \right).$$

Furthermore, since $M(x, x_0)$ is homogeneous of degree -2 , $K(x, x_0)$ is also homogeneous of degree -2 in its six variables ($x_1, x_2, x_3, x_{01}, x_{02}$ and x_{03}). We can therefore apply Euler's homogeneous function theorem [12, Vol. 2, App. Eq. 3.75] and get:

$$x_1 \frac{\partial K}{\partial x_1} + x_{01} \frac{\partial K}{\partial x_{01}} + x_2 \frac{\partial K}{\partial x_2} + x_{02} \frac{\partial K}{\partial x_{02}} + x_3 \frac{\partial K}{\partial x_3} + x_{03} \frac{\partial K}{\partial x_{03}} = -2K.$$

But, since the following relations hold true:

$$\frac{\partial K}{\partial x_{01}} = -\frac{\partial K}{\partial x_1}, \quad \frac{\partial K}{\partial x_{02}} = -\frac{\partial K}{\partial x_2}, \quad \frac{\partial K}{\partial x_{03}} = \frac{\partial K}{\partial x_3} - \frac{2}{x_3} K,$$

we obtain the following equation:

$$-x_3 x_{a1} \frac{\partial K}{\partial x_1} - x_3 x_{a2} \frac{\partial K}{\partial x_2} + x_3 x_{a3} \frac{\partial K}{\partial x_3} = 2(x_{03} - x_3)K. \tag{I.28}$$

Thus, for $x_c \in \mathbb{R}_-^3$ a critical point of I_Π and because of Equation (I.19), $p_0^T(x_{03} - x_{c3})K(x_c, x_0)p_0 = 0$. But, for $x_{03} \neq x_{c3}$, $(x_{03} - x_{c3})K(x_c, x_0)$ is definite which means that $p_0 = 0_{\mathbb{R}^3}$ contradicting hypothesis (I.17). Thus, $x_c \in \mathbb{R}_-^3$ is a critical point of I_Π only if $x_{c3} = x_{03}$.

I.2.3.c Second step: use of strict positivity

Let $x \in \mathbb{R}_-^3$. Let us use polar coordinates in the plane: $x_{a1} = r \cos(\theta)$ and $x_{a2} = r \sin(\theta)$ with $r \geq 0$ and $\theta \in [0, 2\pi[$. Let K_r be the matrix:

$$K_r = K_r(x, x_0) \stackrel{\text{def}}{=} -\frac{\partial}{\partial r} K \left(\begin{pmatrix} x_{01} - r \cos(\theta) \\ x_{02} - r \sin(\theta) \\ x_3 \end{pmatrix}, x_0 \right).$$

Let us prove that unless $(x_1, x_2) = (x_{01}, x_{02})$ (i.e. $r = 0$), $K_r(x, x_0)$ is positive definite. In what follows, we assume that $r \neq 0$. As K_r is symmetric, we have to check that its eigenvalues λ_1 , λ_2 and λ_3 are positive. First, using Equations (I.24), (I.25) and (I.27), one can see that the vector $(\sin(\theta), -\cos(\theta), 0)^T$ is an eigenvector of $M(x, x_0)$, thus of $K(x, x_0)$ and thus of $K_r(x, x_0)$ with the eigenvalue:

$$\lambda_1 = \frac{32x_3^2\pi}{r|x_a|^3} \left(\frac{x_{a3}}{|x_a|} + 1 \right) \frac{4r^2 + 3x_{a3}^2}{2|x_a|^3 - x_{a3}r^2 - 2x_{a3}|x_a|^2} > 0.$$

Furthermore, one can check that:

$$\lambda_2 + \lambda_3 = \text{Tr}(K_r(x, x_0)) - \lambda_1 = \frac{32x_3^2\pi}{r^5|x_a|^6} \frac{\mathcal{A}_t^2 - \mathcal{B}_t^2}{\mathcal{A}_t + \mathcal{B}_t} > 0,$$

where we define the positive quantities:

$$\begin{aligned} \mathcal{A}_t^2 - \mathcal{B}_t^2 &= r^6 (25r^6 + 35r^2x_{a3}^4 + 50r^4x_{a3}^2 + 9x_{a3}^6) > 0, \\ \mathcal{A}_t &= 13r^2x_{a3}^4 + 15r^4x_{a3}^2 + 5r^6 + 4x_{a3}^6 > 0, \\ \mathcal{B}_t &= -x_{a3}|x_a| (4x_{a3}^4 + 10r^4 + 11r^2x_{a3}^2) > 0. \end{aligned}$$

Similarly, we have:

$$\lambda_2\lambda_3 = \frac{\det(K_r(x, x_0))}{\lambda_1} = \frac{64x_3^4\pi^2}{r^4|x_a|^{12}} \frac{\mathcal{A}_d^2 - \mathcal{B}_d^2}{\mathcal{A}_d + \mathcal{B}_d} > 0,$$

where we define the positive quantities:

$$\begin{aligned} \mathcal{A}_d^2 - \mathcal{B}_d^2 &= r^6 (1024r^6 + 1457r^2x_{a3}^4 + 240x_{a3}^6 + 2240r^4x_{a3}^2) > 0, \\ \mathcal{A}_d &= 128r^2x_{a3}^4 + 135r^4x_{a3}^2 + 32r^6 + 24x_{a3}^6 > 0, \\ \mathcal{B}_d &= -x_{a3}|x_a| (24x_{a3}^4 + 80r^4 + 116r^2x_{a3}^2) > 0. \end{aligned}$$

This shows that λ_1 , λ_2 and λ_3 are positive for $r > 0$. The matrix $K_r(x, x_0)$ is thus positive definite if $(x_{a1}, x_{a2}) \neq (0, 0)$. Hence, as $p_0 \neq 0_{\mathbb{R}^3}$, and because $p_0^T K_r(x_c, x_0) p_0 = 0$ for any critical point $x_c \in \mathbb{R}_-^3$ of I_Π , $x \in \mathbb{R}_-^3$ is a critical point of I_Π only if $x_1 = x_{01}$ and $x_2 = x_{02}$.

I.2.3.d Reciprocal

The only remaining possibility is $x_c = x_0$. We first remark from Equation (I.15) that:

$$p(x_0) = M(x_0, x_0)^{-1} M(x_0, x_0)^T p_0 = p_0.$$

Furthermore, (x_0, p_0) is obviously a critical point of J_Π as it is its global minimizer (see e.g. Proposition I.2.1). We can thus conclude that J_Π has a unique critical point: (x_0, p_0) . This ends the proof of Theorem I.2.2. □

I.2.4 Spherical case (Proof of Proposition I.2.3)

Let us fix $p_0 \in \mathbb{R}^3$ and $x_0 = 0_{\mathbb{R}^3}$. In this section, we want to compute the critical points of the criterion J_S . To do so, in Section I.2.4.a we express (I.12) by computing certain integrals. We then show in Section I.2.4.b the uniqueness of the critical point of (I.12) with positivity arguments.

I.2.4.a Explicit computation of the criterion

As part of the following computations can be pursued for any $x_0 \in \mathbb{B}$, we initially consider the general case $x_0 \in \mathbb{B}$ rather than $x_0 = 0_{\mathbb{R}^3}$. As in the half-space case of Section I.2.3, we will need to compute $M(x, x)$ and $M(x, x_0)$ defined by Equation (I.14) with $\partial\Omega = \mathbb{S}$. The elements of these matrices are given for x and x_0 in \mathbb{B} by:

$$\begin{aligned} M_{i,j}(x, x_0) &= \int_{\mathbb{S}} \frac{x_{0i} - z_i}{|x_0 - z|^3} \frac{x_j - z_j}{|x - z|^3} d\sigma(z) \\ &= \partial_{x_j} \partial_{x_{0i}} F(x, x_0), \end{aligned} \quad (\text{I.29})$$

for all $(i, j) \in \{1, 2, 3\}^2$ and where we defined the function:

$$F(x, x_0) = \int_{\mathbb{S}} \frac{1}{|x_0 - z|} \frac{1}{|x - z|} d\sigma(z).$$

Remark 3. One can see that this expression was not usable in the half-space case because $F(x, x_0)$ would be infinite while in this case, it is simply the integral of a continuous function on a compact set.

First, we compute the matrix $M(x, x)$. For all $x \in \mathbb{B}$, let us express $f(x) = F(x, x)$:

$$\begin{aligned} f(x) &= \int_{\mathbb{S}} \frac{1}{|x - z|^2} d\sigma(z) \\ &= \int_{\mathbb{S}} u^2(x, z) d\sigma(z) \\ &= \int_{\theta=0}^{\pi} \int_{\varphi=0}^{2\pi} \frac{\sin(\theta)}{1 + |x|^2 - 2|x|\cos(\theta)} d\varphi d\theta \\ &= \frac{2\pi}{|x|} \ln \left(\frac{1 + |x|}{1 - |x|} \right), \end{aligned}$$

where we define the function:

$$\begin{aligned} u &: \mathbb{B} \times \mathbb{S} \longrightarrow \mathbb{R} \\ (x, z) &\longmapsto \frac{1}{|x - z|}. \end{aligned}$$

For i and j in $\{1, 2, 3\}$ we want to compute:

$$M_{i,j}(x, x) = \int_{\mathbb{S}} \frac{x_i - z_i}{|x - z|^3} \frac{x_j - z_j}{|x - z|^3} d\sigma(z) = \int_{\mathbb{S}} u_i(x, z) u_j(x, z) d\sigma(z), \quad (\text{I.30})$$

where for all k in $\{1, 2, 3\}$, u_k denotes the partial derivative of u with respect to x_k .

For i and j in $\{1, 2, 3\}$, we have:

$$\begin{aligned}\partial_{x_i}\partial_{x_j}f(x) &= \int_{\mathbb{S}} \partial_{x_i}\partial_{x_j} [u^2(x, z)] d\sigma(z) \\ &= 2 \int_{\mathbb{S}} (u_{i,j}(x, z)u(x, z) + u_i(x, z)u_j(x, z)) d\sigma(z),\end{aligned}\tag{I.31}$$

where for all $(x, z) \in \mathbb{B} \times \mathbb{S}$:

$$\begin{aligned}u_{i,j}(x, z) &= \partial_{x_i}\partial_{x_j}u(x, z) \\ &= 3 \frac{(x_i - z_i)(x_j - z_j)}{|x - z|^5} - \frac{\delta_{i,j}}{|x - z|^3} \\ &= 3 \frac{u_i(x, z)u_j(x, z)}{u(x, z)} - \delta_{i,j} \frac{1}{u(x, z)} \frac{1}{|x - z|^4}.\end{aligned}\tag{I.32}$$

Hence, using Equations (I.30), (I.31) and (I.32):

$$\begin{aligned}\partial_{x_i}\partial_{x_j}f(x) &= 2 \int_{\mathbb{S}} (u_{i,j}(x, z)u(x, z) + u_i(x, z)u_j(x, z)) d\sigma(z) \\ &= 8 \int_{\mathbb{S}} u_i(x, z)u_j(x, z) d\sigma(z) - 2\delta_{i,j} \int_{\mathbb{S}} \frac{1}{|x - z|^4} d\sigma(z) \\ &= 8M_{i,j}(x, x) - 2\delta_{i,j} \int_{\mathbb{S}} \frac{1}{|x - z|^4} d\sigma(z).\end{aligned}$$

By using the expression of $a_{\mathbb{S}}(x, x_0)$ (I.53) established in Section I.3.3 for $x_0 = x$, we can deduce that:

$$\int_{\mathbb{S}} \frac{1}{|x - z|^4} d\sigma(z) = \frac{4\pi}{(1 - |x|^2)^2}.$$

This allows us to compute $M(x, x)$. For i and j in $\{1, 2, 3\}$ with $i \neq j$, we get:

$$\begin{aligned}M_{i,j}(x, x) &= \frac{1}{8} \partial_{x_i}\partial_{x_j}f(x) \\ &= \frac{\pi x_i x_j}{4|x|^5(1 - |x|^2)^2} \left[3(1 - |x|^2)^2 \ln \left(\frac{1 + |x|}{1 - |x|} \right) + |x|(10|x|^2 - 6) \right],\end{aligned}\tag{I.33}$$

$$\begin{aligned}M_{i,i}(x, x) &= \frac{1}{8} \left(\partial_{x_i}\partial_{x_i}f(x) + \frac{8\pi}{(1 - |x|^2)^2} \right) \\ &= \frac{\pi}{4|x|^6(1 - |x|^2)^2} \left[|x|(1 - |x|^2)^2 (3x_i^2 - |x|^2) \ln \left(\frac{1 + |x|}{1 - |x|} \right) \right. \\ &\quad \left. + 2|x|^2 (|x|^2 - 3x_i^2 + |x|^4 + 5x_i^2|x|^2) \right].\end{aligned}\tag{I.34}$$

We will suppose in the following that x_0 is the center of \mathbb{B} (i.e. $x_0 = 0_{\mathbb{R}^3}$). Since the problem then becomes symmetric by rotation around the center, x can be chosen in any direction and thus, for simplicity, will be chosen to be of the form $x = (0, 0, x_3)^T$ where $x_3 \in]0, 1[$ (we leave out the value $x_3 = 0$ for now). Using these hypotheses on x and x_0 ,

we have, from Equation (I.29):

$$M_{1,1}(x, x_0) = \int_{\theta=0}^{\pi} \int_{\varphi=0}^{2\pi} \frac{(\cos(\varphi) \sin(\theta))^2}{[1 + x_3^2 - 2x_3 \cos(\theta)]^{3/2}} \sin(\theta) d\varphi d\theta = \frac{4\pi}{3}, \quad (\text{I.35})$$

$$M_{2,2}(x, x_0) = \int_{\theta=0}^{\pi} \int_{\varphi=0}^{2\pi} \frac{(\sin(\varphi) \sin(\theta))^2}{[1 + x_3^2 - 2x_3 \cos(\theta)]^{3/2}} \sin(\theta) d\varphi d\theta = \frac{4\pi}{3}, \quad (\text{I.36})$$

$$M_{3,3}(x, x_0) = \int_{\theta=0}^{\pi} \int_{\varphi=0}^{2\pi} \frac{(x_3 - \cos(\theta)) \cos(\theta)}{[1 + x_3^2 - 2x_3 \cos(\theta)]^{3/2}} \sin(\theta) d\varphi d\theta = \frac{4\pi}{3}, \quad (\text{I.37})$$

$$M_{1,2}(x, x_0) = \int_{\theta=0}^{\pi} \int_{\varphi=0}^{2\pi} \frac{\cos(\varphi) \sin(\theta) \sin(\varphi) \sin(\theta)}{[1 + x_3^2 - 2x_3 \cos(\theta)]^{3/2}} \sin(\theta) d\varphi d\theta = 0, \quad (\text{I.38})$$

$$M_{2,1}(x, x_0) = \int_{\theta=0}^{\pi} \int_{\varphi=0}^{2\pi} \frac{\cos(\varphi) \sin(\theta) \sin(\varphi) \sin(\theta)}{[1 + x_3^2 - 2x_3 \cos(\theta)]^{3/2}} \sin(\theta) d\varphi d\theta = 0, \quad (\text{I.39})$$

$$M_{1,3}(x, x_0) = \int_{\theta=0}^{\pi} \int_{\varphi=0}^{2\pi} \frac{\cos(\varphi) \sin(\theta) (x_3 - \cos(\theta))}{[1 + x_3^2 - 2x_3 \cos(\theta)]^{3/2}} \sin(\theta) d\varphi d\theta = 0, \quad (\text{I.40})$$

$$M_{3,1}(x, x_0) = \int_{\theta=0}^{\pi} \int_{\varphi=0}^{2\pi} \frac{\cos(\varphi) \sin(\theta) \cos(\theta)}{[1 + x_3^2 - 2x_3 \cos(\theta)]^{3/2}} \sin(\theta) d\varphi d\theta = 0, \quad (\text{I.41})$$

$$M_{2,3}(x, x_0) = \int_{\theta=0}^{\pi} \int_{\varphi=0}^{2\pi} \frac{\sin(\varphi) \sin(\theta) (x_3 - \cos(\theta))}{[1 + x_3^2 - 2x_3 \cos(\theta)]^{3/2}} \sin(\theta) d\varphi d\theta = 0, \quad (\text{I.42})$$

$$M_{3,2}(x, x_0) = \int_{\theta=0}^{\pi} \int_{\varphi=0}^{2\pi} \frac{\sin(\varphi) \sin(\theta) \cos(\theta)}{[1 + x_3^2 - 2x_3 \cos(\theta)]^{3/2}} \sin(\theta) d\varphi d\theta = 0. \quad (\text{I.43})$$

Similarly, using the formulas (I.33) and (I.34) previously computed, we get:

$$\begin{aligned} M_{1,1}(x, x) &= \frac{\pi}{4x_3^3(1-x_3^2)^2} \left[(1-x_3^2)^2 \ln \left(\frac{1-x_3}{1+x_3} \right) + 2x_3(1+x_3^2) \right], \\ M_{2,2}(x, x) &= \frac{\pi}{4x_3^3(1-x_3^2)^2} \left[(1-x_3^2)^2 \ln \left(\frac{1-x_3}{1+x_3} \right) + 2x_3(1+x_3^2) \right], \\ M_{3,3}(x, x) &= -\frac{\pi}{2x_3^3(1-x_3^2)^2} \left[(1-x_3^2)^2 \ln \left(\frac{1-x_3}{1+x_3} \right) + 2x_3(1-3x_3^2) \right], \\ M_{1,2}(x, x) &= M_{2,1}(x, x) = M_{1,3}(x, x) = M_{3,1}(x, x) \\ &= M_{2,3}(x, x) = M_{3,2}(x, x) = 0. \end{aligned}$$

I.2.4.b Critical point computation

In the spherical case, using Equation (I.18) and relations (I.35) to (I.43), we have for all $x \in \mathbb{B}$:

$$K(x, x_0) = \left(\frac{4\pi}{3} \right)^2 M(x, x)^{-1}.$$

So, because of Equation (I.19), $x_c \in \mathbb{B}$ is a critical point of $I_{\mathbb{S}}$ only if:

$$p_0^T \frac{d}{dx_3} M^{-1}(x_c, x_c) p_0 = 0.$$

Since the matrix $M(x, x)$ is diagonal, its inverse $M^{-1}(x, x)$ is also diagonal and its diagonal terms are the inverse of the diagonal terms of the matrix $M(x, x)$. Therefore:

$$\frac{dM^{-1}(x, x)}{dx_3} = \begin{pmatrix} \frac{dM_{1,1}(x, x)}{dx_3} \frac{-1}{M_{1,1}^2(x, x)} & 0 & 0 \\ 0 & \frac{dM_{2,2}(x, x)}{dx_3} \frac{-1}{M_{2,2}^2(x, x)} & 0 \\ 0 & 0 & \frac{dM_{3,3}(x, x)}{dx_3} \frac{-1}{M_{3,3}^2(x, x)} \end{pmatrix}.$$

Since this matrix is diagonal, it is negative definite if and only if its diagonal terms are negative. Through simple derivations, we obtain:

$$\begin{aligned} \frac{dM_{1,1}(x, x)}{dx_3} &= \frac{dM_{2,2}(x, x)}{dx_3} \\ &= \frac{\pi}{4x_3^4(1-x_3^2)^3} \left[3(1-x_3^2)^3 \ln\left(\frac{1+x_3}{1-x_3}\right) + 6x_3^5 + 16x_3^3 - 6x_3 \right], \\ \frac{dM_{3,3}(x, x)}{dx_3} &= \frac{\pi}{2x_3^4(1-x_3^2)^3} \left[3(1-x_3^2)^3 \ln\left(\frac{1-x_3}{1+x_3}\right) + 26x_3^5 - 16x_3^3 + 6x_3 \right]. \end{aligned}$$

Since $0 < x_3 < 1$, we can use classical Taylor series expansions [13, Eq. 4.6.5 and 4.6.7]:

$$\begin{aligned} \ln\left(\frac{1+x_3}{1-x_3}\right) &= 2x_3 + \frac{2}{3}x_3^3 + 2 \sum_{n=2}^{\infty} \frac{x_3^{2n+1}}{2n+1}, \\ &= \frac{2x_3}{1-x_3^2} - \frac{4}{3}x_3^3 - \sum_{n=2}^{\infty} \frac{4n}{2n+1} x_3^{2n+1}. \end{aligned}$$

Hence:

$$2x_3 + \frac{2}{3}x_3^3 \leq \ln\left(\frac{1+x_3}{1-x_3}\right) \leq \frac{2x_3}{1-x_3^2} - \frac{4}{3}x_3^3. \quad (\text{I.44})$$

Using Equation (I.44), we get:

$$\begin{aligned} \frac{dM_{1,1}(x, x)}{dx_3} &\geq \frac{\pi}{4x_3^4(1-x_3^2)^3} \left[3(1-x_3^2)^3 \left(2x_3 + \frac{2}{3}x_3^3 \right) + 6x_3^5 + 16x_3^3 - 6x_3 \right] \\ &\geq \frac{\pi x_3}{2(1-x_3^2)^3} (9 - x_3^4) \\ &> 0, \\ \frac{dM_{3,3}(x, x)}{dx_3} &\geq \frac{\pi}{2x_3^4(1-x_3^2)^3} \left[3(1-x_3^2)^3 \left(-\frac{2x_3}{1-x_3^2} + \frac{4}{3}x_3^3 \right) + 26x_3^5 - 16x_3^3 + 6x_3 \right] \\ &\geq \frac{2\pi x_3}{(1-x_3^2)^3} (2 + 3x_3^2 - x_3^4) \\ &> 0. \end{aligned}$$

So, for $x_3 \neq 0$, all the diagonal coefficients of $\frac{dM^{-1}(x, x)}{dx_3}$ are negative and $\frac{dM^{-1}(x, x)}{dx_3}$ is then negative definite. Thus, if $x_3 \neq 0$, x is a critical point of $I_{\mathbb{S}}$ if and only if $p_0 = 0_{\mathbb{R}^3}$. If $p_0 \neq 0_{\mathbb{R}^3}$, the only critical point of $I_{\mathbb{S}}$ is $x_3 = 0$ which means $x = 0_{\mathbb{R}^3} = x_0$. Hence, we have shown Proposition I.2.3. □

I.3 A charge localization electrical inverse problem

In this section, we study the critical points of the criterion $j_{\partial\Omega}$ given by Equation (I.7) for two different geometries, $\partial\Omega$ being a horizontal plane and the unit sphere. It can be noted that these cases are not restrictive as using rotations and homotheties the results can be extended to any plane and sphere.

I.3.1 Main results

A preliminary result is given by Proposition I.3.1 for general geometric situations.

Proposition I.3.1. *For each $(x_0, q_0) \in \Omega \times \mathbb{R}$ with $q_0 \neq 0$, the criterion $j_{\partial\Omega}$ admits a unique global minimizer $(x^*, q^*) \in \Omega \times \mathbb{R}$. It coincides with the original source: $x^* = x_0$ and $q^* = q_0$.*

If $q_0 = 0$, the minimizers of $j_{\partial\Omega}$ are all the $(x, 0)$ with $x \in \Omega$.

Proof. As $j_{\partial\Omega}$ is non-negative and $j_{\partial\Omega}(x_0, q_0) = 0$, $j_{\partial\Omega}$ admits 0 as a global minimum. Let $(x^*, q^*) \in \Omega \times \mathbb{R}$ be a global minimizer of $j_{\partial\Omega}$, we have $j_{\partial\Omega}(x^*, q^*) = 0$. Let us define on Ω^c the difference:

$$\forall z \in \Omega^c, h(z) = q^* \frac{x^* - z}{|x^* - z|^3} - q_0 \frac{x_0 - z}{|x_0 - z|^3},$$

such that:

$$\int_{\partial\Omega} |h|^2 d\sigma = j_{\partial\Omega}(x^*, q^*) = 0. \quad (\text{I.45})$$

Clearly, h is a continuous bounded function on Ω^c , is harmonic in $\Omega^c \setminus \partial\Omega$ and, if Ω^c is unbounded:

$$h(z) \xrightarrow{|z| \rightarrow \infty} 0_{\mathbb{R}^3}.$$

The function h is equal to $0_{\mathbb{R}^3}$ on $\partial\Omega$ according to the strict positivity of the integral (I.45). Therefore the function h is equal to $0_{\mathbb{R}^3}$ on Ω^c according to the uniqueness result [12, Vol. 1, Chap. II, Par. 4, Prop. 1 and 9]. Hence, we have:

$$\forall z \in \Omega^c, Q(z) = q^{*2} |x^* - z|^2 |x_0 - z|^6 - q_0^2 |x_0 - z|^2 |x^* - z|^6 = 0.$$

As Q is a polynomial of the variables (z_1, z_2, z_3) that is null on Ω^c which contains a non-empty open set in \mathbb{R}^3 , it is null in \mathbb{R}^3 . However, as $|z|$ goes to infinity, we have the following asymptotic expansion for Q :

$$\frac{Q(z)}{|z|^6} \underset{|z| \rightarrow \infty}{=} (q^{*2} - q_0^2) |z|^2 + 2 [q^{*2}(x^* \cdot z) - q_0^2(x_0 \cdot z) + 3q^{*2}(x_0 \cdot z) - 3q_0^2(x^* \cdot z)] + O(1).$$

By identifying the first coefficient with 0 we see that $q^* = \pm q_0$. Then if $q_0 \neq 0$, by identifying the second term with 0, we find that $x^* = x_0$. Furthermore, because h is null on $\partial\Omega$, we have $q^* = q_0$. Hence, if $q_0 \neq 0$, there is a unique global minimizer to $j_{\partial\Omega}$: $(x^*, q^*) = (x_0, q_0)$. If $q_0 = 0$, then for all $x \in \Omega$, $(x, 0)$ is a global minimizer of $j_{\partial\Omega}$. \square

The uniqueness of the critical point is given by Theorems I.3.2 and I.3.3 for two different geometries, the half-space case presented on Figure I.3 and the spherical case presented on Figure I.4.

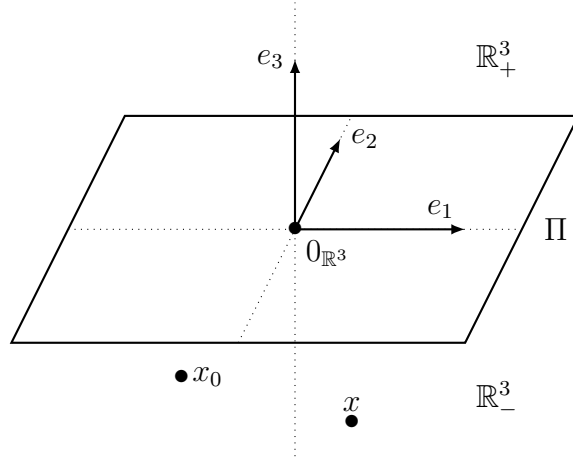


Figure I.3: Schematic geometry in the half-space case.

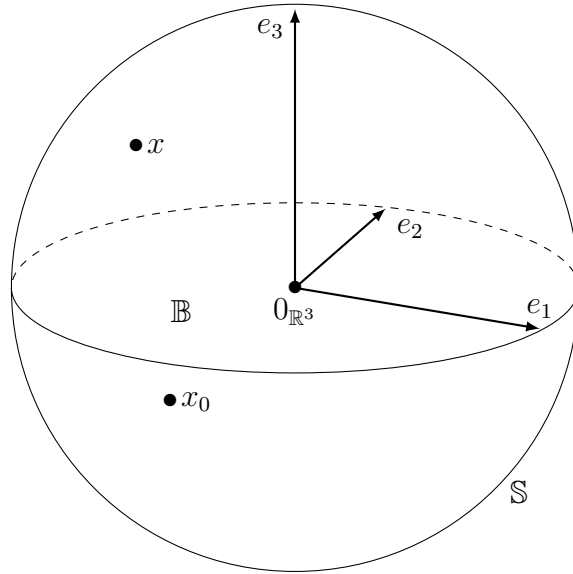


Figure I.4: Schematic geometry in the spherical case.

Theorem I.3.2. For each $(x_0, q_0) \in \mathbb{R}_-^3 \times \mathbb{R}$ with $q_0 \neq 0$, the criterion j_Π admits a unique critical point $(x_c, q_c) \in \mathbb{R}_-^3 \times \mathbb{R}$ such that $\nabla_x j_\Pi(x_c, q_c) = 0_{\mathbb{R}^3}$ and $\frac{\partial}{\partial q} j_\Pi(x_c, q_c) = 0$. It coincides with the global minimizer: $x_c = x_0$ and $q_c = q_0$.

If $q_0 = 0$, the critical points are all the $(x, 0)$ with $x \in \mathbb{R}_-^3$.

Section I.3.2 is devoted to the proof of Theorem I.3.2.

Theorem I.3.3. For each $(x_0, q_0) \in \mathbb{B} \times \mathbb{R}$ with $q_0 \neq 0$, the criterion j_S admits a unique critical point $(x_c, q_c) \in \mathbb{B} \times \mathbb{R}$ such that $\nabla_x j_S(x_c, q_c) = 0_{\mathbb{R}^3}$ and $\frac{\partial}{\partial q} j_S(x_c, q_c) = 0$. It coincides with the global minimizer: $x_c = x_0$ and $q_c = q_0$.

If $q_0 = 0$, the critical points are all the $(x, 0)$ with $x \in \mathbb{B}$.

Section I.3.3 is devoted to the proof of Theorem I.3.3.

Remark 4. Proposition I.3.1 and Theorems I.3.2 and I.3.3 remain true for any dimension $n \geq 3$ as the proofs done in Sections I.3.1, I.3.2 and I.3.3 can be extended to any dimension with minimal changes.

I.3.2 Planar case (Proof of Theorem I.3.2)

Let us fix $x_0 \in \mathbb{R}_-^3$ and $q_0 \in \mathbb{R}$. We want to compute the critical points of the criterion:

$$j_{\Pi} : \mathbb{R}_-^3 \times \mathbb{R} \longrightarrow \mathbb{R}_+$$

$$(x, q) \longmapsto \int_{\Pi} \left| q \frac{x-z}{|x-z|^3} - q_0 \frac{x_0-z}{|x_0-z|^3} \right|^2 d\sigma(z), \quad (\text{I.46})$$

where σ is now the Lebesgue measure on Π : $d\sigma(z) = dz_1 dz_2$ with $z = (z_1, z_2, 0) \in \Pi$. By expanding the square in Equation (I.46), we have for all $x \in \mathbb{R}_-^3$ and $q \in \mathbb{R}$:

$$j_{\Pi}(x, q) = q^2 a_{\Pi}(x, x) + q_0^2 a_{\Pi}(x_0, x_0) - 2qq_0 a_{\Pi}(x, x_0),$$

where:

$$a_{\Pi}(x, x_0) = \int_{\Pi} \frac{x-z}{|x-z|^3} \cdot \frac{x_0-z}{|x_0-z|^3} d\sigma(z).$$

Let us compute $a_{\Pi}(x, x_0)$ as in (I.21) using Clifford analytic calculus presented in Appendix A:

$$\begin{aligned} a_{\Pi}(x, x_0) &= \int_{\Pi} \frac{x_0-z}{|x_0-z|^3} \cdot \frac{x-z}{|x-z|^3} d\sigma(z) \\ &= -\text{Re} \left(\int_{\Pi} \frac{x_0-z}{|x_0-z|^3} \odot \frac{x-z}{|x-z|^3} d\sigma(z) \right) \\ &= -\text{Re} \left(\int_{\Pi} \frac{x_0-z}{|x_0-z|^3} \odot e_3 \odot \frac{x^+-z}{|x^+-z|^3} d\sigma(z) \odot e_3 \right) \\ &= -4\pi \text{Re} \left(\frac{x^+ - x_0}{|x^+ - x_0|^3} \odot e_3 \right) \\ &= -4\pi \frac{x_3 + x_{03}}{|x^+ - x_0|^3}, \end{aligned} \quad (\text{I.47})$$

because $z \mapsto \frac{x^+-z}{|x^+-z|^3}$ is left Clifford analytic in \mathbb{R}_-^3 since $x^+ \in \mathbb{R}_+^3$. Hence, for all $x \in \mathbb{R}_-^3$:

$$j_{\Pi}(x, q) = q^2 \frac{\pi}{x_3^2} + q_0^2 \frac{\pi}{x_{03}^2} + 8\pi q q_0 \frac{x_3 + x_{03}}{|x^+ - x_0|^3}.$$

One can see that if $q_0 = 0$, $(x, 0)$ are the critical points of j_{Π} for all $x \in \mathbb{R}_-^3$. Similarly, if $(x_c, 0)$ for $x_c \in \mathbb{R}_-^3$ is a critical point of j_{Π} then $q_0 = 0$. In the following, we will assume that $q_0 \neq 0$ and $q_c \neq 0$. Simple computations show that:

$$\begin{aligned} \frac{\partial}{\partial x_1} j_{\Pi}(x, q) &= -qq_0 \frac{24\pi(x_3 + x_{03})(x_1 - x_{01})}{|x^+ - x_0|^5}, \\ \frac{\partial}{\partial x_2} j_{\Pi}(x, q) &= -qq_0 \frac{24\pi(x_3 + x_{03})(x_2 - x_{02})}{|x^+ - x_0|^5}. \end{aligned}$$

Hence, $(x_c, q_c) \in \mathbb{R}_-^3 \times \mathbb{R}$ is a critical point of j_{Π} only if $x_{c1} = x_{01}$ and $x_{c2} = x_{02}$. Furthermore:

$$\frac{\partial}{\partial x_3} j_{\Pi} \left(\begin{pmatrix} x_{01} \\ x_{02} \\ x_3 \end{pmatrix}, q \right) = -2\pi \left(\frac{q^2}{x_3^3} - \frac{8qq_0}{(x_3 + x_{03})^3} \right), \quad (\text{I.48})$$

$$\frac{\partial}{\partial q} j_{\Pi} \left(\begin{pmatrix} x_{01} \\ x_{02} \\ x_3 \end{pmatrix}, q \right) = 2\pi \left(\frac{q}{x_3^2} - \frac{4q_0}{(x_3 + x_{03})^2} \right). \quad (\text{I.49})$$

Let $(x_c, q_c) \in \mathbb{R}_-^3 \times \mathbb{R}$ be critical point of j_Π . The cancellation of Equations (I.48) and (I.49) leads to:

$$\frac{q_c}{x_{c3}^3} = \frac{8q_0}{(x_{c3} + x_{03})^3}, \quad (\text{I.50})$$

$$\frac{q_c}{x_{c3}^2} = \frac{4q_0}{(x_{c3} + x_{03})^2}. \quad (\text{I.51})$$

Therefore, by dividing Equation (I.51) by Equation (I.50) and after simplification we get $x_{c3} = x_{03}$. Then, using Equation (I.50), we immediately obtain $q_c = q_0$. This shows that $(x_c, q_c) = (x_0, q_0)$ is the unique critical point of j_Π . Hence, we have shown Theorem I.3.2. \square

Remark 5. We could have shown the same result when only considering the vertical component of the field for the criterion (I.7) with minimal changes.

I.3.3 Spherical case (Proof of Theorem I.3.3)

Let $\mathbb{B} \subset \mathbb{R}^3$ be the open ball of center $0_{\mathbb{R}^3}$ and radius 1 and \mathbb{S} its boundary. Let us fix $x_0 \in \mathbb{B}$ and $q_0 \in \mathbb{R}$. We want to compute the critical points of the criterion:

$$j_{\mathbb{S}} : \mathbb{B} \times \mathbb{R} \longrightarrow \mathbb{R}_+$$

$$(x, q) \longmapsto \int_{\mathbb{S}} \left| q \frac{x-z}{|x-z|^3} - q_0 \frac{x_0-z}{|x_0-z|^3} \right|^2 d\sigma(z), \quad (\text{I.52})$$

where σ is now the Lebesgue measure on \mathbb{S} .

By expanding the square in Equation (I.52), we have for all $x \in \mathbb{B}$ and $q \in \mathbb{R}$:

$$j_{\mathbb{S}}(x, q) = q^2 a_{\mathbb{S}}(x, x) + q_0^2 a_{\mathbb{S}}(x_0, x_0) - 2qq_0 a_{\mathbb{S}}(x, x_0),$$

where:

$$a_{\mathbb{S}}(x, x_0) = \int_{\mathbb{S}} \frac{x-z}{|x-z|^3} \cdot \frac{x_0-z}{|x_0-z|^3} d\sigma(z).$$

Let us compute $a_{\mathbb{S}}(x, x_0)$:

$$\begin{aligned} a_{\mathbb{S}}(x, x_0) &= \int_{\mathbb{S}} \frac{x_0-z}{|x_0-z|^3} \cdot \frac{x-z}{|x-z|^3} d\sigma(z) \\ &= -\text{Re} \left(\int_{\mathbb{S}} \frac{x_0-z}{|x_0-z|^3} \odot \frac{x-z}{|x-z|^3} d\sigma(z) \right) \\ &= \text{Re} \left(\int_{\mathbb{S}} \frac{x_0-z}{|x_0-z|^3} \odot z \odot z \odot \frac{x-z}{|x-z|^3} d\sigma(z) \right) \\ &= \text{Re} \left(\int_{\mathbb{S}} \frac{x_0-z}{|x_0-z|^3} \odot z \odot \frac{z}{|z|^3} \odot \frac{x - \frac{z}{|z|^2}}{\left| x - \frac{z}{|z|^2} \right|^3} d\sigma(z) \right) \\ &= 4\pi \text{Re} \left(\frac{x_0}{|x_0|^3} \odot \frac{x - \frac{x_0}{|x_0|^2}}{\left| x - \frac{x_0}{|x_0|^2} \right|^3} \right) \\ &= 4\pi \frac{1 - x \cdot x_0}{\left| |x|x_0 - \frac{x}{|x|} \right|^3}, \end{aligned} \quad (\text{I.53})$$

because $z \mapsto \frac{z}{|z|^3} \odot \frac{x - \frac{z}{|z|^2}}{\left|x - \frac{z}{|z|^2}\right|^3}$ is left Clifford analytic in \mathbb{B} using [14, Prop. 3.1]. Hence, for all $x \in \mathbb{B}$:

$$j_{\mathbb{S}}(x, q) = q^2 \frac{4\pi}{(1 - |x|^2)^2} + q_0^2 \frac{4\pi}{(1 - |x_0|^2)^2} - 8\pi q q_0 \frac{1 - x \cdot x_0}{\left|x|x_0 - \frac{x}{|x}|\right|^3}.$$

Considering the symmetry under rotation of the problem, we can choose x_0 to be of the form $x_0 = (0, 0, x_{03})^T$ with $x_{03} \geq 0$. We then get:

$$j_{\mathbb{S}}(x, q) = q^2 \frac{4\pi}{(1 - |x|^2)^2} + q_0^2 \frac{4\pi}{(1 - x_{03}^2)^2} - 8\pi q q_0 \frac{1 - x_3 x_{03}}{[1 + |x|^2 x_{03}^2 - 2x_3 x_{03}]^{3/2}}.$$

One can see that if $q_0 = 0$, for all $x \in \mathbb{B}$, $(x, 0)$ are the critical points of $j_{\mathbb{S}}$. Similarly, if $(x_c, 0)$ for $x_c \in \mathbb{B}$ is a critical point of $j_{\mathbb{S}}$ then $q_0 = 0$. In the following, we will assume that $q_0 \neq 0$ and $q_c \neq 0$. Thus, for $i \in \{1, 2\}$:

$$\frac{\partial}{\partial x_i} j_{\mathbb{S}}(x, q) = 8\pi \left[\frac{2q^2}{(1 - |x|^2)^3} + 3 \frac{q q_0 (1 - x_3 x_{03}) x_{03}}{[1 + |x|^2 x_{03}^2 - 2x_3 x_{03}]^{5/2}} \right] x_i, \quad (\text{I.54})$$

$$\frac{\partial}{\partial q} j_{\mathbb{S}}(x, q) = 8\pi \left[\frac{q}{(1 - |x|^2)^2} - \frac{q_0 (1 - x_3 x_{03})}{[1 + |x|^2 x_{03}^2 - 2x_3 x_{03}]^{3/2}} \right]. \quad (\text{I.55})$$

Let $(x_c, q_c) \in \mathbb{B} \times \mathbb{R}$ be a critical point of $j_{\mathbb{S}}$. Because of Equation (I.55), $q_c q_0 \geq 0$. Hence, as the term between the brackets in Equation (I.54) is positive, we get $x_{c1} = x_{01} = 0$ and $x_{c2} = x_{02} = 0$. Then, computing the remaining derivatives leads to:

$$\begin{aligned} \frac{\partial}{\partial x_3} j_{\mathbb{S}} \left(\begin{pmatrix} 0 \\ 0 \\ x_3 \end{pmatrix}, q \right) &= 16\pi \left[\frac{q^2 x_3}{(1 - x_3^2)^3} - \frac{q q_0 x_{03}}{(1 - x_3 x_{03})^3} \right], \\ \frac{\partial}{\partial q} j_{\mathbb{S}} \left(\begin{pmatrix} 0 \\ 0 \\ x_3 \end{pmatrix}, q \right) &= 8\pi \left[\frac{q}{(1 - x_3^2)^2} - \frac{q_0}{(1 - x_3 x_{03})^2} \right]. \end{aligned}$$

Therefore, doing the same operations as in the proof of Theorem I.3.2, we find that $(x_c, q_c) \in \mathbb{B} \times \mathbb{R}$ is a critical point of $j_{\mathbb{S}}$ only if $x_{c3} = x_{03}$ and $q_c = q_0$. This shows that $(x_c, q_c) = (x_0, q_0)$ is the unique critical point of $j_{\mathbb{S}}$. Hence, we have shown Theorem I.3.3. \square

I.4 A dipole localization magnetic inverse problem

I.4.1 Main result

In this part, we only consider the planar case ($\partial\Omega = \Pi$) with the moment p_0 being horizontal ($p_0 \in \Pi$). For this case, we present Theorem I.4.1 which describes the critical points of the criterion (I.9).

Theorem I.4.1. *For each $(x_0, p_0) \in \mathbb{R}_-^3 \times \Pi$ with $p_0 \neq 0_{\mathbb{R}^3}$, the criterion \tilde{J}_Π admits three isolated critical points x_{c0} , x_{c3} and x_{c4} together with two half-lines d_{c1} and d_{c2} of critical points:*

$$\begin{aligned} x_{c0} &= x_0, & p_{c0} &= p_0, \\ d_{c1} &= \{x_0 + r_1(t + x_{03})u_\theta(\theta_0) + tu_z, t \in]-\infty, 0[\}, & p_{c1} &= 0_{\mathbb{R}^3}, \\ d_{c2} &= \{x_0 - r_1(t + x_{03})u_\theta(\theta_0) + tu_z, t \in]-\infty, 0[\}, & p_{c2} &= 0_{\mathbb{R}^3}, \\ x_{c3} &= x_0 + r_2(2x_{03})u_\theta(\theta_0), & p_{c3} &= \tilde{\mu}(x_{03})p_0, \\ x_{c4} &= x_0 - r_2(2x_{03})u_\theta(\theta_0), & p_{c4} &= \tilde{\mu}(x_{03})p_0. \end{aligned}$$

where:

$$\begin{aligned} \theta_0 &= -\arctan(p_{01}/p_{02}), \\ u_\theta(\theta_0) &= (\sin(\theta_0), -\cos(\theta_0), 0)^T, \\ u_z &= (0, 0, 1)^T, \\ r_1(x_{a3}) &= |x_{a3}| \sqrt{3 - 2\sqrt{3}} \neq 0, \\ r_2(x_{a3}) &= |x_{a3}| \sqrt{\frac{1}{12} \left(61 + \left(286417 - 2592\sqrt{202} \right)^{1/3} + \left(286417 + 2592\sqrt{202} \right)^{1/3} \right)} \neq 0, \\ \tilde{\mu}(x_{03}) &= \frac{-8x_{03}^2 \left(6r_2^2(2x_{03})x_{03} + (r_2^2(2x_{03}) + (2x_{03})^2)^{3/2} + 8x_{03}^2 \right)}{3r_2^2(2x_{03}) (r_2^2(2x_{03}) + (2x_{03})^2)^{3/2}} \neq 0. \end{aligned}$$

If $p_0 = 0_{\mathbb{R}^3}$, the critical points are all the $(x, 0_{\mathbb{R}^3})$ with $x \in \mathbb{R}_-^3$.

The sequel of this section is dedicated to the proof of Theorem I.4.1.

I.4.2 Proof of Theorem I.4.1

As in Section I.2.2.a, by expanding the square in Equation (I.9), we have for all $(x, p) \in \Omega \times \mathbb{R}^3$:

$$\tilde{J}_{\partial\Omega}(x, p) = p^T \tilde{M}_{\partial\Omega}(x, x)p + p_0^T \tilde{M}_{\partial\Omega}(x_0, x_0)p_0 - 2p_0^T \tilde{M}_{\partial\Omega}(x, x_0)p, \quad (\text{I.56})$$

where the 3×3 matrix $\tilde{M}_{\partial\Omega}(x, x_0)$ is given by:

$$\tilde{M}_{\partial\Omega}(x, x_0) = \text{tr}(M_{\partial\Omega}(x, x_0)) I_d - M_{\partial\Omega}^T(x, x_0). \quad (\text{I.57})$$

where the matrix I_d is the 3×3 identity matrix and the matrix $M_{\partial\Omega}(x, x_0)$ is defined as in (I.14).

Due to the similarity in the structure between $\tilde{J}_{\partial\Omega}$ and $J_{\partial\Omega}$, we see that the computations done in Section I.2.2 are valid for this criterion by replacing J , $p(\cdot)$, I , M and K by their magnetic counterpart \tilde{J} , $\tilde{p}(\cdot)$, \tilde{I} , \tilde{M} and \tilde{K} in Equations (I.15) and (I.18) to get:

$$\begin{aligned} \tilde{I}_{\partial\Omega} : \Omega &\longrightarrow \mathbb{R}_+ \\ x &\longmapsto p_0^T \tilde{K}(x, x_0)p_0 - p_0^T \tilde{M}(x_0, x_0)p_0. \end{aligned} \quad (\text{I.58})$$

Here, we study the planar case ($\Omega = \mathbb{R}_-^3$) for which the matrix $M_\Pi(x, x_0)$ is given by Equations (I.23) to (I.27) hence $\tilde{M}_\Pi(x, x_0)$ is also known. Let $p_0 = (p_{01}, p_{02}, 0) \in \Pi$ and $\theta_0 = -\arctan(p_{01}/p_{02})$. First, as in Section I.2.2.a, if $p_0 = 0_{\mathbb{R}^3}$, then for all $x \in \mathbb{R}_-^3$, $\tilde{p}(x) = 0_{\mathbb{R}^3}$ and $(x, 0_{\mathbb{R}^3})$ is a critical point of \tilde{J} hence we assume in what follows that $p_0 \neq 0_{\mathbb{R}^3}$.

In the following of the proof, we first use homogeneity of the problem in order to reduce the search of critical points to two possibilities in Section I.4.2.a. Then, in Section I.4.2.b we consider the tangential derivative of the criterion in order to describe three possibilities and we use the radial derivative to characterize them. Finally, by combining these possibilities, we find potential critical points which are the critical points given in Theorem I.4.1 and finally check their criticality property in Section I.4.2.c.

I.4.2.a First step: use of homogeneity

Because of Equation (I.57), the homogeneity properties of the problem are similar to those of the electric potential presented in Section I.2.3.b hence we get an Euler relation similar to equation (I.28):

$$-x_3 x_{a1} \frac{\partial \tilde{K}}{\partial x_1} - x_3 x_{a2} \frac{\partial \tilde{K}}{\partial x_2} + x_3 x_{a3} \frac{\partial \tilde{K}}{\partial x_3} = 2(x_{03} - x_3) \tilde{K}. \quad (\text{I.59})$$

Hence, using the same argument as in Section I.2.3.b, $x \in \mathbb{R}_-^3$ is a critical point of \tilde{I}_Π only if $x_3 = x_{03}$ or $\det(\tilde{M}(x, x_0)) = 0$. For the second case, we see that:

$$r^4 \det(\tilde{M}(x, x_0)) = \frac{-16\pi^3 |x_{a3}|^7}{|x_a|^9} (v-1)^2 (v+2) (v^2 - 2v - 2),$$

where $r = \sqrt{x_{a1}^2 + x_{a2}^2}$ and $v = \sqrt{1 + \left(\frac{r}{x_{a3}}\right)^2} \geq 1$. Hence, $\det(\tilde{M}(x, x_0)) \neq 0$ except for $v = 1 + \sqrt{3}$ thus $r = r_1(x_{a3}) \stackrel{\text{def}}{=} |x_{a3}| \sqrt{3 - 2\sqrt{3}}$. Hence, $x \in \mathbb{R}_-^3$ is a critical point of \tilde{I}_Π only if one of the two following conditions is fulfilled;

$$x_3 = x_{03} \quad (\text{I.60})$$

$$r = r_1(x_{a3}). \quad (\text{I.61})$$

I.4.2.b Second step: derivatives in the plane

Let $x \in \mathbb{R}_-^3$. Let us use polar coordinates in the plane: $x_{a1} = r \cos(\theta)$ and $x_{a2} = r \sin(\theta)$ with $r \geq 0$ and $\theta \in [0, 2\pi[$. Let \tilde{K}_r be the matrix:

$$\tilde{K}_r = \tilde{K}_r(x, x_0) = -\frac{\partial}{\partial r} \tilde{K} \left(\left(\begin{array}{c} x_{01} - r \cos(\theta) \\ x_{02} - r \sin(\theta) \\ x_3 \end{array} \right), x_0 \right).$$

Similarly, let \tilde{K}_θ be the matrix:

$$\tilde{K}_\theta = \tilde{K}_\theta(x, x_0) = -\frac{\partial}{\partial \theta} \tilde{K} \left(\left(\begin{array}{c} x_{01} - r \cos(\theta) \\ x_{02} - r \sin(\theta) \\ x_3 \end{array} \right), x_0 \right).$$

In what follows, we assume that $r \neq 0$. We can see that:

$$\tilde{K}_\theta = \begin{bmatrix} -\alpha \sin(2\theta) & \alpha \cos(2\theta) & \beta \sin(\theta) \\ \alpha \cos(2\theta) & \alpha \sin(2\theta) & -\beta \cos(\theta) \\ \beta \cos(\theta) & -\beta \cos(\theta) & 0 \end{bmatrix}$$

where:

$$\alpha = \frac{8\pi x_3^2}{r^2 |x_a|^6} (6r^2 x_{a3}^2 + 4x_{a3} |x_a|^3 - r^4 + 4x_{a3}^4),$$

$$\beta = \frac{8\pi x_3^2}{r |x_a|^6} (2|x_a|^3 + 3r^2 x_{a3} + 2x_{a3}^3).$$

Let us use the cylindrical orthonormal bases (u_r, u_θ, u_z) given by:

$$u_r = \begin{pmatrix} \cos(\theta) \\ \sin(\theta) \\ 0 \end{pmatrix}, \quad u_\theta = \begin{pmatrix} \sin(\theta) \\ -\cos(\theta) \\ 0 \end{pmatrix}, \quad u_z = \begin{pmatrix} 0 \\ 0 \\ 1 \end{pmatrix}.$$

One can see that:

$$\begin{aligned} \tilde{K}_\theta u_r &= -\alpha u_\theta, \\ \tilde{K}_\theta u_\theta &= -\alpha u_r + \beta u_z, \\ \tilde{K}_\theta u_z &= \beta u_\theta. \end{aligned} \tag{I.62}$$

Hence, by writing $p_0 \in \Pi$ in this base $p_0 = p_{0r} u_r + p_{0\theta} u_\theta$, we see that:

$$p_0^T \tilde{K}_\theta p_0 = -2\alpha p_{0\theta} p_{0r}.$$

Thus, $x \in \mathbb{R}_-^3$ is a critical point of \tilde{I}_π only if one of the three following properties is satisfied:

$$\alpha = 0, \tag{I.63}$$

$$p_{0\theta} = 0, \tag{I.64}$$

$$p_{0r} = 0. \tag{I.65}$$

Condition (I.63) One can see that:

$$\alpha = -\frac{8\pi x_3^2}{r^2 |x_a|^6} |x_{a3}|^4 (v-1)^2 (v^2 + 6v + 3),$$

where $v = \sqrt{1 + \left(\frac{r}{x_{a3}}\right)^2} \geq 1$. Hence the condition (I.63) is verified only if $v = 1$ hence $r = 0$.

Condition (I.64) Let us assume that we are in configuration (I.64) hence, as $p_0 \neq 0_{\mathbb{R}^3}$, we can assume that $p_0 = u_r$. We can then compute the radial derivative of the criterion and get:

$$u_r^T \tilde{K}_r u_r = \frac{16\pi x_3^2}{3r^2 |x_a|^8} \frac{\mathcal{A}_r^2 - \mathcal{B}_r^2}{\mathcal{A}_r + \mathcal{B}_r} > 0,$$

where we define the positive quantities:

$$\mathcal{A}_r^2 - \mathcal{B}_r^2 = r^6 (100r^{10} + 260r^8 x_{a3}^2 + 649r^6 x_{a3}^4 + 948r^4 x_{a3}^6 + 600r^2 x_{a3}^8 + 132x_{a3}^{10}) > 0,$$

$$\mathcal{A}_r = 26r^2 x_{a3}^6 + 24r^4 x_{a3}^4 + 13r^6 x_{a3}^2 + 10r^8 + 8x_{a3}^8 > 0,$$

$$\mathcal{B}_r = -x_{a3} |x_a|^3 (14r^2 x_{a3}^2 + 8x_{a3}^4) > 0.$$

Thus, we have shown that the condition (I.64) leads to $r = 0$.

Condition (I.65) Finally, let us consider the situation (I.65). Using Equations (I.24), (I.25), (I.27) and (I.57), one can see that as in Section I.2.3.c, the vector u_θ is an eigenvector of $\tilde{M}(x, x_0)$, thus of $\tilde{K}(x, x_0)$ and thus of $\tilde{K}_r(x, x_0)$ with the eigenvalue:

$$\tilde{\lambda}_1 = \frac{32x_3^2\pi|x_{a3}|^8}{3r^5|x_a|^8}(v-1)^3(v^2-2v-2)(2v^3-5v^2-12v-6),$$

where $v = \sqrt{1 + \left(\frac{r}{x_{a3}}\right)^2} \geq 1$. So, we see that $\tilde{\lambda}_1 = 0$ hence $x \in \mathbb{R}_-^3$ cancels the normal derivative, only if one of these conditions is satisfied:

$$r = 0,$$

$$r = r_1(x_{a3}) \stackrel{\text{def}}{=} |x_{a3}| \sqrt{3 - 2\sqrt{3}},$$

$$r = r_2(x_{a3}) \stackrel{\text{def}}{=} |x_{a3}| \sqrt{\frac{1}{12} \left(61 + \left(286417 - 2592\sqrt{202} \right)^{1/3} + \left(286417 + 2592\sqrt{202} \right)^{1/3} \right)}.$$

Furthermore, condition (I.65) implies that $\theta = \theta_0$ or $\theta = \theta_0 + \pi$ as a given vector is tangential to a circle only twice on the plane.

I.4.2.c Reciprocal

Hence, combining all conditions (I.60) to (I.61) and the conclusions of (I.63) to (I.65) leads to the possibility of three isolated critical points and two half-lines:

$$\begin{aligned} x_{c0} &= x_0, \\ d_{c1} &= \{x_0 + r_1(t + x_{03})u_\theta(\theta_0) + tu_z, t \in]-\infty, 0[\}, \\ d_{c2} &= \{x_0 - r_1(t + x_{03})u_\theta(\theta_0) + tu_z, t \in]-\infty, 0[\}, \\ x_{c3} &= x_0 + r_2(2x_{03})u_\theta(\theta_0), \\ x_{c4} &= x_0 - r_2(2x_{03})u_\theta(\theta_0). \end{aligned}$$

These critical points are illustrated on Figure I.5 for $x_{01} = x_{02} = 0$, $x_{03} = -1$ and $p_0 = (0, 1, 0)^T$.

Point x_{c0} Let us study the criticality of x_{c0} . First, we can compute:

$$\tilde{p}(x_{c0}) = \tilde{M}(x_0, x_0)^{-1} \tilde{M}(x_0, x_0)^{-1} p_0 = p_0.$$

Furthermore, (x_0, p_0) is obviously a critical point of the criterion as it is a global minimizer.

Half-lines d_{c1} and d_{c2} Let us study the criticality of points belonging to d_{c1} and d_{c2} . Let $i \in \{1, 2\}$ and x_{ci} a point on d_i . First, we compute the eigenvalue of $\tilde{M}(x, x_0)$ for the vector u_θ and see that:

$$\tilde{\lambda} = \frac{-2\pi|x_{a3}|^3}{r^2|x_a|^3}(v-1)(v^2-2v-2).$$

Thus, $\tilde{\lambda} = 0$ as $r = r_1(x_{a1})$. As p_0 is proportional to u_θ , this shows that:

$$p(x_{ci}) = \tilde{M}(x_{ci}, x_{ci})^{-1} \tilde{M}(x_{ci}, x_0) p_0 = 0_{\mathbb{R}^3}.$$

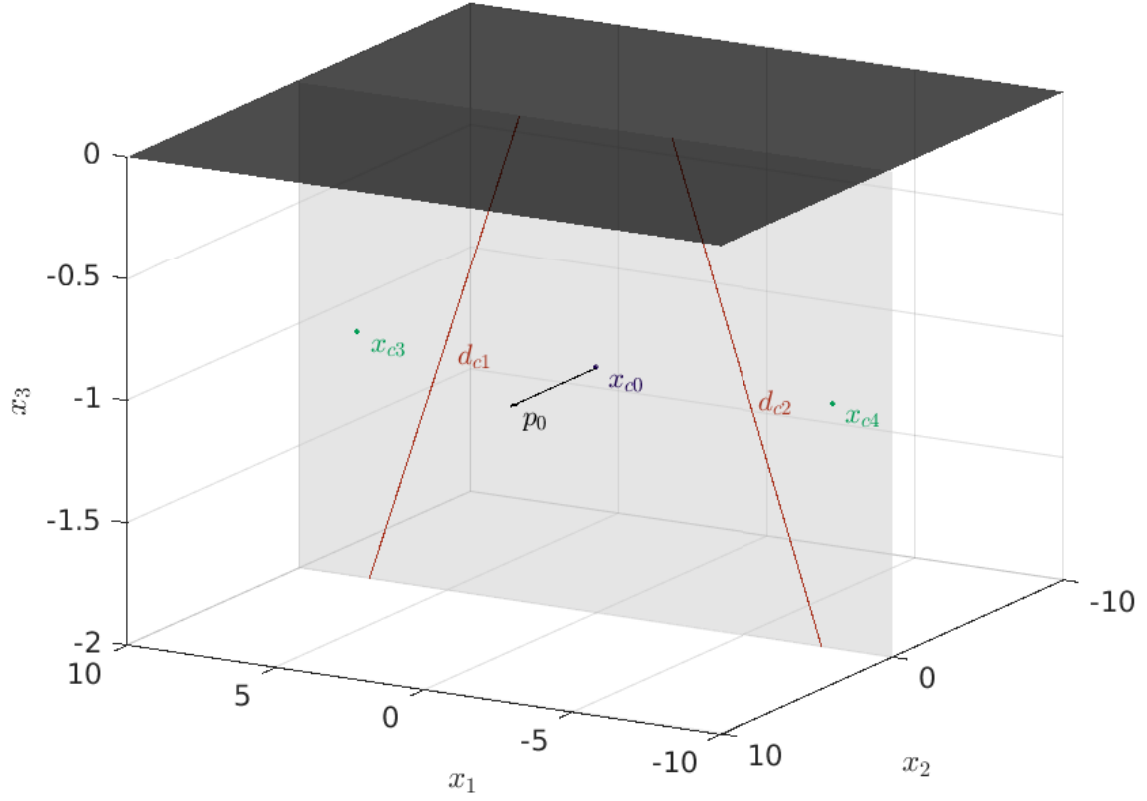


Figure I.5: Locations of the critical points of the criterion (I.9).

Furthermore, by computing the radial and tangential derivatives of \tilde{I} , we find for :

$$\begin{aligned}
\partial_r \tilde{I}(x_{ci}) &= p_0^T \partial_r \tilde{K} p_0 \\
&= p_0^T \partial_r \tilde{M}(x_{ci}, x_0) \tilde{M}(x_{ci}, x_{ci}) \tilde{M}(x_{ci}, x_0)^T p_0 \\
&\quad + p_0^T \tilde{M}(x_{ci}, x_0) \tilde{M}(x_{ci}, x_{ci}) \partial_r \tilde{M}(x_{ci}, x_0)^T p_0 \\
&= 0, \\
\partial_\theta \tilde{I}(x_{ci}) &= p_0^T \partial_\theta \tilde{K} p_0 \\
&= p_0^T \partial_\theta \tilde{M}(x_{ci}, x_0) \tilde{M}(x_{ci}, x_{ci}) \tilde{M}(x_{ci}, x_0)^T p_0 \\
&\quad + p_0^T \tilde{M}(x_{ci}, x_0) \tilde{M}(x_{ci}, x_{ci}) \partial_\theta \tilde{M}(x_{ci}, x_0)^T p_0 \\
&= 0.
\end{aligned} \tag{I.66}$$

Finally, using Euler's Equation (I.59) together with (I.66), we find that:

$$\partial_{x_3} \tilde{I}(x_{ci}) = 0.$$

So, we have shown that any points of the half-lines d_{c1} and d_{c1} are critical points of \tilde{I} . Hence, because of the definition of \tilde{p} , $(x_{c1}, 0_{\mathbb{R}^3})$ and $(x_{c2}, 0_{\mathbb{R}^3})$ are critical points of the criterion (I.9).

Points x_{c3} and x_{c4} Let us study the criticality of x_{c3} and x_{c4} . Let $i \in \{3, 4\}$. First, we have shown when studying the condition (I.65) that x_{ci} cancels the radial derivative $\partial_r \tilde{I}$. Furthermore, using the Euler's equation (I.59), we see that it also cancels the vertical derivative $\partial_{x_3} \tilde{I}$. Finally, as p_0 is proportional to u_θ we can compute:

$$\begin{aligned} \partial_\theta \tilde{I}(x_{ci}) &= |p_0|^2 u_\theta^T \partial_\theta \tilde{K}(x_{ci}, x_0) u_\theta \\ &= 0, \end{aligned}$$

because of (I.62). Hence, we have shown that x_{c3} and x_{c4} are indeed critical points of \tilde{I} . Also, we can see that:

$$\tilde{p}(x_{ci}) = \tilde{\mu}(x_{03}) p_0,$$

where we define:

$$\tilde{\mu}(x_{03}) \stackrel{\text{def}}{=} \frac{-8x_{03}^2 \left(6r_2(2x_{03})^2 x_{03} + (r_2^2(2x_{03}) + (2x_{03})^2)^{3/2} + 8x_{03}^2 \right)}{3r_2(2x_{03})^2 (r_2^2(2x_{03}) + (2x_{03})^2)^{3/2}} \neq 0.$$

Hence, because of the definition of \tilde{p} , $(x_{c3}, \tilde{\mu}(x_{03})p_0)$ and $(x_{c4}, \tilde{\mu}(x_{03})p_0)$ are critical points of the criterion (I.9). □

We shall see on the numerical simulations that x_{c0} is the unique local minimizer, x_{c1} and x_{c2} are local maximizers and x_{c3} and x_{c4} are saddle points of \tilde{I} .

I.5 Numerical illustration

I.5.1 Dipole and charge localization electric inverse problems

For illustration purposes, we define $i_{\partial\Omega}$ in a similar manner as $I_{\partial\Omega}$ in Section I.2.2.b such that for all $x \in \Omega$:

$$i_{\partial\Omega}(x) = j_{\partial\Omega}(x, q(x)), \quad (\text{I.67})$$

where:

$$q(x) \stackrel{\text{def}}{=} q_0 \frac{a_{\partial\Omega}(x, x_0)}{a_{\partial\Omega}(x, x)}. \quad (\text{I.68})$$

I.5.1.a Planar case

To illustrate the uniqueness of the critical point of i_{Π} and I_{Π} , we consider $x_0 = (0, 0, -1)$, $q_0 = 1$ and $p_0 = (1, -5, 0.1)$ and study $i_{\Pi}(x)$ and $I_{\Pi}(x)$ for $x = (x_1, x_2, -1)$ in the same horizontal plane as x_0 with $(x_1, x_2) \in [-4, 4]^2$. The quantities i_{Π} and ∇i_{Π} were computed using their expressions in Equations (I.67) and (I.68) together with Equation (I.47) using a Matlab code. Similarly, the quantities I_{Π} and ∇I_{Π} were computed using their expressions in Section I.2.2.b together with the formulas (I.23), (I.24), (I.25), (I.26) and (I.27) using a Matlab code. Figure I.6 represents the criteria i_{Π} and I_{Π} and their variations on the horizontal square $[-4, 4]^2 \times \{-1\}$ while Figure I.8 illustrates their vertical variation on the segment $\{0\} \times \{0\} \times [-5, 0]$. Figure I.7 shows the squared norms of the gradients of the criteria i_{Π} and I_{Π} on the horizontal square $[-4, 4]^2 \times \{-1\}$. The behaviors of j_{Π} with respect to q and J_{Π} with respect to p are not represented as they are quadratic hence strictly convex.

Figures I.6 and I.8 illustrate the non-convexity of the criteria hence the need of this study for the convergence of optimization schemes. These figures also illustrate the convergence of the criteria i_{Π} and I_{Π} to $\|E_0\|_{L^2(\Pi)}$ and $\|u_0\|_{L^2(\Pi)}$ as $|x| \rightarrow \infty$ or $x_3 \rightarrow 0$ and show that there is a unique global minimizer of i_{Π} and I_{Π} on the plane of height x_{03} and on the vertical line passing through x_0 respectively. Figure I.7 shows the uniqueness of the critical point of i_{Π} and I_{Π} in the plane of height x_{03} . One can see that the main difference between the two studied problems is the symmetry under rotation around the vertical axis of i_{Π} which is absent for I_{Π} as can be seen on Figure I.7.

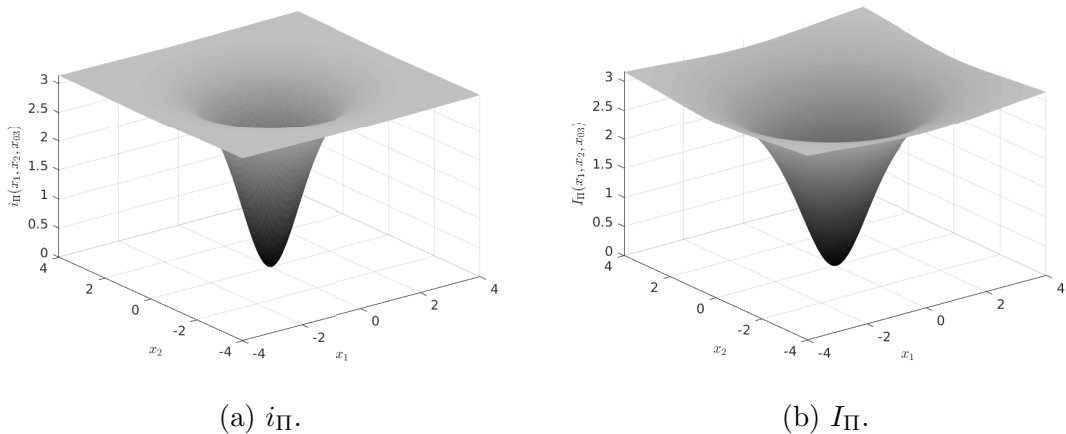
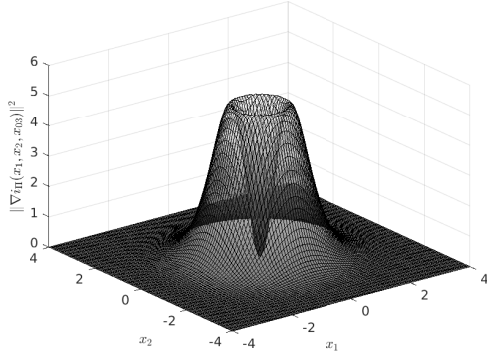
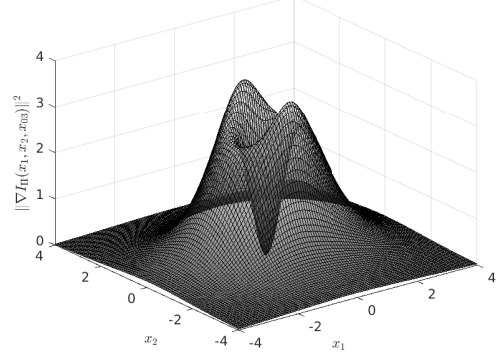


Figure I.6: Criteria on the horizontal square $[-4, 4]^2 \times \{-1\}$.

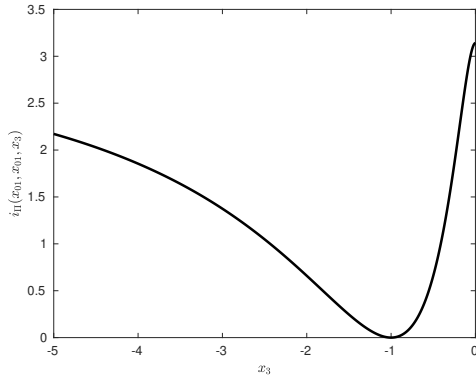


(a) ∇i_{II} .

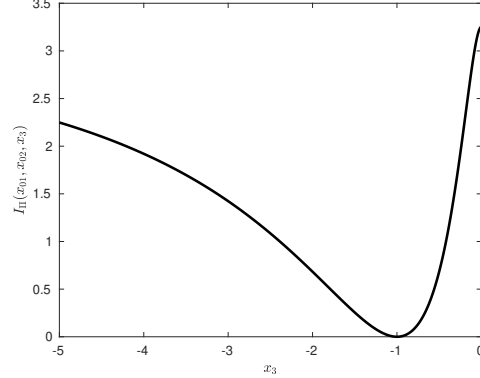


(b) ∇I_{II} .

Figure I.7: Squared norms of the gradients of the criteria on the horizontal square $[-4, 4]^2 \times \{-1\}$.



(a) i_{II} .



(b) I_{II} .

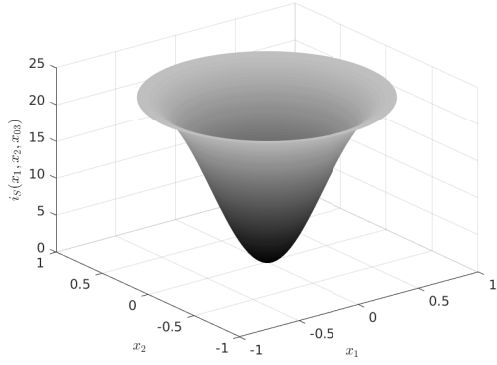
Figure I.8: Criteria on the vertical line $\{0\} \times \{0\} \times [-5, 0]$.

I.5.1.b Spherical case

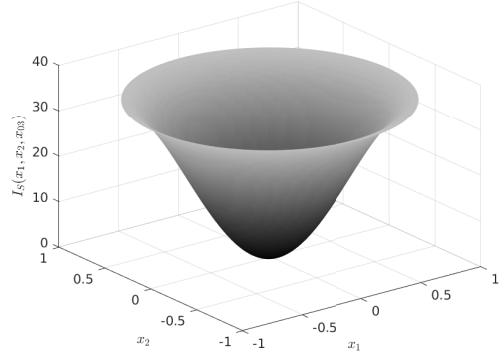
To illustrate the uniqueness of the critical point of $i_{\mathbb{S}}$ and $I_{\mathbb{S}}$, we consider $x_0 = (0, 0, 0.5)$ (for $i_{\mathbb{S}}$) and $x_0 = (0, 0, 0)$ (for $I_{\mathbb{S}}$), $q_0 = 1$ and $p_0 = (1, -5, 0.1)$ and study $i_{\mathbb{S}}(x)$ and $I_{\mathbb{S}}(x)$ for $x = (x_1, x_2, x_{03})$ in the same horizontal plane as x_0 with (x_1, x_2) in the disk $D\left(0, \sqrt{1 - x_{03}^2}\right)$. The quantities $i_{\mathbb{S}}$ and $\nabla i_{\mathbb{S}}$ were computed using their expressions in Equations (I.67) and (I.68) together with Equation (I.53) using a Matlab code. Similarly, the quantities $I_{\mathbb{S}}$ and $\nabla I_{\mathbb{S}}$ were computed using their expressions in Section I.2.4.a using a Matlab code. Figure I.9 represent the criteria $i_{\mathbb{S}}$ and $I_{\mathbb{S}}$ and their variations on the horizontal plane while Figure I.11 illustrates their vertical variation. Figure I.10 shows the squared norms of the gradients of $i_{\mathbb{S}}$ and $I_{\mathbb{S}}$. The behavior of $j_{\mathbb{S}}$ with respect to q and of $J_{\mathbb{S}}$ with respect to p are not represented as they are quadratic hence strictly convex.

Figures I.9 and I.11 illustrate the non-convexity of the criteria hence the need of this study for the convergence of optimization schemes. These figures also illustrate the convergence of the criteria $i_{\mathbb{S}}$ and $I_{\mathbb{S}}$ to $\|E_0\|_{L^2(\mathbb{S})}$ and $\|u_0\|_{L^2(\mathbb{S})}$ as $|x| \rightarrow 1$ and show that there is a unique global minimizer of $i_{\mathbb{S}}$ and $I_{\mathbb{S}}$ on respectively the plane of height x_{03} and the vertical line passing through x_0 . Figure I.10 shows the uniqueness of the critical point

of $i_{\mathbb{S}}$ and $I_{\mathbb{S}}$ in the plane of height x_{03} . One can see that the main difference between the two studied problems in the rotational symmetry around the vertical axis of $i_{\mathbb{S}}$ which is absent for $I_{\mathbb{S}}$ as can be seen on Figure I.10.

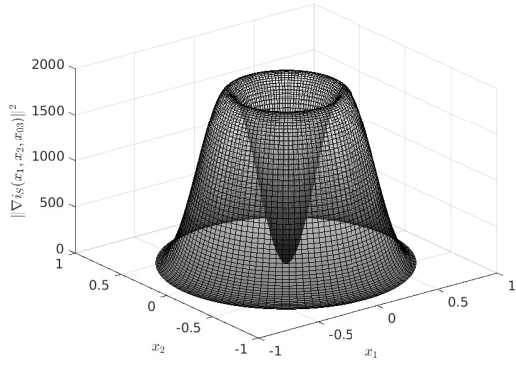


(a) $i_{\mathbb{S}}$ on $D\left(0, \frac{\sqrt{3}}{2}\right) \times \left\{\frac{1}{2}\right\}$.

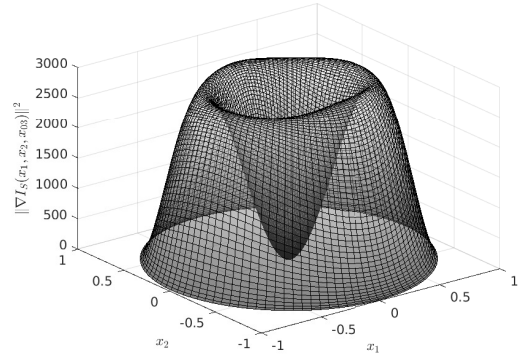


(b) $I_{\mathbb{S}}$ on $D(0, 1) \times \{0\}$.

Figure I.9: Criteria on the horizontal disk containing x_0 .



(a) $\nabla i_{\mathbb{S}}$ on $D\left(0, \frac{\sqrt{3}}{2}\right) \times \left\{\frac{1}{2}\right\}$.



(b) $\nabla I_{\mathbb{S}}$ on $D(0, 1) \times \{0\}$.

Figure I.10: Squared norms of the gradients of the criteria on the horizontal disk containing x_0 .

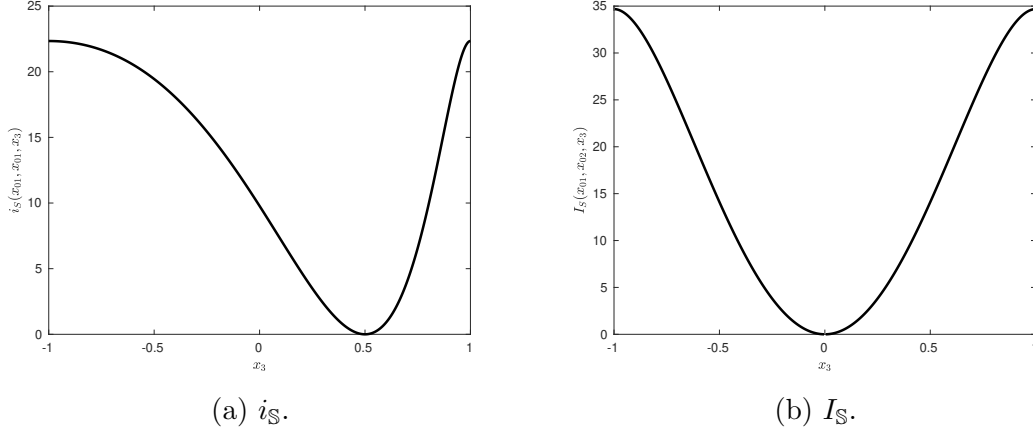


Figure I.11: Criteria on the vertical line $\{0\} \times \{0\} \times [-1, 1]$.

I.5.2 Dipole localization magnetic inverse problem

To illustrate the different critical points \tilde{I}_Π , we consider $x_0 = (0, 0, -1)$, and $p_0 = (0, 1, 0)$ and study the criterion \tilde{I}_Π . On Figure I.12 we plot $\tilde{I}_\Pi(x)$ for $x = (x_1, x_2, -1)$ in the same horizontal plane as x_0 with $(x_1, x_2) \in [-10, 10]^2$. On Figure I.13 and I.14, we plot the criterion \tilde{I}_Π around x_{c3} and x_{c4} . Figure I.13 shows \tilde{I}_Π on the horizontal disk $x_{c3} + (D(0, 1) \times \{0\})$ and on the vertical line $\{x_{c3} + tu_z, t \in [-1, 1]\}$. Figure I.14 shows \tilde{I}_Π on the horizontal disk $x_{c4} + (D(0, 1) \times \{0\})$ and on the vertical line $\{x_{c4}tu_z, t \in [-1, 1]\}$. Finally, to illustrate d_{c1} and d_{c2} , let us first define for $t \in [0, +\infty[$, $x_{c1}(t)$ the intersection of d_{c1} and the horizontal plane of height $x_3 = t$ and $x_{c2}(t)$ the intersection of d_{c2} and the horizontal plane of height $x_3 = t$. We then plot on Figures I.15, I.16 and I.17 the criterion around $x_{c1}(x_{03}/2)$, $x_{c1}(x_{03})$ and $x_{c1}(3x_{03}/2)$ respectively. Figures I.15 shows \tilde{I}_Π on the horizontal disk $x_{c1}(x_{03}/2) + (D(0, 1) \times \{0\})$ and on the vertical line $\{x_{c1}(x_{03}/2) + tu_z, t \in [-3/2, 1/2]\}$. Figures I.16 shows \tilde{I}_Π on the horizontal disk $x_{c1}(x_{03}) + (D(0, 1) \times \{0\})$ and on the vertical line $\{x_{c1}(x_{03}) + tu_z, t \in [-1, 1]\}$. Figures I.17 shows \tilde{I}_Π on the horizontal disk $x_{c1}(3x_{03}/2) + (D(0, 1) \times \{0\})$ and on the vertical line $\{x_{c1}(3x_{03}/2) + tu_z, t \in [-1/2, 3/2]\}$. The quantity \tilde{I}_Π was computed using its expression in Section I.58 together with the formulas (I.57), (I.23), (I.24), (I.25), (I.26) and (I.27) using a Matlab code.

These figures illustrate the criticality property of the different critical points described in Theorem I.4.1. Furthermore, they show that x_{c0} is the global minimum, x_{c3} and x_{c4} are saddle points and points on d_{c1} and d_{c2} are global maxima of the criterion \tilde{I}_Π .

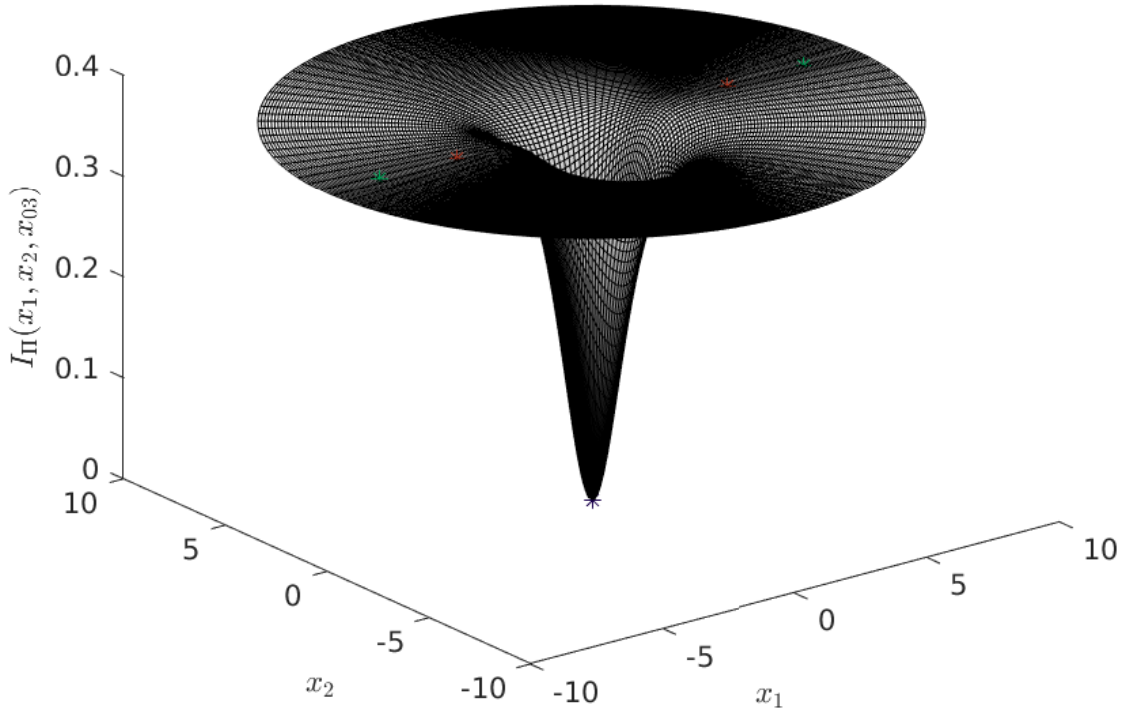
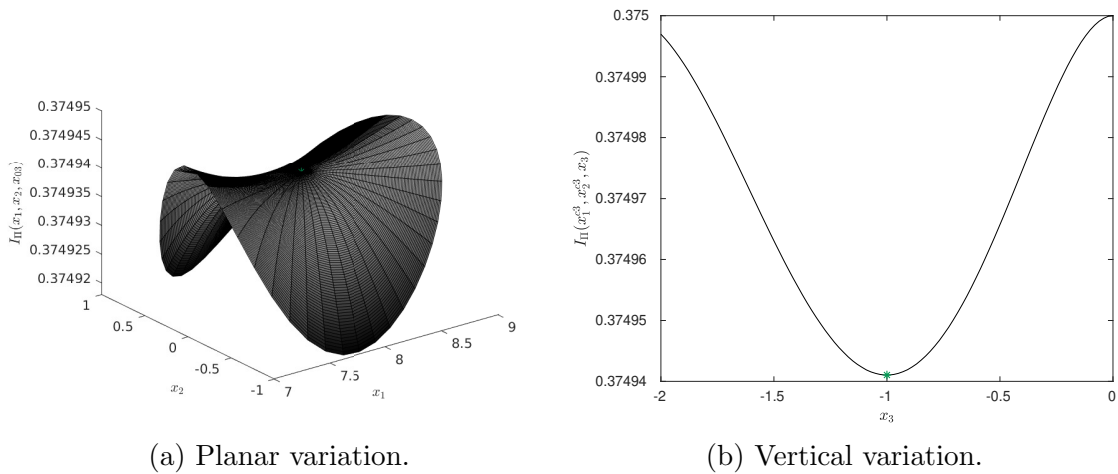


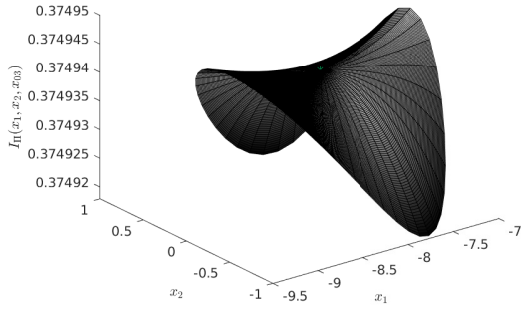
Figure I.12: Criterion \tilde{I}_Π on the horizontal square $[-10, 10]^2 \times \{-1\}$. The stars indicate the locations of the critical points: x_{c0} (blue), $x_{c1}(x_{03})$ and $x_{c2}(x_{03})$ (red) and $x_{c3}(x_{03})$ and $x_{c4}(x_{03})$ (green).



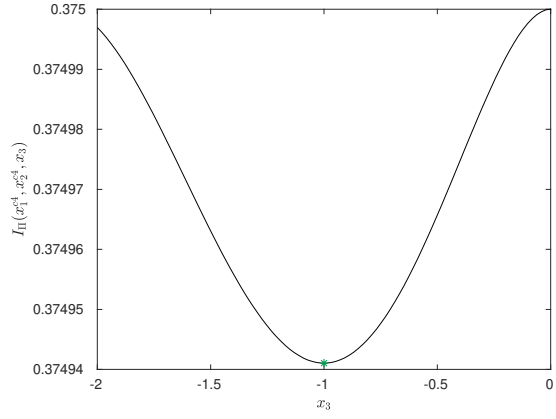
(a) Planar variation.

(b) Vertical variation.

Figure I.13: Criterion \tilde{I}_Π on the horizontal disk $x_{c3} + (D(0, 1) \times \{0\})$ and on the vertical line $\{x_{c3} + tu_z, t \in [-1, 1]\}$.

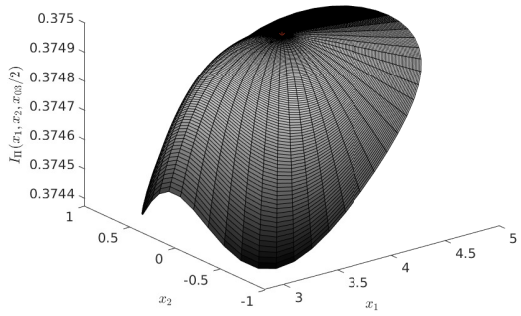


(a) Planar variation.

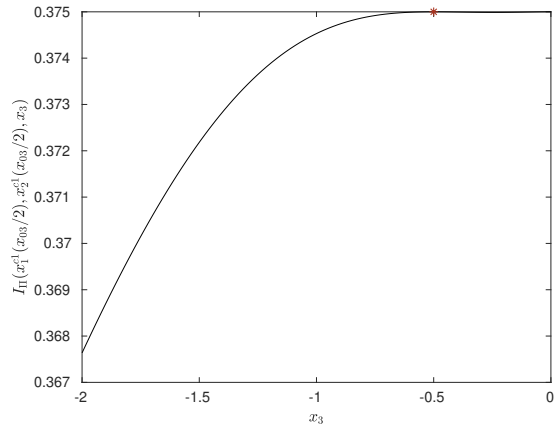


(b) Vertical variation.

Figure I.14: Criterion \tilde{I}_{Π} on the horizontal disk $x_{c4} + (D(0, 1) \times \{0\})$ and on the vertical line $\{x_{c4} + tu_z, t \in [-1, 1]\}$.

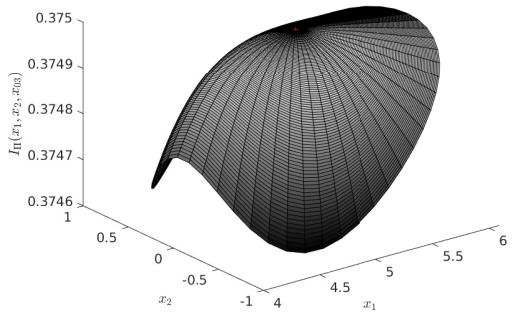


(a) Planar variation.

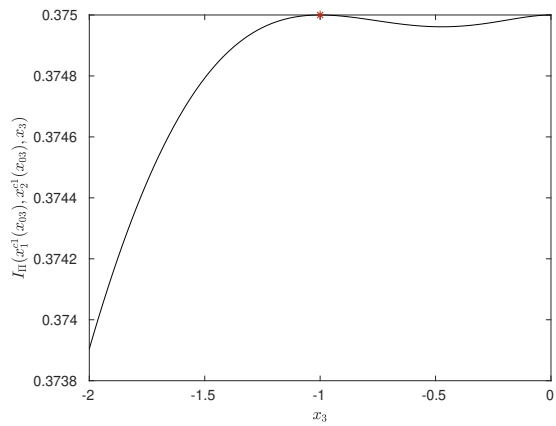


(b) Vertical variation.

Figure I.15: Criterion \tilde{I}_{Π} on the horizontal disk $x_{c1}(x_{03}/2) + (D(0, 1) \times \{0\})$ and on the vertical line $\{x_{c1}(x_{03}/2) + tu_z, t \in [-3/2, 1/2]\}$.

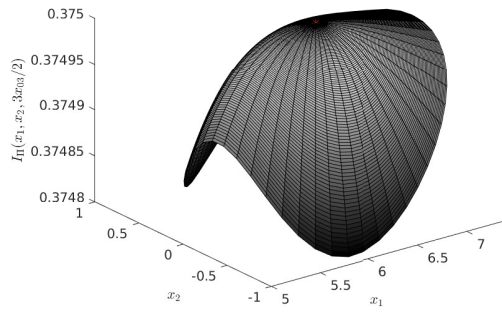


(a) Planar variation.

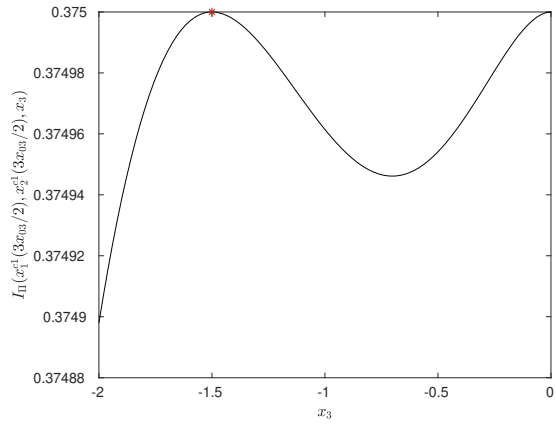


(b) Vertical variation.

Figure I.16: Criterion \tilde{I}_{Π} on the horizontal disk $x_{c1}(x_{03}) + (D(0, 1) \times \{0\})$ and on the vertical line $\{x_{c1}(x_{03}) + tu_z, t \in [-1, 1]\}$.



(a) Planar variation.



(b) Vertical variation.

Figure I.17: Criterion \tilde{I}_{Π} on the horizontal disk $x_{c1}(3x_{03}/2) + (D(0, 1) \times \{0\})$ and on the vertical line $\{x_{c1}(3x_{03}/2) + tu_z, t \in [-1/2, 3/2]\}$.

I.6 Conclusion

In this chapter, for the dipole localization from measurements of the electric potential we proved the uniqueness of the critical point of the least-squares criterion J_{Π} in the Euclidean geometry ($\partial\Omega = \Pi$). We studied the same problem in the spherical setting ($\partial\Omega = \mathbb{S}$). This setting leads to complications in the absence of homogeneity of the functions considered. Yet, we managed to establish the uniqueness in the particular case where $x_0 = 0_{\mathbb{R}^3}$ is at the center of the sphere. Unlike in the two-dimensional case, the result does not directly generalize to other surfaces.

The study of $j_{\partial\Omega}$ for the charge localization from measurements of the electric field was also done for these two different geometries (the horizontal plane Π and the sphere \mathbb{S}) and we showed the uniqueness of the critical point in both cases.

Finally, we studied $\tilde{J}_{\partial\Omega}$ for the dipole localization from measurements of the magnetic field in the Euclidean geometry ($\partial\Omega = \Pi$) with a horizontal moment $p_0 \in \Pi$ for which we proved the existence of three isolated critical points and two half-lines of critical points. This shows that the uniqueness of the critical point of least-square criteria from solution to these Poisson equations is not systematic and there can even be degenerated cases for which the critical points are not discrete.

Further generalizations are still expected for the criteria $J_{\partial\Omega}$ given by (I.5), $j_{\partial\Omega}$ given by (I.7) and $\tilde{J}_{\partial\Omega}$ given by (I.9) for multiple dipolar sources, for incomplete or noisy data and for more sophisticated geometries.

II.1 Introduction

II.1.1 Scattering

We are studying the scattering of electromagnetic waves by a perfect electric conductor Ω . The experimental setting is described on Figure II.1: an antenna is used to send an electromagnetic plane wave on an object and the electric field scattered by this object at is measured the same antenna. Our aim is to find the shape of this object knowing the electric field it scatter at different frequencies. In order to do this recovery different machine learning algorithms can be used [15] which used poles of the transfer function as variables. In order to get these poles from finite measurements of the field, several algorithm of rational approximation has been used [16]. In this work, we study the theory around different rational approximations rather than the different existing algorithms and will stick to the vector-fitting algorithm introduced in [17], [18] and [19] for the numerical examples. The use of rational approximation to the frequency response is justified by the meromorphic nature of the field as a function of the frequency [20, Thm 3.1].

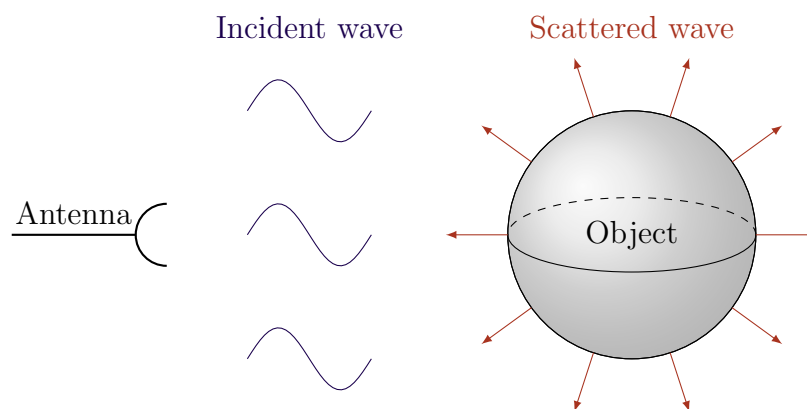


Figure II.1: Geometric situation of the scattering of an incident wave on an object.

The incident field electromagnetic field is expressed for all x in \mathbb{R}^3 by:

$$\begin{aligned} E_{inc}(x) &= E_0 \exp(-iv \cdot x), \\ H_{inc}(x) &= H_0 \exp(-iv \cdot x), \end{aligned}$$

where:

- E_{inc} is the \mathbb{C}^3 -valued incident electric field,
- H_{inc} is the \mathbb{C}^3 -valued incident magnetic field,
- $k \in \mathbb{R}_+$ is the wave number of the incident fields,
- $v \in \mathbb{R}^3$, is the direction of propagation of the incident wave with $|v| = 1$,
- $E_0 \in \mathbb{C}^3$ and $H_0 \in \mathbb{C}^3$ are the electromagnetic fields at $x = 0$ with the conditions that $E_0 \cdot H_0 = 0$, $E_0 \cdot v = 0$ and $H_0 \cdot v = 0$.

This problem is described by Maxwell equations for time-harmonic waves in vacuum (II.1) and (II.2) with a Dirichlet condition on the object (II.3) and the Silver-Müller radiation condition (II.4) [21]:

$$\nabla \times (E_{sc}) - ikH_{sc} = 0, \text{ in } \mathbb{R}^3 \setminus \overline{\Omega}, \quad (\text{II.1})$$

$$\nabla \times (H_{sc}) + ikE_{sc} = 0, \text{ in } \mathbb{R}^3 \setminus \overline{\Omega}, \quad (\text{II.2})$$

$$(E_{sc} + E_{inc}) \times \nu = 0, \text{ on } \partial\Omega, \quad (\text{II.3})$$

$$\lim_{|x| \rightarrow \infty} (H_{sc} \times x - |x|E_{sc}) = 0, \quad (\text{II.4})$$

where:

- E_{sc} is the \mathbb{C}^3 -valued scattered electric field,
- H_{sc} is the \mathbb{C}^3 -valued scattered magnetic field.
- ν is the outgoing unit vector normal to $\partial\Omega$.

Remark 6. One can see that (E_{inc}, H_{inc}) does not satisfy (II.4). Indeed, plane wave are not considered to be physical and can only be considered locally which is the case here as only the boundary value on $\partial\Omega$ of E_{inc} appears in Equation (II.1) to (II.4).

This electromagnetic field is also solution of Helmholtz equation:

$$\Delta E_{sc} + k^2 E_{sc} = 0, \text{ in } \mathbb{R}^3 \setminus \overline{\Omega} \quad (\text{II.5})$$

$$\Delta H_{sc} + k^2 H_{sc} = 0, \text{ in } \mathbb{R}^3 \setminus \overline{\Omega}$$

with the a zero-divergence condition:

$$\begin{aligned} \nabla \cdot E_{sc} &= 0, \text{ in } \mathbb{R}^3 \setminus \overline{\Omega} \\ \nabla \cdot H_{sc} &= 0, \text{ in } \mathbb{R}^3 \setminus \overline{\Omega} \end{aligned} \quad (\text{II.6})$$

In this section, we consider a spherical conductor of center $0_{\mathbb{R}^3}$ and radius $a > 0$ with the notation $\Omega = \mathbb{B}_a$ and $\partial\Omega = \mathbb{S}_a$. For such a spherical conductor, there exists a formula for E_{sc} [21, Eq. (6-104)] given by the Mie series:

$$E_{sc}^\theta(x) = -\frac{E_0}{kr} \cos(\varphi) \sum_{n=1}^{\infty} \left[-ib_n \hat{H}'_n^{(2)}(kr) \sin(\theta) P_n^1(\cos(\theta)) + c_n \hat{H}_n^{(2)}(kr) \frac{P_n^1 \cos(\theta)}{\sin(\theta)} \right],$$

where $(r, \theta, \varphi) \in \mathbb{R}^+ \times [0, \pi] \times [0, 2\pi[$ are the spherical coordinates of $x \in \mathbb{R}^3 \setminus \mathbb{B}_a$ and for all $n \in \mathbb{N}$:

- $\hat{H}_n^{(2)}$ is the n -th spherical Hankel function of the second kind,
- \hat{J}_n is the n -th spherical Bessel function of the first kind,
- P_n^1 is the associated Legendre function of order $(1, n)$,
- $b_n = -\frac{i^{-n}(2n+1)}{n(n+1)} \frac{\hat{J}'_n(ka)}{\hat{H}_n^{(2)}(ka)}$ and $c_n = -\frac{i^{-n}(2n+1)}{n(n+1)} \frac{\hat{J}_n(ka)}{\hat{H}_n^{(2)}(ka)}$.

In this study, we only consider the back-scattering position ($\theta = \pi$) hence the formula we are interested in is:

$$E_{sc}(r) = \frac{E_0}{kr} \sum_{n=1}^{\infty} i^n \left(n + \frac{1}{2} \right) \left[\frac{\hat{J}_n(ka) \hat{H}_n^{(2)}(kr)}{\hat{H}_n^{(2)}(ka)} - i \frac{\hat{J}'_n(ka) \hat{H}_n^{(2)}(kr)}{\hat{H}_n^{(2)}(ka)} \right]. \quad (\text{II.7})$$

As for all $n \in \mathbb{N}$, $\hat{H}_n^{(2)}$ and \hat{J}_n are analytic functions, we can immediately check the meromorphic nature of E_{sc} and determine its poles are they are the $k \in \mathbb{C}$ such that there exists $n \in \mathbb{N}$ with $\hat{H}_n^{(2)}(ka) = 0$ or $\hat{H}'_n^{(2)}(ka)$. Figure II.2 shows the first 120 poles of E_{sc} in this case.

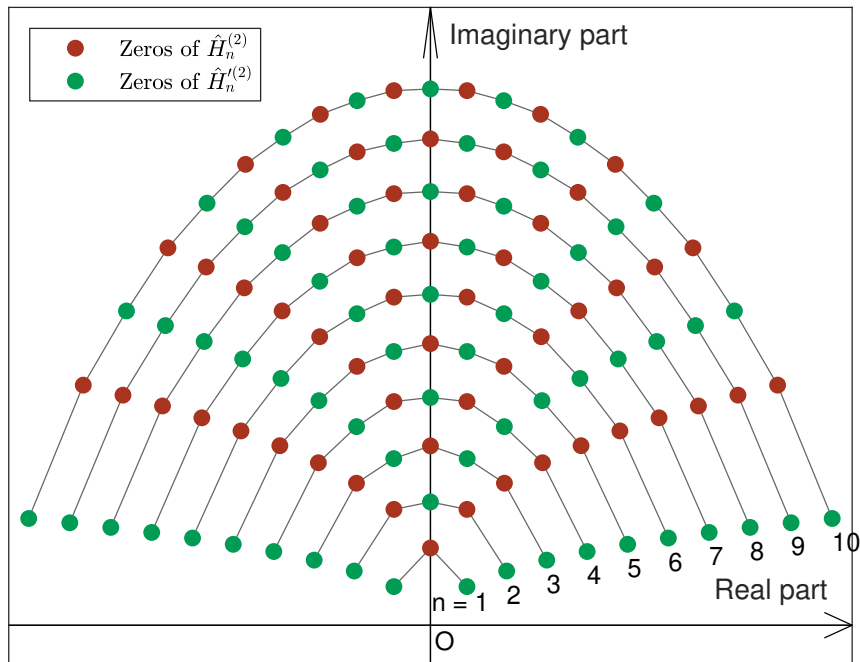


Figure II.2: Poles of E_{sc} for a metallic sphere of radius $a = 1$.

When studying the poles of E_{sc} , we can consider its far-field expansion:

$$\begin{aligned}
E_{sc}(r) &= P(\rho) \frac{i \exp(-ikr)}{kr} E_0, \\
P(\rho) &= \sum_{n=1}^{\infty} (-1)^n \left(n + \frac{1}{2}\right) \left(\frac{\hat{J}_n(\rho)}{\hat{H}_n^{(2)}(\rho)} - \frac{\hat{J}'_n(\rho)}{\hat{H}'_n^{(2)}(\rho)} \right) \\
&= \sum_{n=0}^{\infty} (-1)^n \left(n + \frac{1}{2}\right) \left(\frac{\hat{J}_n(\rho)}{\hat{H}_n^{(2)}(\rho)} - \frac{\hat{J}'_n(\rho)}{\hat{H}'_n^{(2)}(\rho)} \right) - \frac{1}{2} \exp(2i\rho), \quad (\text{II.8}) \\
\rho &= ka,
\end{aligned}$$

computed from Equation (II.7) using the following expansions:

$$\begin{aligned}
\hat{H}_n^{(2)}(x) &\underset{x \rightarrow \infty}{\sim} i^{n+1} \exp(-ix), \\
\hat{H}'_n^{(2)}(x) &\underset{x \rightarrow \infty}{\sim} i^n \exp(-ix).
\end{aligned}$$

This allows simplification in the computations done in Section II.2 and one can see that E_{sc} and P have the same poles.

II.1.2 Rational approximation

In the chapter, we study a family of rational approximations of meromorphic functions. The different approximation schemes studied are generalization of Padé approximation [22] presented below. Other schemes exist as in [23], [24],[25] and [26]. The different studied properties of these approximants use the notion of logarithmic capacity which is presented in Appendix B.

II.1.2.a Padé approximation at 0

Definition II.1.1. Let f be analytic in a neighborhood 0. For $m, n \in \mathbb{N}$, the Padé approximant to f at 0, is the rational function $p_{m,n}^0/q_{m,n}^0$ where $p_{m,n}^0 \in \mathcal{P}_m$, $q_{m,n}^0 \in \mathcal{P}_n$ with $q_{m,n}^0 \not\equiv 0$ and

$$(p_{m,n}^0 - f q_{m,n}^0)(z) = O(z^{m+n+1}) \text{ as } z \rightarrow 0. \quad (\text{II.9})$$

For a given function f analytic in a neighborhood of 0, its Padé approximant exists and is unique. Indeed, even though there exist an infinite number of duets $(p_{m,n}^0, q_{m,n}^0)$ solutions of Equation (II.9), they all lead to the same fractional function $p_{m,n}^0/q_{m,n}^0$ [27, Thm 1.4.3]. The following theorem, proven iteratively in [28] and [29] describes the approximation error made with this approximant and how it evolves when we increase the order of approximation (m and n).

Theorem II.1.1 (Nuttall-Pommerenke). *Let $E \subset \overline{\mathbb{C}}$ be a close set with $\text{cap}(E) = 0$ and $0 \notin E$ and let f be analytic in the complement of E . Let $K \subset \mathbb{C}$ be a compact set, $\varepsilon > 0$, $\delta > 0$, $\lambda > 1$. Then there exists $m_0 \in \mathbb{N}$ such that for all natural numbers m and n which satisfy:*

$$\begin{aligned}
m/\lambda &\leq n \leq \lambda m, \\
m_0 &\leq m,
\end{aligned}$$

we have:

$$|p_{m,n}^0/q_{m,n}^0 - f| < \varepsilon^m,$$

on $K \setminus E_{m,n}$ where $\text{cap}(E_{m,n}) \leq \delta$.

II.1.2.b Multipoint Padé approximation

A natural generalization of this approximation is the multipoint Padé approximation.

Definition II.1.2. For $m, n \in \mathbb{N}$ and $(z_i)_{i \in \llbracket 1, m+n+1 \rrbracket} \in \mathbb{C}^{m+n+1}$ be a collection of points. Let f be analytic in a neighborhood of each of these points. The multipoint Padé approximant to f at $(z_i)_{i \in \llbracket 1, m+n+1 \rrbracket}$ is the rational function $p_{m,n}/q_{m,n}$ where $p_{m,n} \in \mathcal{P}_m$, $q_{m,n} \in \mathcal{P}_n$ with $q_{m,n} \not\equiv 0$ and for all $i \in \llbracket 1, m+n+1 \rrbracket$:

$$(p_{m,n} - fq_{m,n})(z_i) = 0.$$

For a given function f analytic in neighborhood of each of points of a collection of points $(z_i)_{i \in \llbracket 1, m+n+1 \rrbracket} \in \mathbb{C}^{m+n+1}$, its multipoint Padé approximant exists and is unique. Nevertheless, this approximation is not an interpolation as the numerator and the denominator can vanish at a point z_i hence preventing interpolation at this point after simplification. A generalization of Theorem II.1.1 for the multipoint Padé approximation is given by [30, Thm 4]:

Theorem II.1.2. Let E and F be two closed sets in $\overline{\mathbb{C}}$ with $\text{cap}(F) = 0$ and $E \cap F = \emptyset$. Let $(z_i)_{i \in \mathbb{N}}$ be a family of distinct points in E . Let f be analytic in $\overline{\mathbb{C}} \setminus F$. Let $K \subset \mathbb{C}$ be a compact set, $\varepsilon > 0$, $\delta > 0$, $\lambda \geq 1$. Then, there exists m_0 such that for all natural numbers m and n which satisfy:

$$\begin{aligned} m/\lambda &\leq n \leq \lambda m, \\ m_0 &\leq m, \end{aligned}$$

we have:

$$|p_{m,n}/q_{m,n} - f| < \varepsilon^m,$$

in $K \setminus E_{m,n}$ where $\text{cap}(E_{m,n}) < \delta$.

Remark 7. This result needs to be compared to the existing ones for least-squares polynomial approximation. Indeed, for Padé approximation this theorem does not require any assumptions for the points $(z_i)_{i \in \mathbb{N}}$ which are completely independent of the set K . Nevertheless, the obtained convergence (in capacity) is weaker than the uniform convergence which can be achieved through least-squares polynomial approximation [31]. There, in order for uniform convergence to hold true, points have to be chosen in some admissible meshes (defined by inequalities).

Theorems II.1.1 and II.1.2 only specify a ‘weak’ kind of convergence of the approximant to the approximated function. Yet, Proposition II.1.3 shows that this convergence in capacity (defined by B.0.1 in Appendix B) also induces a form of convergence of the poles of the approximant towards the poles of the approximated function when it is meromorphic. This proposition is a direct application of Rouché theorem [32, Thm 10.43].

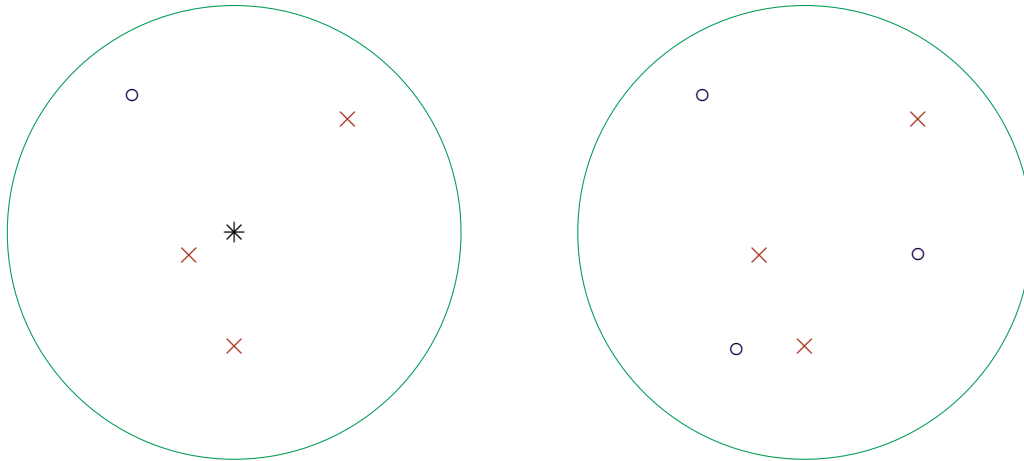
Proposition II.1.3. Let f be a meromorphic function and $(g_n)_{n \in \mathbb{N}}$ be a sequence of meromorphic functions which converges in capacity to f . Then for any open set $O \subset \mathbb{C}$ in which f admits a finite number of poles and zeros, for any point z in O there exist a disk $D(z, r) \subset O$ of radius $r > 0$ and an integer $k_0 \in \mathbb{N}$ such that for all $k \geq k_0$:

$$p_f - z_f = p_n - z_n,$$

where p_f and z_f are respectively the number of poles and zeros of f in K counted with their multiplicities and p_n and z_n are respectively the number of poles and zeros of g_n in $D(z, r)$ counted with their multiplicities.

Proposition II.1.3 illustrates the link between convergence in capacity as in Theorem II.1.1 and the present goal of retrieving the poles of a meromorphic function. Indeed, let f a meromorphic and $a \in \mathbb{C}$ one of its poles of multiplicity $d \in \mathbb{N}$. We consider a compact set $K \subset \mathbb{C}$ such that K does not contain any zeros of f and contains no other poles than a . Let $(g_n)_{n \in \mathbb{N}}$ be a sequence of meromorphic functions which converges in capacity to f . By applying Proposition II.1.3 to f , g_n and K , we see that for all $n \geq n_0$ the approximant g_n admits at least d poles in K and that any additional poles that g_n might have shall be compensated by a zero of g_n . As we can choose K as small as want, this shows that at least a part of the poles of the approximant g_n shall be arbitrarily close to the poles of the approximated function f . Nevertheless, this result does not prevent g_n to have other poles as long as they are compensated by zeros nearby. Indeed, the same argument applied to a compact set in the analyticity domain of f show that g_n can have poles far from the poles of f as long as it possess zeros nearby.

This property is illustrated on Figure II.3. On the left side (Figure II.3a), we consider a compact set (a disk) which contains a double pole of f and we see that the approximant g_n has three poles and a zero in this set. On the right side (Figure II.3b), we consider a compact set (a disk) which contains no pole of f and we see that the approximant g_n has three poles and three zeros in this set.



(a) Compact set which contains a double pole of f . (b) Compact set which contains no poles of f .

Figure II.3: Poles and zeros of f and its approximant g_n different compact sets. Red crosses are poles of g_n , blue circles are zeroes of g_n and the black star is a double pole of f .

The goal of this chapter is to study the pole recovery of the far field term P as defined in Equation (II.8). This recovery is done using the Vector-Fitting algorithm which is an implementation of a generalization of the multipoint Padé approximation described in Section (II.4). The results achieved on the convergence in capacity of this approximant, done in Section (II.4), justifies the use of this method in pole recovering.

II.1.3 Overview

In Section II.2, we study an approximation process of the scattered field for a metallic sphere at high-frequency in an attempt to extend the data for a given range of frequency.

In Section II.3, we introduce least-squares Padé approximation at 0 which is a generalization of Padé approximation at 0 presented in Section II.1.2.a. For this approximation we study the existence and uniqueness of the approximant in section II.3.1, then prove a generalization of Nuttall-Pommerenke theorem in Section II.3.2. Finally, in Section II.4, we introduce monic least-squares multipoint Padé approximation which is a generalization of multipoint Padé approximation presented in Section II.1.2.b. For this approximation, we introduce Theorem II.1.2 and Conjecture II.4.1, which are generalizations of Nuttall-Pommerenke theorem. Theorem II.1.2 is proven in Section II.4.1, while Conjecture II.4.1 is discussed in Section II.4.2.

II.2 High-frequency approximation

In this section, we study the behavior of the field at high frequency (as $k \rightarrow +\infty$). In Section II.2.1, we construct a high-frequency equivalent in the form of a series which can be computed for any convex object and is here computed for a spherical object. In Section II.2.2 we study a finer approximation of the field at high-frequency for the spherical object in the back-scattering position. This approximation is decomposed into an optic part similar to the previous series and a creeping wave part whose behavior is more complex. Finally, in Section II.2.3 we apply a rational approximation scheme to these different high-frequency extension in order to study their usability for our purpose.

II.2.1 Luneburg-Kline series

In this section, the computations can be done outside the spherical case and we only assume that $\Omega \subset \mathbb{R}^3$ is convex and smooth. To study this problem, we will assume that E_{sc} can be expanded in a Luneburg-Kline series [33]:

$$E_{sc}(k, x) \sim \sum_{n=0}^{\infty} \frac{A_n(x)}{(ik)^n} \exp(-ikS(x)), \quad (\text{II.10})$$

where for all $n \in \mathbb{N}$:

$$\begin{aligned} A_n &: \mathbb{R}^3 \setminus \bar{\Omega} \longrightarrow \mathbb{C}^3, \\ S &: \mathbb{R}^3 \setminus \bar{\Omega} \longrightarrow \mathbb{R}, \end{aligned}$$

are respectfully the amplitudes of the expansion and the phase. This expansion is to be understood in the Poincaré sense, meaning that for all $x \in \mathbb{R}^3 \setminus \bar{\Omega}$ and $N \in \mathbb{N}$:

$$E_{sc}(k, x) = \sum_{n=0}^N \frac{A_n(x)}{(ik)^n} \exp(-ikS(x)) + o\left(\frac{1}{k^N}\right) \text{ as } k \rightarrow +\infty.$$

This series does not need to converge. Indeed if it converged, because of the uniqueness of the solution of the system of equations (II.1) to (II.4), the equivalence would be an equality. In this series, we are mainly interested in A_0 and S as they indicate the first order behavior of E_{sc} when k goes to $+\infty$.

Substituting the expansion II.10 into Equations (II.5) and (II.6) and identifying the terms as powers of ik we get for all $n \in \mathbb{N}$ the system of equations:

$$|\nabla S|^2 = 1, \quad (\text{II.11})$$

$$(\Delta S + 2\nabla S \cdot \nabla)A_n = -\Delta A_{n-1}, \quad (\text{II.12})$$

$$\nabla S \cdot A_n = -\nabla \cdot A_{n-1},$$

with the convention $A_{-1} = 0$. Equation (II.11) is the eikonal equation and Equation (II.12) is a transport equation. The Dirichlet condition (II.3) gives, for all $y \in \partial\Omega$:

$$S(y) = v \cdot y, \quad (\text{II.13})$$

$$A_0 \times \nu(y) = -E_0 \times \nu(y), \quad (\text{II.14})$$

where $\nu(y)$ is the unit vector which is outgoing and normal to $\partial\Omega$ at y .

II.2.1.a Solving the eikonal equation

Let us define rays as the integral curves of the gradient of the phase S . Let A and B to points on the ray path and Γ be the curve from A to B on this path. We have:

$$S(B) - S(A) = \int_{\Gamma} \nabla S \cdot ds = \int_{\Gamma} ds \stackrel{\text{def}}{=} \ell^{\Gamma}(A, B), \quad (\text{II.15})$$

as on the ray, ∇S and ds are parallel (since A and B are on the same ray) and ∇S is of norm 1 because of Equation (II.11). Now, if we integrate the same quantity on the line segment $[AB]$, we get from Cauchy-Schwarz inequality:

$$S(B) - S(A) = \int_A^B \nabla S \cdot ds \leq \int_A^B ds = |AB|. \quad (\text{II.16})$$

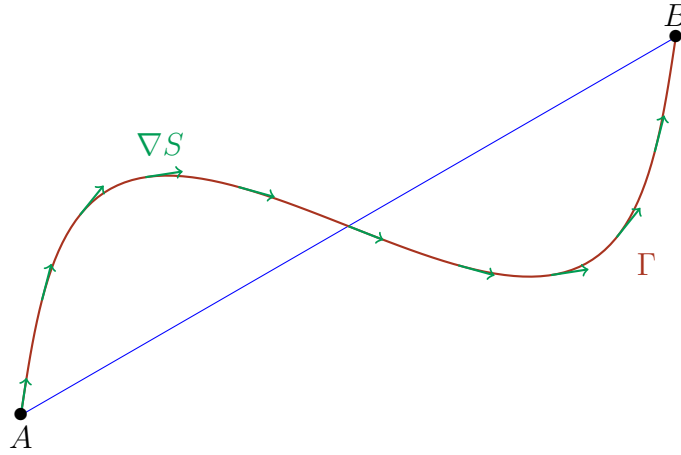


Figure II.4: Geometrical representation of the path Γ in the resolution of the eikonal equation.

Using Equations (II.15) and (II.16) we see that $\ell^{\Gamma}(A, B) \leq |AB|$ and thus, as straight lines are length minimizers, the rays must be straight lines. Let $u \in \mathbb{R}^3$ be a unit outgoing director vector of a ray passing through $\partial\Omega$ at a point $y \in \partial\Omega$. Using the Dirichlet condition (II.14) and taking the tangential derivative, we see that for all $y \in \partial\Omega$:

$$\nabla S \times \nu(y) = v \times \nu(y).$$

Hence, as $u(y) = \pm \nabla S(y)$, we see that u has the same tangential component than v at y . Since it is unitary and outgoing, we find that we have to distinguish between two regions: the lit side and the shadow side. Indeed for all $y \in \partial\Omega$:

$$u(y) = \begin{cases} v - 2(v \cdot \nu(y))\nu(y) & \text{if } v \cdot \nu(y) \leq 0, \\ v & \text{else.} \end{cases} \quad (\text{II.17})$$

So, to solve the eikonal equation (II.11) at a point x outside of $\overline{\Omega}$, one needs to find $y(x) \in \partial\Omega$ such that x and $y(x)$ are on the same ray (this is known as Alhazen's Problem [34]). The situation is illustrated on Figure II.6 for a precise configuration and on Figure II.7 for general reflections. Then, using Equations (II.13) and (II.16) we find:

$$\begin{aligned} S(x) &= S(y(x)) + |x - y(x)| \\ &= v \cdot y(x) + |x - y(x)|. \end{aligned} \quad (\text{II.18})$$

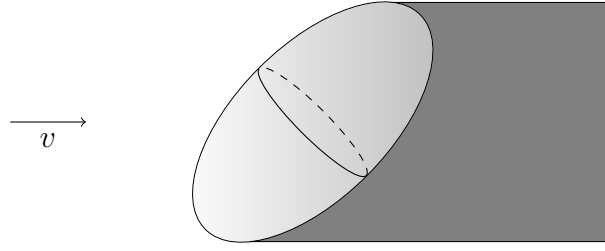


Figure II.5: Distinction between the lit region (in white) and the shadow region (in gray) for a spheroid.

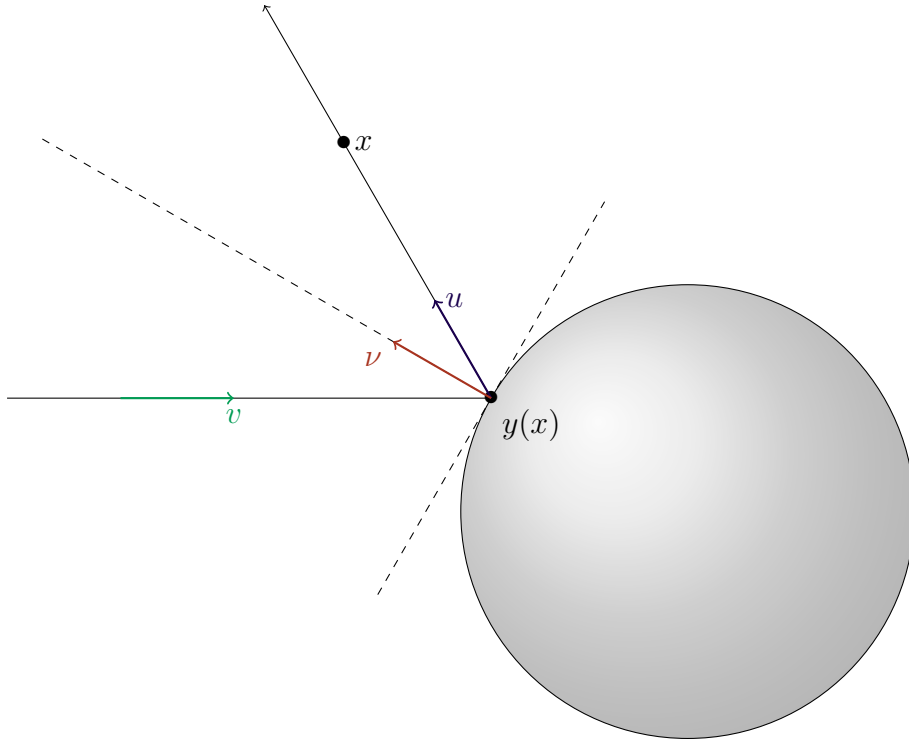


Figure II.6: Schema of the reflection of an electromagnetic wave on a metallic sphere.

From now on, we assume that Ω is the ball \mathbb{B}_a of radius $a > 0$ and we consider back-scattering situation for which, given $x = -rv$, we can easily find $y(x)$ using the formula:

$$y(x) = a \frac{x}{|x|} = -av.$$

Hence for $x = -rv$ in the back scattering position we have:

$$S(x) = -a + r - a = r - 2a.$$

II.2.1.b Solving the transport equation

Let us solve the transport equation (II.12) for $n = 0$. Let a_0 be any Cartesian component of A_0 ($a_0 = e_i \cdot A_0$ for $i \in \{1, 2, 3\}$). First, by multiplication of Equation (II.12) with a_0 we have:

$$\nabla \cdot (a_0^2 \nabla S) = 0, \text{ in } \mathbb{R}^3 \setminus \overline{\mathbb{B}_a}. \quad (\text{II.19})$$

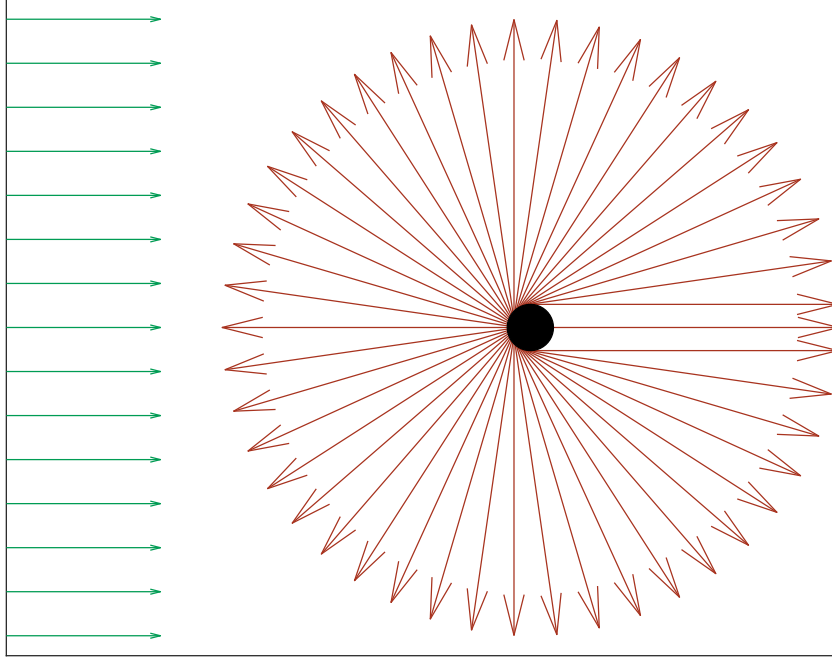


Figure II.7: Schematic illustration of ray paths from the scattering of a metallic sphere.

Let us define the following parametrization of points on the sphere:

$$y : [0, \pi] \times [0, 2\pi[\longrightarrow \mathbb{S}_a$$

$$(\theta, \varphi) \longmapsto a \begin{pmatrix} \cos(\varphi) \sin(\theta) \\ \sin(\varphi) \sin(\theta) \\ \cos(\theta) \end{pmatrix}.$$

Similarly, for all $s \in \mathbb{R}_+$, we define:

$$x_s : [0, \pi] \times [0, 2\pi[\longrightarrow \mathbb{R}^3$$

$$(\theta, \varphi) \longmapsto y(\theta, \varphi) + su(y(\theta, \varphi)),$$

where u is as defined in Equation (II.17). Let $\theta^0 \in [0, \pi]$ and $\varphi^0 \in [0, 2\pi[$ and $y^0 = y(\theta^0, \varphi^0)$ be a fixed point on the sphere \mathbb{S}_a . Similarly, for all $s \in \mathbb{R}_+$, we define:

$$\hat{x}_s : [0, \pi] \times [0, 2\pi[\longrightarrow \mathbb{R}^3$$

$$(\theta, \varphi) \longmapsto y(\theta, \varphi) + g(s, \theta, \varphi)u(y(\theta, \varphi)),$$

where $g(s, \theta, \varphi) \in \mathbb{R}_+$ is chosen such that:

$$S(\hat{x}_s(\theta, \varphi)) = S(x_s(\theta_0, \varphi_0)).$$

Let s_1 and s_2 in \mathbb{R}^+ and $x_1 = x_{s_1}(\theta_0, \varphi_0)$ and $x_2 = x_{s_2}(\theta_0, \varphi_0)$. Let W_1 and W_2 be the surfaces defined by for all $\varepsilon > 0$:

$$W_1(\varepsilon) = \{ \hat{x}_{s_1}(\theta, \varphi), \theta \in [\theta^0 - \varepsilon, \theta^0 + \varepsilon], \varphi \in [\varphi^0 - \varepsilon, \varphi^0 + \varepsilon] \},$$

$$W_2(\varepsilon) = \{ \hat{x}_{s_2}(\theta, \varphi), \theta \in [\theta^0 - \varepsilon, \theta^0 + \varepsilon], \varphi \in [\varphi^0 - \varepsilon, \varphi^0 + \varepsilon] \}.$$

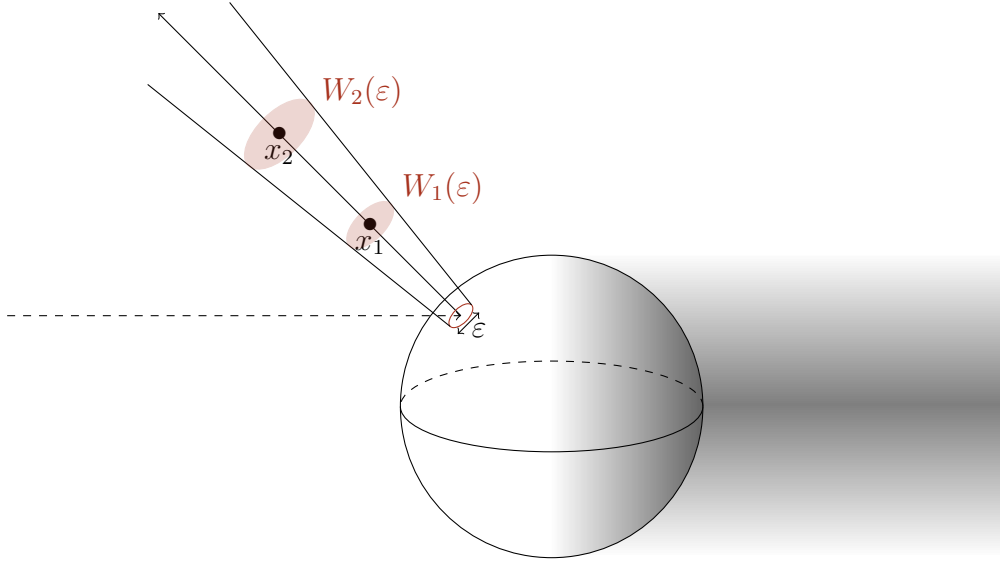


Figure II.8: Geometric description of the surfaces W_1 and W_2 used in the resolution of the transport equation.

Let us consider the volume $V = V(\varepsilon, s_1, s_2)$ which is surrounded by the rays through the boundaries of both surfaces $W_1(\varepsilon)$ and $W_2(\varepsilon)$ and the surfaces themselves. The different surfaces introduced here are presented on Figure II.8. By integrating the quantity (II.19) on this volume and using the divergence theorem, one gets:

$$\frac{1}{\text{surf}(W_1(\varepsilon))} \int_{W_1(\varepsilon)} a_0^2(s) ds = \frac{\text{surf}(W_2(\varepsilon))}{\text{surf}(W_1(\varepsilon)) \text{surf}(W_2(\varepsilon))} \int_{W_2(\varepsilon)} a_0^2(s) ds.$$

Because a_0 is assumed to be continuous, we also know that for $i \in \{1, 2\}$:

$$\lim_{\varepsilon \rightarrow 0} \frac{1}{\text{surf}(W_i(\varepsilon))} \int_{W_i(\varepsilon)} a_0^2(s) ds = a_0^2(x_i).$$

Let us now compute the ratio of the two surfaces. In what follows, a case distinction has to be done between the lit side ($\theta_0 \in [\pi/2, \pi]$) and the dark side ($\theta_0 \in [0, \pi/2[$). Let us start with the lit side. Because $x = \hat{x}_{s_i}(\theta, \varphi)$ is defined by being on the same ray as $y = y(\theta, \varphi)$ and being on the same wavefront as $x_i^0 = x_{s_i}(\theta_0, \varphi_0)$, we see from Equations (II.17) and (II.18) that it solves the system:

$$\begin{aligned} \frac{x - y}{|x - y|} &= v - 2 \frac{v \cdot y}{a^2} y, \\ |x - y| + v \cdot y &= s + v \cdot y^0. \end{aligned}$$

This allows us to express $x = x_{s_i}(\theta, \varphi)$ as:

$$x = y(\theta, \varphi) + \left(s + v \cdot y^0 - v \cdot y(\theta, \varphi) \right) \left(v - 2 \frac{v \cdot y(\theta, \varphi)}{a^2} y(\theta, \varphi) \right).$$

Using the known formula for the area of a surface defined this way [13, Eq. 1.6.48] defined as such we have:

$$\begin{aligned} \text{surf}(W_i(\varepsilon)) &= \int_{\theta^0 - \varepsilon}^{\theta^0 + \varepsilon} \int_{\varphi^0 - \varepsilon}^{\varphi^0 + \varepsilon} X_i(\theta, \varphi) d\varphi d\theta \\ &= 4\varepsilon^2 X_i(\theta^0, \varphi^0) + o(\varepsilon^2), \end{aligned}$$

where for all $(\theta, \varphi) \in [0, \pi] \times [0, 2\pi[$:

$$X_i(\theta, \varphi) = |\partial_\theta x_{s_i}(\theta, \varphi) \times \partial_\varphi x_{s_i}(\theta, \varphi)|.$$

After computation, which as been done using a symbolic computation program, we find:

$$X_i(\theta^0, \varphi^0) = |\sin(\theta_0)| (a^2 \cos(\theta_0) - 2as \cos(\theta_0)^2 - 2as_i + 4s_i^2 \cos(\theta_0)).$$

Thus we get:

$$\begin{aligned} \lim_{\varepsilon \rightarrow 0} \frac{\text{surf}(W_2(\varepsilon))}{\text{surf}(W_1(\varepsilon))} &= \frac{X_2(\theta^0, \varphi^0)}{X_1(\theta^0, \varphi^0)} \\ &= \frac{a^2 \cos(\theta_0) - 2as_2 \cos(\theta_0)^2 - 2as_2 + 4s_2^2 \cos(\theta_0)}{a^2 \cos(\theta_0) - 2as_1 \cos(\theta_0)^2 - 2as_1 + 4s_1^2 \cos(\theta_0)}. \end{aligned}$$

By taking $x_2^0 = x \in \mathbb{R}^3 \setminus \overline{\mathbb{B}_a}$ and $x_1^0 \rightarrow y(x) \in \mathbb{S}_a$, one get:

$$a_0(x)^2 = \frac{a^4}{(a^2 - 2v \cdot y(x)|x - y(x)|) \left(a^2 - 2\frac{a^2}{v \cdot y(x)}|x - y(x)| \right)} a_0(y(x))^2.$$

So, by continuity of A_0 , we finally find:

$$A_0(x) = \frac{a^2}{(a^2 - 2v \cdot y(x)|x - y(x)|)^{1/2} \left(a^2 - 2\frac{a^2}{v \cdot y(x)}|x - y(x)| \right)^{1/2}} A_0(y(x)).$$

Similarly, on the shadow side ($\theta_0 \in [0, \pi/2]$), as $u = v$, the areas of those surfaces $W_1(\varepsilon)$ and $W_2(\varepsilon)$ are equal for all $\varepsilon > 0$ small enough thus:

$$\lim_{\varepsilon \rightarrow 0} \frac{\text{surf}(W_2(\varepsilon))}{\text{surf}(W_1(\varepsilon))} = 1.$$

And, we finally find:

$$A_0(x) = A_0(y(x)).$$

Hence, we have computed the following asymptotic expansion, for all $x \in \mathbb{R}^3 \setminus \mathbb{B}_a$ and $y = y(x)$ as defined before:

$$\begin{aligned} E_{sc}(x) &\underset{k \rightarrow \infty}{\sim} \frac{a^2}{(a^2 - 2(v \cdot y)|x - y|)^{1/2} \left(a^2 - 2\frac{a^2}{v \cdot y}|x - y| \right)^{1/2}} && \text{if } v \cdot y \leq 0, \\ &\times \left[-E_0 + 2\frac{(E_0 \cdot y)}{a^2}y \right] \exp(-ik(v \cdot y + |x - y|)) \\ &\underset{k \rightarrow \infty}{\sim} -E_0 \exp(-ik(v \cdot x)) && \text{if } v \cdot y > 0. \end{aligned}$$

The comparison between the Luneburg-Kline series first term $A_0 \exp(-ikS)$ we calculated and the accurate truncated Mie series is shown on Figure II.9. We see on that figure that the approximation made using the first Luneburg-Kline term A_0 is only valid around the back scattering position and its accuracy decreases when approaching the lit/shadow limit represented as dashed vertical lines on Figure II.9.

One can now compute similarly A_1 , A_2 and so on from Equation (II.10) which in the back-scattering configuration simplifies to:

$$\begin{aligned} E_{sc}(-rv) &\underset{k \rightarrow \infty}{\sim} \left(-\frac{a}{2r-a} - 2\frac{(r-a)^2}{(2r-a)^3} \frac{1}{ik} + 2\frac{(r-a)(2r^2 - 4ra + 3a^2)}{(2r-a)^5} \frac{1}{(ik)^2} \right) \\ &\times E_0 \exp(-ik(r-2a)). \end{aligned} \quad (\text{II.20})$$

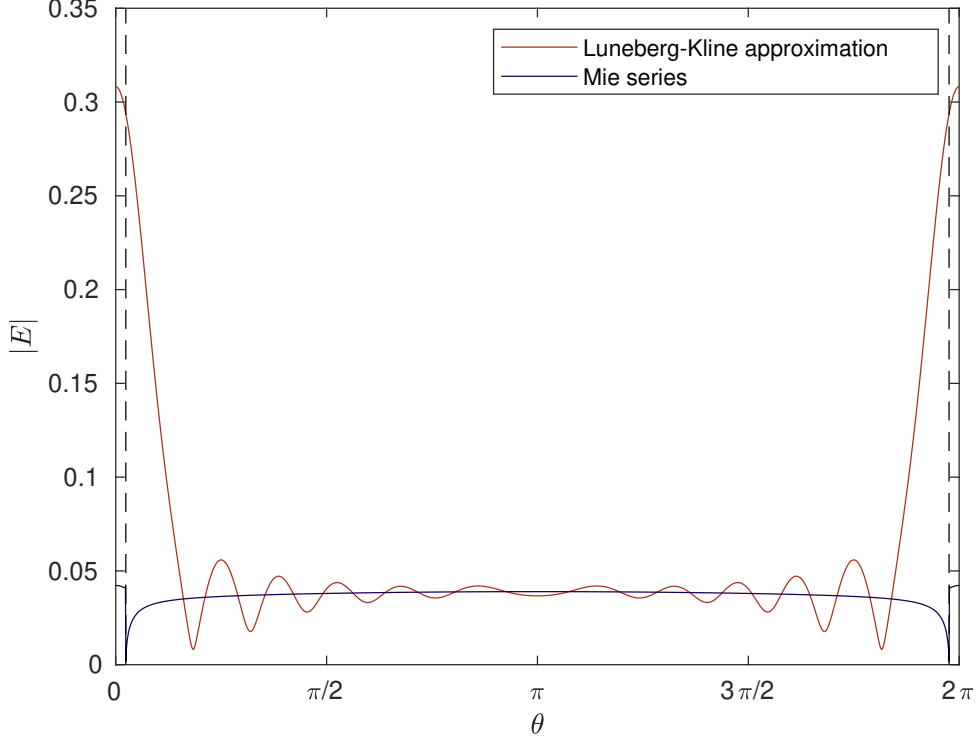


Figure II.9: Comparison between Mie (blue) series and the first Luneberg-Kline term A_0 (red) with $a = 0.15/2$ m, at a distance $r = 1$ m at a frequency $f = 5$ GHz for all $\theta \in [0, 2\pi]$.

II.2.2 Creeping Waves

In this section we only consider the far field given by Equation (II.8) in the back-scattering configuration. We use Watson transformation [35] which transforms a sum into an integral using the residue theorem to get a simpler form. One of the form Watson transformations can have is given by:

$$\sum_{n=0}^{\infty} f\left(n + \frac{1}{2}\right) = 2 \int_C \frac{\exp(-i\nu\pi)}{\cos(\nu\pi)} f(\nu) d\nu,$$

where C is a curve passing through 0 which surrounds the half integers and f is an analytic function in the interior of C . The curve C is illustrated on Figure II.10. In this case, we take advantage of the analytic nature of $\nu \mapsto \hat{H}_\nu^{(2)}$ and $\nu \mapsto \hat{J}_\nu$ with respect to their index [13, Sec. 10.2(ii)]. Let us apply this formula to evaluate the sum:

$$\begin{aligned} \mathfrak{S}(\rho) &\stackrel{\text{def}}{=} \sum_{n=0}^{\infty} (-1)^n \left(n + \frac{1}{2}\right) \left(\frac{\hat{J}_n(\rho)}{\hat{H}_n^{(2)}(\rho)} - \frac{\hat{J}'_n(\rho)}{\hat{H}'_n{}^{(2)}(\rho)} \right) \\ &= 2 \int_C \frac{\exp(-i\nu\pi) \exp(i\pi(\nu - 1/2))}{\cos(\nu\pi)} f_\rho(\nu) \nu d\nu \\ &= -2i \int_C \frac{f_\rho(\nu) \nu}{\cos(\nu\pi)} d\nu, \end{aligned} \tag{II.21}$$

where for all ρ in \mathbb{R}_+ we define the meromorphic function:

$$f_\rho : \mathbb{C} \longrightarrow \overline{\mathbb{C}}$$

$$\nu \longmapsto \frac{\hat{J}_{\nu-1/2}(\rho)}{\hat{H}_{\nu-1/2}^{(2)}(\rho)} - \frac{\hat{J}'_{\nu-1/2}(\rho)}{\hat{H}'_{\nu-1/2}^{(2)}(\rho)}.$$

Because of [13, Eq. 10.4.8], we see that for all ρ in \mathbb{R}_+ , f_ρ admits the following parity symmetry:

$$f_\rho(-\nu) = \exp(2i\nu\pi)f_\rho(\nu). \quad (\text{II.22})$$

Let C_+ and C_- be sections of C of respectively positive and negative imaginary parts and C_-^S the symmetric of C_- with respect to the point 0 in \mathbb{C} . Using Equation (II.22), we have:

$$\begin{aligned} \int_{C_-} \frac{f_\rho(\nu)\nu}{\cos(\nu\pi)} d\nu &= \int_{C_-} \frac{\exp(2i\nu\pi)}{\cos(\nu\pi)} f_\rho(\nu)\nu d\nu - 2i \int_{C_-} \exp(i\nu\pi) \tan(\nu\pi) f_\rho(\nu)\nu d\nu \\ &= - \int_{C_-^S} \frac{\exp(-2i\nu\pi)}{\cos(\nu\pi)} f_\rho(-\nu)\nu d\nu - 2i \int_{C_-} \exp(i\nu\pi) \tan(\nu\pi) f_\rho(\nu)\nu d\nu \\ &= - \int_{C_-^S} \frac{f_\rho(\nu)\nu}{\cos(\nu\pi)} d\nu - 2i \int_{C_-} \exp(i\nu\pi) \tan(\nu\pi) f_\rho(\nu)\nu d\nu, \end{aligned} \quad (\text{II.23})$$

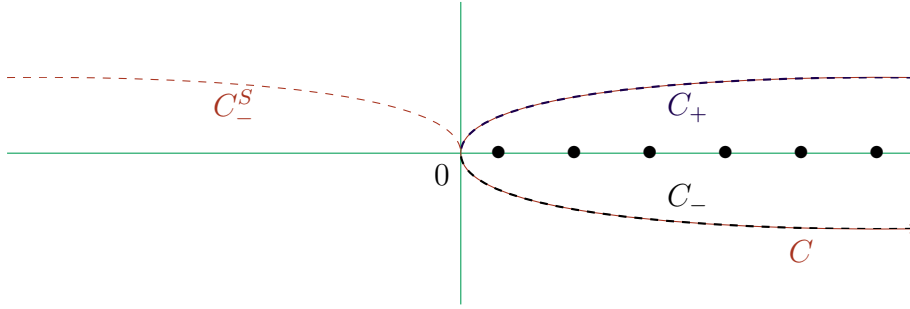


Figure II.10: Schematic representation of the curves C (red), C_- (dashed blue), C_+ (dashed black) and C_-^S (dashed red).

where we used the identity:

$$\forall \nu \in \mathbb{C} : \frac{1}{\cos(\nu\pi)} = \exp(2i\nu\pi) \frac{1}{\cos(\nu\pi)} - 2i \exp(i\nu\pi) \tan(\nu\pi).$$

Using Equations (II.21) and (II.23), we have for all ρ in \mathbb{R}_+ :

$$\mathfrak{S}(\rho) = -2i \int_{C_+ \cup C_-^S} \frac{f_\rho(\nu)\nu}{\cos(\nu\pi)} d\nu - 4 \int_{C_-} \exp(i\nu\pi) \tan(\nu\pi) f_\rho(\nu)\nu d\nu.$$

The first integral on the right-hand side has an integrand which decreases exponentially when $|\nu|$ goes to $+\infty$ with $\text{Im}(\nu) > 0$ hence we can close the contour using Cauchy theorem and apply the residue theorem in the upper half plane to finally find the following decomposition:

$$P(\rho) = P_c(\rho) + P_o(\rho), \quad (\text{II.24})$$

where P_o is the optic part of P and P_c is the creeping wave part of P given by:

$$P_o(\rho) = -\frac{1}{2} \exp(2i\rho) - 4 \int_{C_-} \exp(i\nu\pi) \tan(\nu\pi) f_\rho(\nu) \nu d\nu,$$

$$P_c(\rho) = 4\pi \sum_{n=1}^{+\infty} \frac{\hat{J}_{\nu-1/2}(\rho)}{\partial_\nu \hat{H}_{\nu-1/2}^{(2)}(\rho) \cos(\pi\nu)} \Big|_{\nu=\nu_n} - 4\pi \sum_{m=1}^{+\infty} \frac{\hat{J}'_{\nu-1/2}(\rho)}{\partial_\nu \hat{H}'_{\nu-1/2}^{(2)}(\rho) \cos(\pi\nu)} \Big|_{\nu=\tilde{\nu}_m}.$$

where for all $\rho \in \mathbb{C}$, $\nu_n = \nu_n(\rho)$ and $\tilde{\nu}_m = \tilde{\nu}_m(\rho)$ are the countable values such that:

$$\hat{H}_{\nu_n-1/2}^{(2)}(\rho) = 0,$$

$$\hat{H}'_{\tilde{\nu}_m-1/2}(\rho) = 0.$$

Using the approximations of these (ν_n) and $(\tilde{\nu}_n)$ given by [36, Eq. 21 and 85] and after keeping the dominant term, we get:

$$P_c(\rho) \underset{\rho \rightarrow +\infty}{\sim} \tau^4 e^{i\frac{\pi}{3}} \frac{1}{\beta_1 \text{Ai}(\beta_1)^2} \exp(i\pi\rho - e^{-i\frac{\pi}{6}} \tau \pi \beta_1 + O(\tau^{-1})), \quad (\text{II.25})$$

where:

- $\tau = \tau(\rho) = \left(\frac{\rho}{2}\right)^{1/3}$,
- $\beta_1 \approx -1.019$ is the smallest (in absolute value) zero of the Airy function's derivative Ai' [13, Tb. 9.9.1].

Remark 8. The optic part has a similar high-frequency behavior as the Luneberg-Kline series (II.20) computed in the previous section. We see that the creeping wave part of the field decreases exponentially as k goes to $+\infty$. Hence, this part of the field is, as predicted in the previous section, negligible compared to any polynomial of $1/k$ hence to the optic part.

In order to evaluate the contribution of each term in this decomposition, we compute the error made when only considering the first, the two first and the three first optic terms and when considering the two first optic terms together with the first creeping wave term. The evaluated error is displayed on Table II.1 for a metallic sphere of radius $a = 0.15/2$ m seen in the back-scattering position at a distance $r = 1$ m at a frequency of 5 GHz ($\rho = 7.9$).

Approximate	1 optic	2 optic	3 optic	2 optic and 1 creeping
Error(%)	13.89	9.02	9.01	1.46

Table II.1: Error made in the approximation with respectively one, two and three terms of the optics part and two terms of the optics part and one term of the creeping wave part at frequency 5 GHz for $a = 0.15/2$ m and $r = 1$ m.

Using the results listed in Table II.1, one can see that at 5 GHz the first optic term accounts for 86.11% of the field while the second and third one account only for respectively 4.87% and 0.01%. On the other hand, the first term of the creeping wave part of the field accounts for 7.55%. Hence, even though this part is asymptotically negligible when compared to the optic part, it cannot be neglected at high but finite frequencies. In

Figures II.11, II.12 and II.13, a comparison is made between the different approximations. From the Figures II.11 and II.12, we see that A_0 and $-A_1/k$ are good approximations of respectively the real and imaginary parts of the mean value of the field while Figure II.13 shows that the creeping part corresponds to the local variations in frequency.

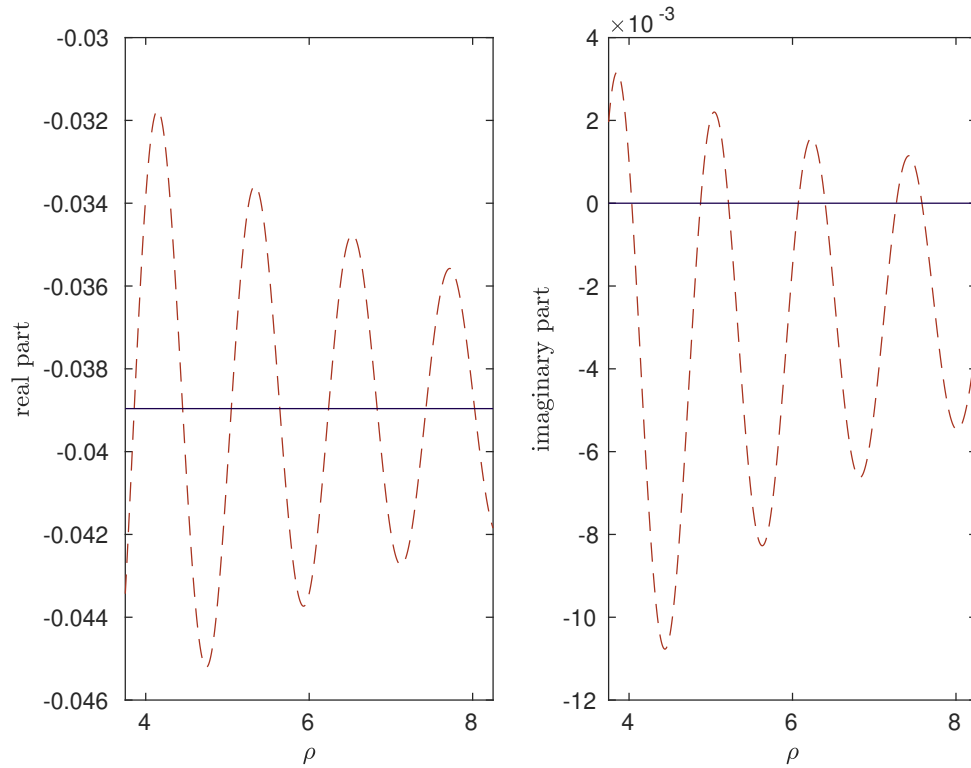


Figure II.11: Comparison between the compensated Mie series $P(\rho) \exp(2i\rho)$ (in red) and the first optic term A_0 (in blue).

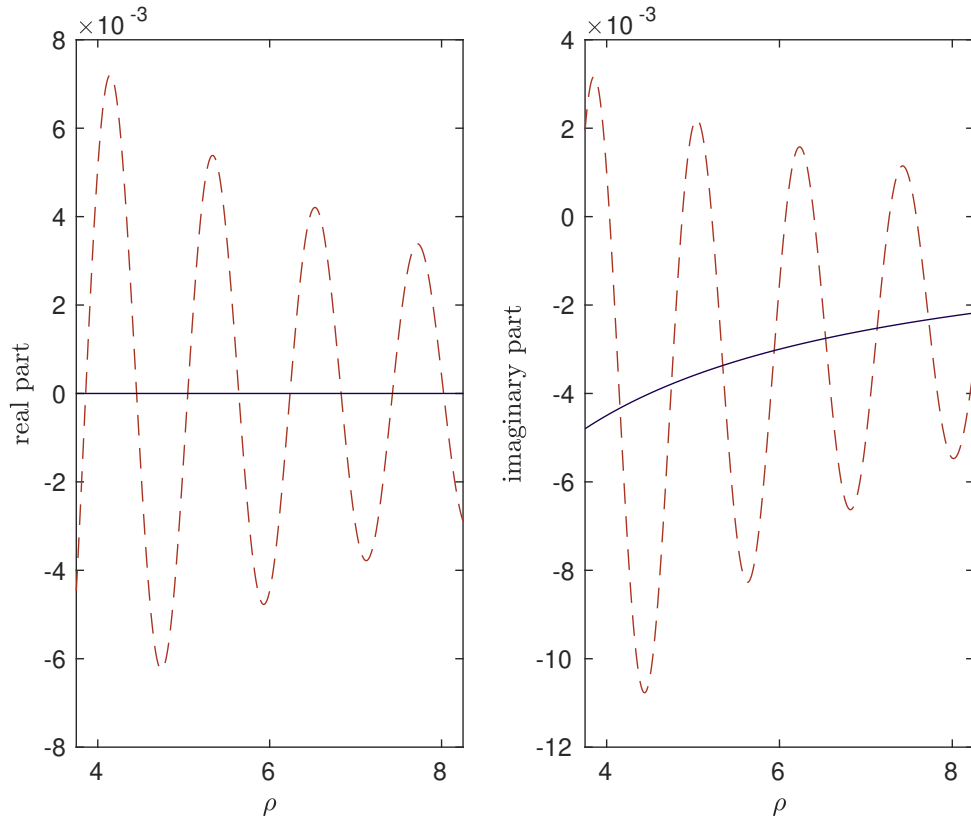


Figure II.12: Comparison between the compensated Mie series $P(\rho) \exp(2i\rho) - A_0$ (in red) and the second optic term $A_1/(ik)$ (in blue).

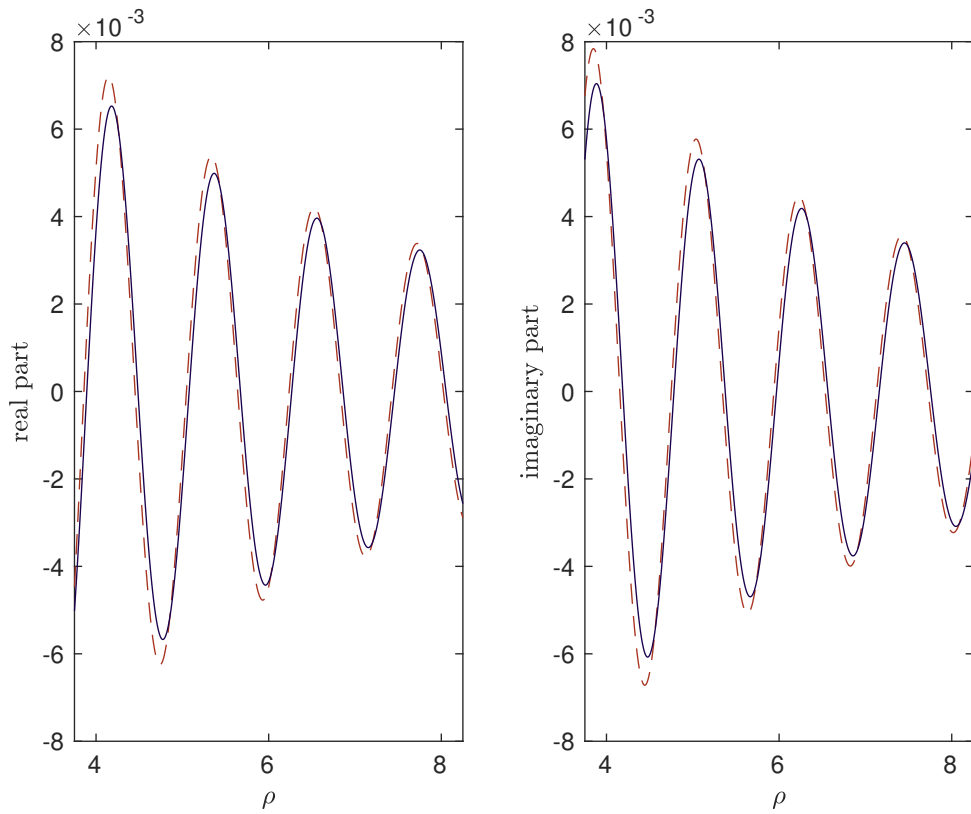


Figure II.13: Comparison between the compensated Mie serie $P(\rho) \exp(2i\rho) - A_0 - A_1/(ik)$ (in red) and the first creeping term (in blue).

II.2.3 Rational approximation using high-frequency behavior

In order to illustrate the use of the previously computed expansions, we apply a rational approximation scheme linked to the least-squares multipoint Padé approximation. On the field for a metallic sphere of radius $a = 0.15/2$ m seen in the back-scattering position at a distance $r = 1$ m. We consider 500 frequency measures uniformly distributed between $k = 0$ GHz and $k = 5$ GHz computed using an appropriate truncation of the Mie series (II.7). We then extend the data on 500 frequency measures uniformly distributed between $k = 5$ GHz and $k = 10$ GHz using iteratively the computed Luneberg-Kline series terms (II.20), then the association between the optic part / Luneberg-Kline series and the creeping wave part (II.25). The data is symmetrized with respect to the imaginary axis using the conjugation symmetry of the field. We further apply the vector-fitting algorithm presented in [17], [18] and [19] using 100 poles. We do a selection of poles using criteria given by [37] in order to avoid poles that are irrelevant, as in the case presented on Figure II.3b. The reconstructed poles are presented on Figures II.14, II.15 and II.16. On these figures, we plot the exact poles in red (\times), the reconstructed poles in blue (+), and the measure points in green (\cdot).

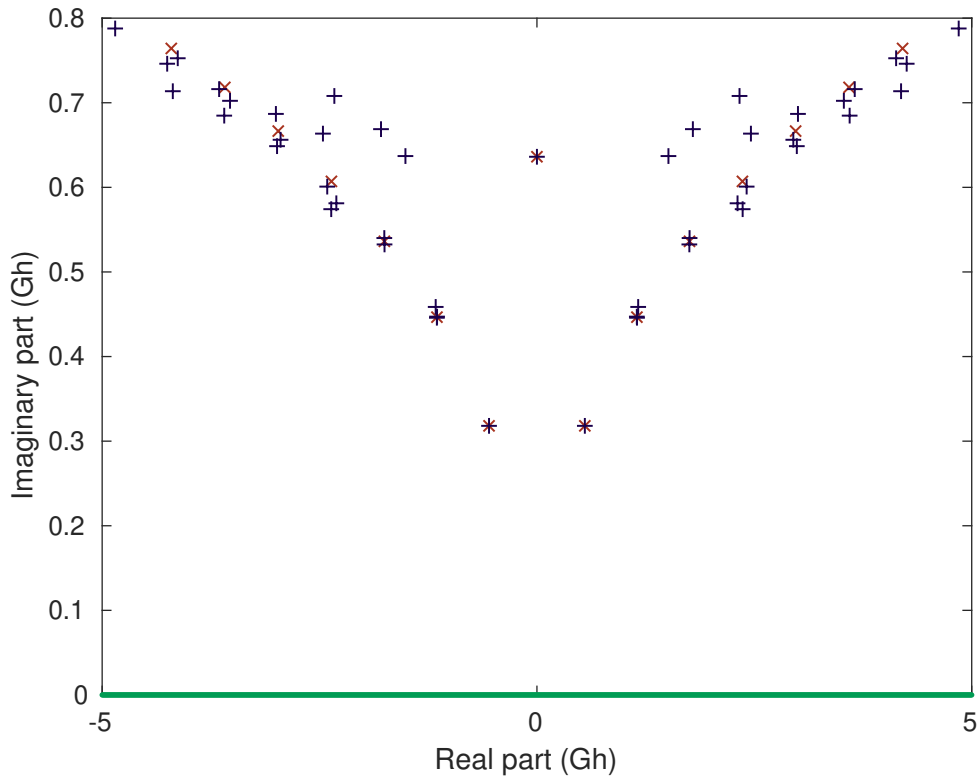


Figure II.14: Exact poles (red) and reconstructed poles (blue) using 500 frequencies uniformly distributed from 0 to 5 GHz.

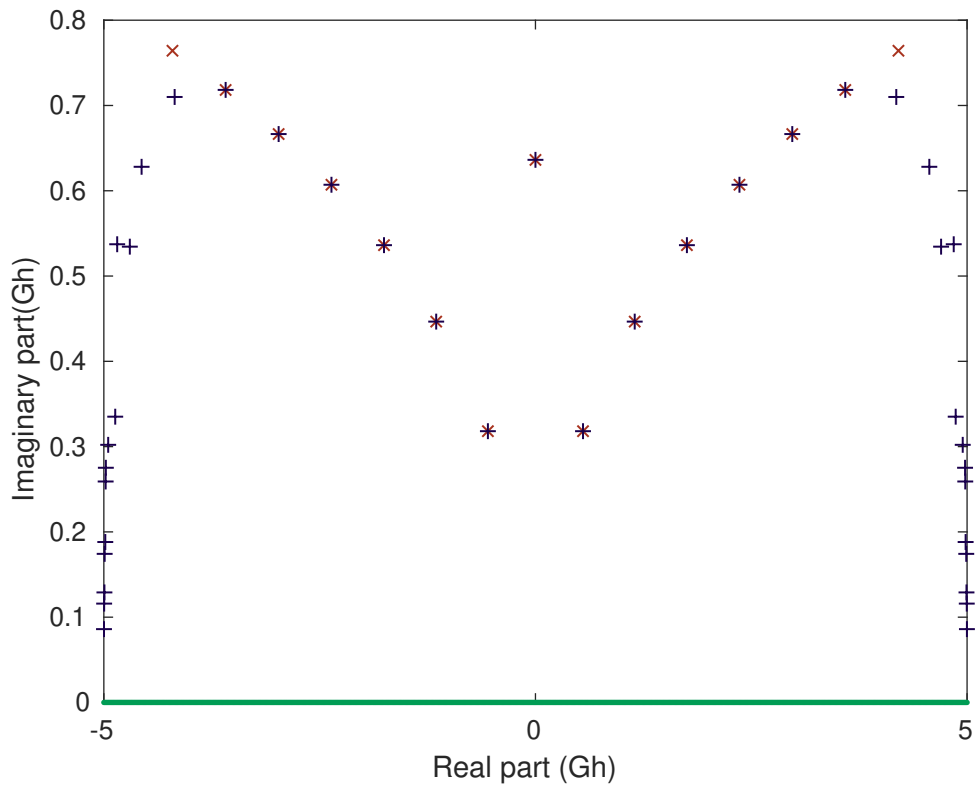


Figure II.15: Exact poles (red) and reconstructed poles (blue) using 500 frequencies uniformly distributed from 0 to 5 GHz and extended to 10 GHz with the Luneberg-Kline approximation.

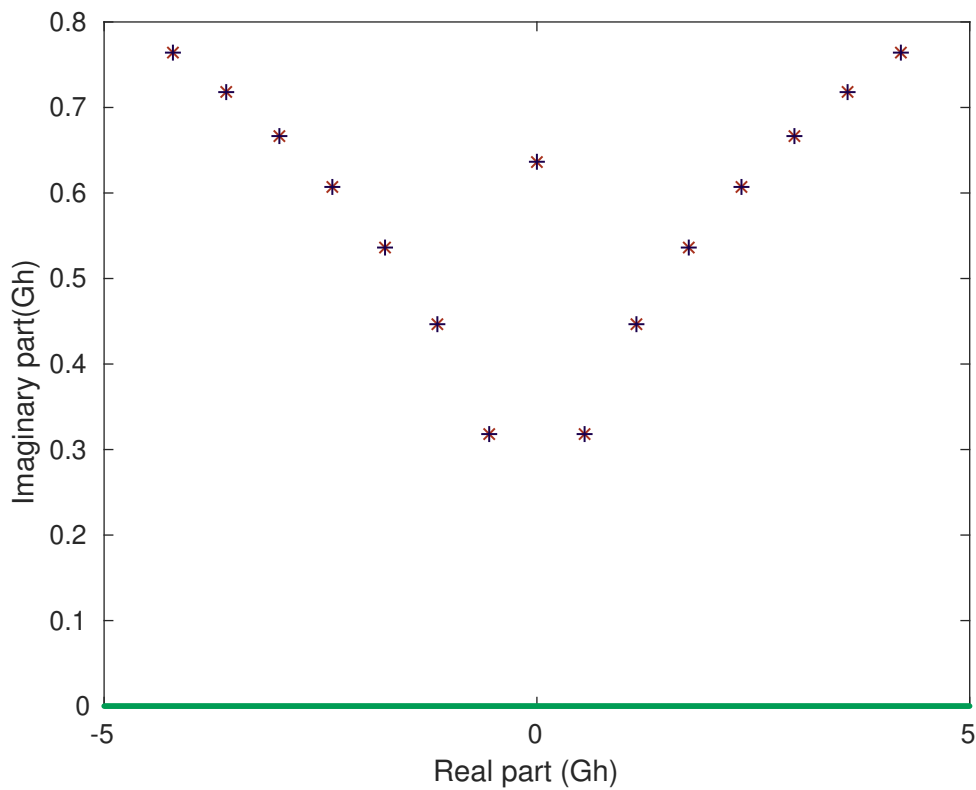


Figure II.16: Exact poles (red) and reconstructed poles (blue) using 500 frequencies uniformly distributed from 0 to 5 GHz and extended to 10 GHz with the complete approximation.

On Figure II.14 we plot the poles computed using the Mie series data. We can see that the computed poles are too numerous in the plotted region. On Figure II.15 we plot the poles computed using the Mie series data and the optic extension. We see that this extension is not proper, as the transition between the Mie series and the optic part induces an accumulation of poles not related to the field but rather to the rough switch of behavior. Finally, on Figure II.16 we plot the poles computed using the Mie series data and the optic and creeping extensions together. We can see that the computed poles are accurate. This illustrates the possibility of extending the field using the form (II.20) and a given set of data in order to improve the pole reconstruction.

This illustrates the convergence properties of the least-squares multipoint Padé approximant studied in the Section II.4. Indeed, extending the field allowed us to increase the number N of (measurement) points, hence also the degrees m and n of the approximant p/q . Such increases induce the convergence behavior of the poles described by Proposition II.1.3 and Conjecture II.4.1.

II.3 Least-squares Padé approximant at 0

Let F be a compact set in \mathbb{C} such that $\text{cap}(F) = 0$ and $0 \notin F$. Let f be analytic in $\overline{\mathbb{C}} \setminus F$. F is the singular set of f . For $m \in \mathbb{N}$, $n \in \mathbb{N}$ and $N \in \mathbb{N}$ such that $m + n + 1 \leq N$, we consider the criterion:

$$J_0 : \mathcal{P}_n \times \mathcal{P}_m^0 \longrightarrow \mathbb{R}_+$$

$$(p, q) \longmapsto \sum_{i=0}^{N-1} |c_i(p, q, f)|^2, \quad (\text{II.26})$$

where $c_i = c_i(p, q, f)$ is the i -th Taylor coefficient of $p - qf$:

$$(p - qf)(x) = \sum_{i=0}^{+\infty} c_i x^i.$$

We intend to find the best rational approximation of f at 0 of type m and n in the least-squares sense by minimizing this least-squares criterion:

Problem II.3.1. *Given $m \in \mathbb{N}$, $n \in \mathbb{N}$ and $N \in \mathbb{N}$ such that $m + n + 1 \leq N$, find $p_{m,n,N}^0 \in \mathcal{P}_n$ and $q_{m,n,N}^0 \in \mathcal{P}_m^0$ such that:*

$$(p_{m,n,N}^0, q_{m,n,N}^0) \in \underset{p \in \mathcal{P}_n, q \in \mathcal{P}_m^0}{\text{Arg min}} J_0(p, q).$$

We call a fraction $p_{m,n,N}^0/q_{m,n,N}^0$ a least-squares Padé approximant of f at 0. It always exists but its uniqueness is not systematic and is discussed in Section. For given integers m, n and N with $N \geq m + n + 1$ we define the strong uniqueness property of a solution to Problem II.3.1 as the uniqueness of both its numerator $p_{m,n,N}^0$ and its denominator $q_{m,n,N}^0$, and its weak uniqueness property as the uniqueness of the quotient $p_{m,n,N}^0/q_{m,n,N}^0$ itself. Let us introduce the notation:

$$p_{m,n,N}^0(x) = \sum_{i=0}^n p_i x^i, \quad f(x) = \sum_{i=0}^{\infty} f_i x^i,$$

$$q_{m,n,N}^0(x) = \sum_{i=0}^m q_i x^i.$$

Hence, for all $i \in \mathbb{N}$:

$$c_i = p_i - \sum_{s=0}^i q_s f_{i-s}. \quad (\text{II.27})$$

Through differentiation of the criterion (II.26) with respect to the coefficients of p and q and using the formula (II.27), we see that $p_{m,n,N}^0$ and $q_{m,n,N}^0$ satisfy the critical points equations:

$$\forall d \in \llbracket 0, n \rrbracket : c_d = 0, \quad (\text{II.28})$$

$$\forall d \in \llbracket 1, m \rrbracket : \sum_{i=d}^{N-1} \bar{c}_i f_{i-d} = 0. \quad (\text{II.29})$$

As for Padé approximant at 0, we proved a result analogous to Theorem II.1.1 (Nuttall-Pommerenke) for this approximation which is stated in Theorem II.3.2 and proven in Section II.3.2.

Theorem II.3.2. *Let F be a compact set in \mathbb{C} such that $\text{cap}(F) = 0$ and $0 \notin F$. Let f be analytic in $\overline{\mathbb{C}} \setminus F$. Then for all compact sets $K \subset \mathbb{C}$, for all $\varepsilon > 0$, $\delta > 0$, $\mu > 1$, $\lambda \geq 1$, there exists $m_0 \in \mathbb{N}$ such that for all natural numbers m , n and N which satisfy:*

$$\begin{aligned} m + n + 1 &\leq N \leq \mu m, \\ m/\lambda &\leq n \leq \lambda m, \\ m_0 &\leq m, \end{aligned}$$

we have:

$$|f - p_{m,n,N}^0/q_{m,n,N}^0| < \varepsilon^m,$$

on $K \setminus E_{m,n}$ with $\text{cap}(E_{m,n}) \leq \delta$.

II.3.1 Existence and uniqueness

In Section II.3.1.a, we prove the existence of minimizers of the criterion II.26. In Section II.3.1.b, we study the strong uniqueness property for any given function f while in Section II.3.1.c we study the set of functions f for which there exists a triple m , n , and N in \mathbb{N} for which the strong uniqueness property does not hold true, and show that it is of empty interior in the ℓ^2 topology. Then, in Section II.3.1.d, we discuss the case in which strong uniqueness does not hold true and show that it induces weak uniqueness for some lower orders m , n and N . Finally, in Section II.3.1.e, we discuss the normalization choice and show that it has no effect on the solutions when the strong uniqueness holds true for all normalization.

II.3.1.a Existence

As the criterion (II.26) is continuous on $\mathcal{P}_n \times \mathcal{P}_m \simeq \mathbb{R}^{n+m+1}$, there exists (at least) a minimum if there exists a bounded minimizing sequence. Let $(p^k, q^k)_{k \in \mathbb{N}}$ be a minimizing sequence of polynomials in $\mathcal{P}_n \times \mathcal{P}_m^0$ which satisfy Equation (II.28) (it is always possible) and Q^k be the vector (q_1^k, \dots, q_m^k) . Using equations (II.27) and (II.28) we see that the criterion evaluated on the minimizing sequence is for all $k \in \mathbb{N}$:

$$J_0(p^k, q^k) = \left\| \begin{pmatrix} f_{n+1} & \cdots & \cdots & f_{n+1-m} \\ f_{n+2} & \cdots & \cdots & f_{n+2-m} \\ \vdots & & & \vdots \\ f_{N-1} & \cdots & \cdots & f_{N-1-m} \end{pmatrix} \begin{pmatrix} 1 \\ q_1^k \\ \vdots \\ q_m^k \end{pmatrix} \right\|_{\ell^2}^2. \quad (\text{II.30})$$

Let \mathfrak{A} be the $(N - n - 1) \times m$ matrix:

$$\mathfrak{A} = \begin{pmatrix} f_n & \cdots & \cdots & f_{n+1-m} \\ f_{n+1} & \cdots & \cdots & f_{n+2-m} \\ \vdots & & & \vdots \\ f_{N-2} & \cdots & \cdots & f_{N-1-m} \end{pmatrix}.$$

For all $k \in \mathbb{N}$, we define the vector \tilde{Q}^k to be the orthogonal projection of Q^k on $\ker(\mathfrak{A})^\perp$ and we define the polynomials $\tilde{q}^k = 1 + \sum_{i=1}^m Q_i^k X^i$ and \tilde{p}^k according to Equation (II.28). Clearly, the pair $(\tilde{p}^k, \tilde{q}^k)_{k \in \mathbb{N}}$ is also a minimizing sequence as for all $k \in \mathbb{N}$ we have $J_0(p^k, q^k) = J_0(\tilde{p}^k, \tilde{q}^k)$. If the sequence $(\tilde{q}^k)_{k \in \mathbb{N}}$ is bounded then so is $(\tilde{p}^k)_{k \in \mathbb{N}}$ because

of Equation (II.28). Hence, $(\tilde{p}^k, \tilde{q}^k)_{k \in \mathbb{N}}$ is a bounded minimizing sequence and we can conclude that there exists a minimum of the criterion (II.26).

Otherwise, let us define the sequence $(\hat{q}^k)_{k \in \mathbb{N}} \stackrel{\text{def}}{=} (\tilde{q}^k / |\tilde{q}^k|)_{k \in \mathbb{N}}$. As the sequence $(\hat{q}^k)_{k \in \mathbb{N}}$ is bounded, we can extract a subsequence that converges towards a polynomial $q^* \in X\mathcal{P}_{m-1}$ and define the polynomial p^* according to Equation (II.28) and the vector $Q^* = (q_1^*, \dots, q_m^*)$.

On the one hand, we see that $|Q^*| = 1$ as for all $k \in \mathbb{N}$, we have $|\hat{q}^k| = 1$ and $q_0^* = 0$. On the other hand, as $(J(\tilde{p}^k, \tilde{q}^k))_{k \in \mathbb{N}}$ is bounded, we see that:

$$J(p^*, q^*) = \lim_{k \rightarrow +\infty} \frac{J(\hat{p}^k, \hat{q}^k)}{|\hat{q}^k|^2} = 0.$$

Hence, because of Equation (II.30), the vector Q^* belongs to $\ker(\mathfrak{A})$ and, as it also belongs $\ker(\mathfrak{A})^\perp$, it is equal to zero. Hence, we have found the contradiction that the vector Q^* is both 0 and of norm 1. Thus the sequence $(\hat{q}^k)_{k \in \mathbb{N}}$ is bounded. So, we have shown that there exists a bounded minimizing sequence hence the criterion J_0 admits a minimum in $\mathcal{P}_n \times \mathcal{P}_m^0$.

II.3.1.b Strong uniqueness property

As the criterion (II.26) is differentiable and convex on $\mathcal{P}_n \times \mathcal{P}_m^0 \simeq \mathbb{R}^{n+m+1}$, the uniqueness of the minimizer, hence the strong uniqueness property, is induced by the uniqueness of the solution to the critical point equations (II.28) and (II.29). Let $n \geq m$. Using the system of equations (II.27) and (II.28), we see that the numerator $p_{m,n,N}^0$ is uniquely and explicitly defined by $q_{m,n,N}^0$ through:

$$\forall d \in \llbracket 0, n \rrbracket : p_d = \sum_{s=0}^d q_s f_{d-s}.$$

In contrast, using the systems of equations (II.27) and (II.29), we see that $q_{m,n,N}^0$ is only implicitly given by:

$$\forall d \in \llbracket 1, m \rrbracket : \sum_{s=1}^m q_s \sum_{i=n+1}^{N-1} \overline{f_{i-d}} f_{i-s} = - \sum_{i=n+1}^{N-1} \overline{f_{i-d}} f_i.$$

Hence, we see that $q_{m,n,N}^0$ is uniquely defined if and only if the matrix $G \in M_m(\mathbb{C})$ defined by:

$$\forall d \in \llbracket 1, m \rrbracket, \forall s \in \llbracket 1, m \rrbracket, G_{s,d} = \sum_{i=n+1}^{N-1} f_{i-s} \overline{f_{i-d}},$$

is invertible. One can see that G is a Gram matrix for the vectors:

$$\begin{pmatrix} f_{n+1-m} \\ \vdots \\ f_{N-1-m} \end{pmatrix}, \begin{pmatrix} f_{n+1-(m-2)} \\ \vdots \\ f_{N-1-(m-2)} \end{pmatrix}, \dots, \begin{pmatrix} f_n \\ \vdots \\ f_{N-2} \end{pmatrix}.$$

So, uniqueness of $q_{m,n,N}^0$ and $p_{m,n,N}^0$ is ensured by the linear independence of those m vectors of \mathbb{C}^{N-n-1} . Using [38, Lem. 3 (Kronecker)], we see that if f is a rational function, $q_{m,n,N}^0$ and $p_{m,n,N}^0$ are not unique if m and N are big enough hence the strong uniqueness property does not hold true. On the contrary, if f is not rational, for all $m, n \in \mathbb{N}$ there exists $N_0 \geq n + m + 1$ such that for all $N \geq N_0$, $q_{m,n,N}^0$ and $p_{m,n,N}^0$ the strong uniqueness property holds true.

II.3.1.c Functions for which the strong uniqueness property fails

Lemma II.3.3. *The set of functions f in ℓ^2 such that there exist natural numbers n, m and N for which the the strong uniqueness property of the solutions to Problem II.3.1 does not hold true is of empty interior for the ℓ^2 topology.*

Proof. Let:

$$\ell^2 = \left\{ \sum_{i=0}^{+\infty} f_i x^i, \sum_{i=0}^{+\infty} |f_i|^2 < \infty \right\},$$

endowed with the norm: $\|f\| = (\sum_{i=0}^{+\infty} |f_i|^2)^{1/2}$. The space $(\ell^2, \|\cdot\|)$ is a complete normed space. For all $m, n \in \mathbb{N}$, let us consider the application:

$$H_{m,n} : \ell^2 \longrightarrow \mathbb{C}$$

$$f \longmapsto \det \begin{pmatrix} f_n & f_{n-1} & \cdots & f_{n-m+1} \\ f_{n+1} & f_n & \cdots & f_{n-m+2} \\ \vdots & \vdots & \ddots & \vdots \\ f_{n+m-1} & f_{n+m-2} & \cdots & f_n \end{pmatrix}.$$

We see that the set of all functions in ℓ^2 such that there exist a choice of m, n and N such that the criterion does not have a unique minimum is:

$$B = \bigcup_{n=0}^{+\infty} \bigcup_{m=0}^{+\infty} H_{m,n}^{-1}(\{0\}).$$

For all $m, n \in \mathbb{N}$, as a polynomial function, $H_{m,n}$ is continuous and not constant on any open set hence $H_{m,n}^{-1}(\{0\})$ is closed and is of empty interior. Hence, applying Baire category theorem [39, Thm 3.9.3], B is of empty interior. \square

II.3.1.d Weak uniqueness property

In this section, we discuss the weak uniqueness property of the approximant hence the uniqueness of the quotient $p_{m,n,N}^0/q_{m,n,N}^0$. Let f be a function analytic around 0. We show the following property:

Proposition II.3.4. *For all $a > 2$, there exist three increasing sequences $(m_k)_{k \in \mathbb{N}}$, $(n_k)_{k \in \mathbb{N}}$ and $(N_k)_{k \in \mathbb{N}}$ of integer numbers satisfying $a(n_k + m_k) \geq N_k \geq a(m_k + n_k) - m_k$ for all $k \in \mathbb{N}$, such that the weak uniqueness property holds true.*

This proposition illustrates that for any function f analytic around 0, we can construct an infinite sequence of approximations verifying the hypothesis of Theorem II.3.2 and for which the approximant is unique.

Proof. First, if f is rational, then for m and n large enough and all $N \geq m + n + 1$, there exists a Padé approximant of order m, n , and N . Hence, because of the uniqueness of the quotient in Padé approximation, the approximant is unique in this case.

Then, if the strong uniqueness property holds true as studied in Section II.3.1.b, the quotient is obviously unique hence the weak uniqueness property holds true.

Finally, let us study the case in which the strong uniqueness property does not hold true. Let m, n and N be three positive integers verifying $m + n + 1 \leq N$ for which Problem

II.3.1 does not have a unique solution. Let $(p, q) \in \mathcal{P}_n \times \mathcal{P}_m^0$ and $(p+r, q+s) \in \mathcal{P}_n \times \mathcal{P}_m^0$ be two solutions of Problem II.3.1. As we assumed that the solution pair is not unique, we have $s \neq 0$ and because of the normalization, $s(0) = 0$. Furthermore, by linearity of the critical points equations (II.28) and (II.29), s is in $\ker(\mathfrak{A})$. Thus because of the definition of \mathfrak{A} , there exists a polynomial $\pi \in \mathcal{P}_n$ such that:

$$sf = \pi + O(X^N). \quad (\text{II.31})$$

Let $d \in \llbracket 1, m \rrbracket$ be the maximal integer such that $s \in X^d \mathcal{P}_{m-d}$ and let us write $s = s_d X^d \tilde{q}$ and $\pi = s_d X^d \tilde{p}$ with $\tilde{q} \in \mathcal{P}_{m-d}^0 \subset \mathcal{P}_m^0$, $\tilde{p} \in \mathcal{P}_{n-d} \subset \mathcal{P}_n$ and $s_d \neq 0$. Simplifying the Equation (II.31), we get:

$$\tilde{q}f = \tilde{p} + O(X^{N-d}),$$

where $\tilde{p} \in \mathcal{P}_n$ and $\tilde{q} \in \mathcal{P}_m^0$.

We see that (\tilde{p}, \tilde{q}) is a minimizer of Problem II.3.1 for m, n and $N-d$, as $J_0(\tilde{p}, \tilde{q}) = 0$, and it is a Padé approximant with degrees m, n , and $N-d$, with $d \in \llbracket 1, m \rrbracket$ as long as $N-d \geq m+n+1$. Because of the uniqueness of the quotient in Padé approximation, this shows the uniqueness of the quotient for the least-squares Padé approximation at 0 with degrees m, n , and $N-d$. Hence, if the problem does not enjoy the strong uniqueness property with degrees m, n , and N , it enjoys the weak uniqueness property with degrees m, n , and $N-d$ with $d \in \llbracket 1, m \rrbracket$ as long as $N-d \geq m+n+1$.

Let $a > 2$ and let us define three increasing sequences $(m_k)_{k \in \mathbb{N}}$, $(n_k)_{k \in \mathbb{N}}$ and $(N_k^0)_{k \in \mathbb{N}}$ of integer numbers satisfying $N_k^0 = a(m_k + n_k)$ for all $k \in \mathbb{N}$. For all $k \in \mathbb{N}$, either the strong uniqueness property holds true with degrees m_k, n_k and N_k^0 or the weak uniqueness property holds true for some degrees m_k, n_k and $N_k = N_k^0 - d_k$ with $d_k \leq m_k$. Hence, we have shown that we can construct three increasing sequences $(m_k)_{k \in \mathbb{N}}$, $(n_k)_{k \in \mathbb{N}}$ and $(N_k)_{k \in \mathbb{N}}$ of integer numbers, satisfying $N_k \in \llbracket N_k^0 - m_k, N_k^0 \rrbracket$ for all $k \in \mathbb{N}$, for which the weak convergence property holds. By construction, the sequence satisfy $a(m_k + n_k) \geq N_k \geq a(m_k + n_k) - m_k$ for all $k \in \mathbb{N}$. Furthermore, as $a > 2$, we have $m_k + n_k + 1 < N_k$ which concludes this proof. \square

II.3.1.e Choice of the normalization

Let us fix n, m and N in \mathbb{N} satisfying $n+m+1 \geq N$. When approximating a function which is analytic at 0 in a least-squares sense, we have a choice for the normalization. Indeed in Section II.3 we have chosen $q_{m,n,N}^0(0) = 1$. Nevertheless a valid choice can be for any $d \in \llbracket 0, m \rrbracket$:

$$q_d^d = 1,$$

where we write $q^d = q_{m,n,N}^0$ for this choice of normalization:

$$(p^d, q^d) \in \underset{p \in \mathcal{P}_n, q \in \mathcal{P}_m, q_d=1}{\text{Arg min}} J_0(p, q).$$

Indeed, for any of these normalization choices, Equation (II.29) becomes for all $k \in \llbracket 0, m \rrbracket$, $k \neq d$:

$$(GQ^d)_k = 0,$$

where Q^d is the coefficients vector of q^d and the $m \times m$ matrix G is defined for all $(i, j) \in \llbracket 0, m \rrbracket^2$:

$$G_{i,j} = \sum_{k=n+1}^{N-1} f_{k-i} \overline{f_{k-j}}.$$

Hence, if G is invertible:

$$Q = q_d^d G^{-1} G_d,$$

where G_d is the d -th column of G .

We see that if G is invertible (hence q^d is uniquely defined for any normalization), two different normalizations $d = d_1 \in \llbracket 0, m \rrbracket$ and $d = d_2 \in \llbracket 0, m \rrbracket$ will lead to two proportional q^{d_1} and q^{d_2} . Hence, because of Equation (II.28) which defines $p^d = p_{m,n,N}^d$, the fractions p^{d_1}/q^{d_1} and p^{d_2}/q^{d_2} they induce will be the same.

Nevertheless, the choice $d = 0$ is natural has when $f = p_f/q_f$ is a rational function analytic at 0 with $p_f \in \mathcal{P}_n$ and $q_f \in \mathcal{P}_m$, (p_f, q_f) is among the minimizers of the criterion (II.26) which is not necessarily true for other normalizations. For example, if we choose $f : z \mapsto z$, $n = 1$ and $m = 1$, $(p_f, q_f) = (z \mapsto z, z \mapsto 1)$ is a solution for $d = 0$ but not for $d = 1$.

II.3.2 Proof of Theorem II.3.2

First, we see that if f is a rational fraction then for m and n large enough, the approximation error $|p_{m,n,N}^0/q_{m,n,N}^0 - f|$ is uniformly zero in $\mathbb{C} \setminus F$ hence the theorem is trivial in this case.

In the following, we assume that f is not a rational function. We can consider the case where the compact set K coincides with $D(0, r)$, the disk of center 0 and radius $r > 1$ chosen such that $F \subset D(0, r)$. Let $2\rho > 0$ be the distance between F and 0. Let m, n in \mathbb{N} such that $1/\lambda \leq n/m \leq \lambda$ with $\lambda \geq 1$. Let $0 < \varepsilon < 1/3$ and $\delta > 3r\varepsilon^{1/3}$. As $\text{cap}(F) = 0$, for all $\eta > 0$, there exists a natural number k and a polynomial h in \mathcal{P}_m^1 such that $F \subset D_\eta$ where:

$$D_\eta = \{z \in \mathbb{C}, |h(z)| < \eta^k\}.$$

For the purpose of this proof, we choose:

$$\eta = \frac{\varepsilon^{2+\mu} \rho^\mu}{3r^{\mu+1}} \leq \varepsilon.$$

Hence, because of the definition (B.1) of the capacity, $\text{cap}(D_\eta) \leq \eta \leq \varepsilon$. Let $n \geq m > k$ and $\ell \in \mathbb{N}$ such that $m - k < k\ell \leq m$. Let us introduce the notation:

$$h^\ell(x) = \sum_{i=0}^m h_i^\ell x^i.$$

Let $(a_0, \dots, a_{N-m-n-1})$ and (b_1, \dots, b_m) be two vectors of \mathbb{C}^{N-n-m} and \mathbb{C}^m respectively which solve the system:

$$\forall i \in \llbracket n+1, N-1 \rrbracket : \sum_{t=0}^{N-1-i} a_t h_{N-1-i-t}^\ell - \sum_{d=1}^m b_d \overline{f_{i-d}} = 0. \quad (\text{II.32})$$

It is an homogeneous linear system of $N - n - 1$ equations and $N - n$ unknowns so there exists a non trivial vector space of solutions. One can see that the solutions of the system (II.32) are such that $(a_0, \dots, a_{N-m-n-1})$ is not the null vector. Indeed, (b_1, \dots, b_m) would then be such that:

$$\forall i \in \llbracket n+1, N-1 \rrbracket : \sum_{d=1}^m b_d \overline{f_{i-d}} = 0,$$

which, according to [38, Lem. 3 (Kronecker) p.5] would lead (b_1, \dots, b_m) to also be the null vector for f not a rational function. Hence, we can choose the solution that has the property:

$$\sup_{z \in D(0,r)} |a(z)| = 1, \quad (\text{II.33})$$

where we defined the polynomial $a \in \mathcal{P}_{N-m-n-1}$ by:

$$a(z) = \sum_{i=0}^{N-m-n-1} a_i z^i.$$

Using the systems (II.28), (II.29) and (II.32), we see that this choice of a leads to:

$$\sum_{i=0}^{N-1} c_i \sum_{t=0}^{N-1-i} a_t h_{N-1-i-t}^\ell = 0. \quad (\text{II.34})$$

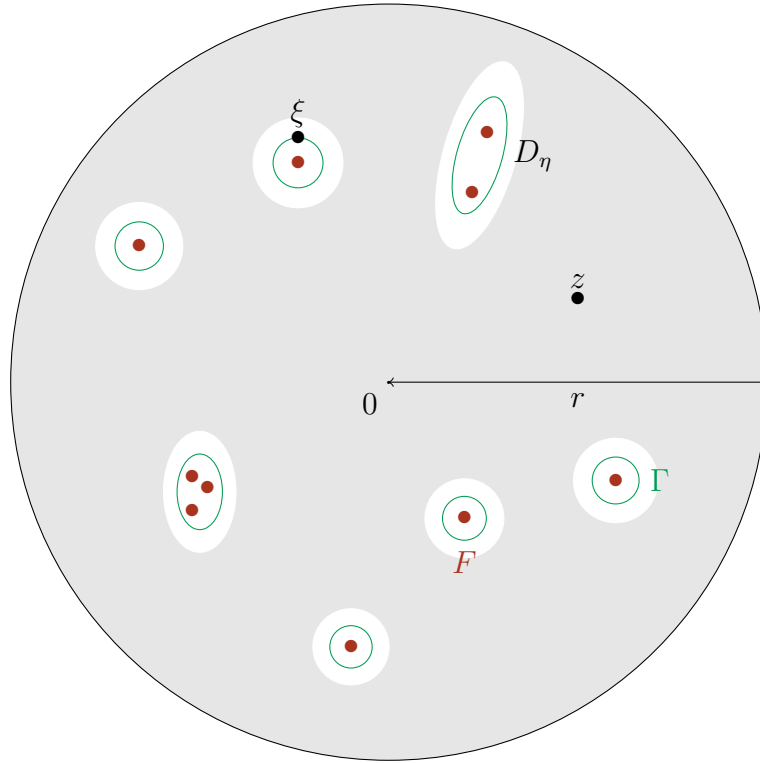


Figure II.17: Scheme of the geometrical setting of the different sets and points considered in the proof of Theorem II.3.2.

Let Γ be a cycle in D_η surrounding F . The situation is summarized on Figure II.17 where F is represented by red points, Γ is represented as green curves and D_η is represented as white regions in the gray disk $D(0, r)$. By applying Cauchy's integral formula for $z \in \mathbb{C} \setminus D_\eta$:

$$\begin{aligned} \frac{1}{2\pi i} \int_{\Gamma} \frac{h^\ell(\xi)(p_{m,n,N}^0 - q_{m,n,N}^0 f)(\xi)a(\xi)}{\xi^N(\xi - z)} d\xi &= \frac{1}{z} \sum_{i=0}^{N-1} c_i \sum_{t=0}^{N-1-i} a_t h_{N-1-i-t}^\ell \\ &+ \frac{h^\ell(z)(p_{m,n,N}^0 - q_{m,n,N}^0 f)(z)a(z)}{z^N}, \end{aligned}$$

because the residue at infinity is null. Using Equation (II.34) and because the function $\xi \mapsto \frac{h^\ell(\xi)p_{m,n,N}^0(\xi)a(\xi)}{\xi^N(\xi-z)}$ is analytic in the interior of Γ for all $z \in \mathbb{C} \setminus D_\eta$, this leads to:

$$\frac{h^\ell(z)(p_{m,n,N}^0 - q_{m,n,N}^0 f)(z)a(z)}{z^N} = -\frac{1}{2\pi i} \int_\Gamma \frac{h^\ell(\xi)q_{m,n,N}^0(\xi)f(\xi)a(\xi)}{\xi^N(\xi-z)} d\xi. \quad (\text{II.35})$$

Using Equation (II.35), we can estimate the error for all $z \in \mathbb{C} \setminus D_\eta$:

$$\left| \frac{p_{m,n,N}^0}{q_{m,n,N}^0} - f \right| (z) \leq C_0 \frac{\eta^{k\ell}}{|h^\ell(z)|} \sup_{\xi \in \Gamma} \left| \frac{a(\xi)}{a(z)} \right| \sup_{\xi \in \Gamma} \left| \frac{q_{m,n,N}^0(\xi)}{q_{m,n,N}^0(z)} \right| \sup_{\xi \in \Gamma} \left| \frac{z^N}{\xi^N} \right|,$$

where $C_0 = C_0(\eta, \Gamma, f)$ is independent of n . We estimate the above right hand side by using the following:

- $\eta^{k\ell} < \eta^{m-k}$ because $m - k < k\ell$,
- by choosing η small enough, we can assume that for all $\xi \in \Gamma$, $|\xi| > \rho$. Furthermore, as $z \in D(0, r)$, we have the estimation: $\sup_{\xi \in \Gamma} \left| \frac{z^N}{\xi^N} \right| \leq \left(\frac{r}{\rho} \right)^N$,
- using Lemma B.0.3, for all $z \in D(0, r)$, $\sup_{\xi \in \Gamma} \left| \frac{q_{m,n,N}^0(\xi)}{q_{m,n,N}^0(z)} \right| \leq \frac{(3r)^m}{|q^*(z)|}$ where q^* is polynomial in $\mathcal{P}_{m^*}^1$ with $m^* \leq m$,
- using the normalization (II.33), $\sup_{\xi \in \Gamma} |a(\xi)| \leq 1$,
- using Lemma B.0.2, because of the normalization (II.33), $|a(z)| \geq \varepsilon^{N-m-n-1}$ for $z \in D(0, r) \setminus \Theta$ where $\text{cap}(\Theta) \leq 3r\varepsilon$,
- $h^\ell q^* \in \mathcal{P}_{2m}$ is a monic polynomial so, by definition (B.1) of the capacity, $|h^\ell q^*(z)| \geq \varepsilon^{2m}$ for $z \in D(0, r) \setminus \Phi$ where Φ is a set of capacity bounded by ε .

Thus, for all $z \in D(0, r) \setminus E_{m,n}$ with $E_{m,n} = D_\eta \cup \Theta \cup \Phi$:

$$\left| \frac{p_{m,n,N}^0}{q_{m,n,N}^0} - f \right| (z) \leq C_0 \eta^{m-k} \frac{(3r)^m}{\varepsilon^{N-1}} \left(\frac{r}{\rho} \right)^N.$$

Using our choice of η and the linear growth of N with m , we get for $m > m_0(\varepsilon)$:

$$\left| \frac{p_{m,n,N}^0}{q_{m,n,N}^0} - f \right| (z) < \varepsilon^m,$$

for all $z \in D(0, r) \setminus E_{m,n}$.

Applying Lemma B.0.1 with $\alpha = \varepsilon$ and $d = 2$, we get that the exceptional set has a capacity:

$$\text{cap}(E_{m,n}) \leq (3r\varepsilon)^{1/3} (2r)^{2/3} \leq 3r\varepsilon^{1/3} \leq \delta,$$

which concludes our proof. The case $n \leq m$ can be shown similarly by appropriately changing the definition of ℓ into $n - k < k\ell \leq n$.

II.4 Least-squares multipoint Padé approximant

Let E and F be compact sets in \mathbb{C} such that $\text{cap}(F) = 0$ and $E \cap F = \emptyset$. Let f be analytic in $\overline{\mathbb{C}} \setminus F$. F is the singular set of f and E is the set at which we can measure f . For $m \in \mathbb{N}$, $n \in \mathbb{N}$ and $N \in \mathbb{N}$ such that $m + n + 1 \leq N$, we consider the criterion:

$$J : \mathcal{P}_n \times \mathcal{P}_m^1 \longrightarrow \mathbb{R}_+$$

$$(p, q) \longmapsto \sum_{i=1}^N |p(z_i) - q(z_i)f(z_i)|^2, \quad (\text{II.36})$$

where $(z_i)_{i \in [1, N]}$ is a collection of N points in E .

We intend to extend the multipoint Padé approximation described in the previous section order to find the best rational approximation of f at 0 of type m and n in the least-squares sense by minimizing this least-squares criterion:

Problem II.4.1. *Given $m \in \mathbb{N}$, $n \in \mathbb{N}$ and $N \in \mathbb{N}$ such that $m + n + 1 \leq N$, find $p_{m,n,N} \in \mathcal{P}_n$ and $q_{m,n,N} \in \mathcal{P}_m^1$ such that:*

$$(p_{m,n,N}, q_{m,n,N}) \in \underset{p \in \mathcal{P}_n, q \in \mathcal{P}_m^1}{\text{Arg min}} J(p, q).$$

We call the fraction $p_{m,n,N}/q_{m,n,N}$ the monic multipoint least-squares Padé approximation of f . As the criterion (II.36) is convex we respect to p and q , a minimizer always exists but the uniqueness of the minimizer is not systematic. The existence of a minimizer can be shown in a similar manner as in Section II.3.1.a.

For $m \geq 1$, by differentiation of (II.36) we respect to the coefficients of p and q , we see that $p_{m,n,N}$ and $q_{m,n,N}$ are such that for all polynomials $\chi \in \mathcal{P}_n$ and $\psi \in \mathcal{P}_{m-1}$:

$$\sum_{i=1}^N \overline{(\chi - \psi f)(z_i)} (p_{m,n,N} - q_{m,n,N} f)(z_i) = 0. \quad (\text{II.37})$$

For $m = 0$, the critical point equation (II.37) becomes: for all $\chi \in \mathcal{P}_n$,

$$\sum_{i=1}^N \overline{\chi}(z_i) (p_{0,n,N} - q_{0,n,N} f)(z_i) = 0.$$

Remark 9. When $N = m + n + 1$, the minimum of the criterion (II.36) is equal to 0 and the monic multipoint least-squares Padé approximation coincides with the multipoint Padé approximation presented in section II.1.2.b.

A weak extension of the Nuttall-Pommerenke theorem (Theorem II.1.2) for these approximant is given by the Theorem II.4.2. Furthermore the Conjecture II.4.1, if proven, could be a more powerful generalization of Theorem II.1.2. Indeed, the difference between Theorem II.4.2 and Conjecture II.4.1 is the dependency of $(z_i)_{i \in [1, N]}$ with respect to m , n and N which is not needed for the classical Nuttall-Pommerenke theorem.

Theorem II.4.2. *Let E and F be two compact sets in \mathbb{C} such that $0 \notin E$, $\text{cap}(F) = 0$ and $E \cap F = \emptyset$. Let f be analytic in $\overline{\mathbb{C}} \setminus F$. Let $K \subset \mathbb{C}$ be a compact set, $\varepsilon > 0$, $\delta > 0$, $\mu > 1$, $\lambda \geq 1$. Then, there exists n_0 such that for all natural numbers m , n and N which satisfy:*

$$m + n + 1 \leq N \leq \mu n, \quad (\text{II.38})$$

$$m/\lambda \leq n \leq \lambda m, \quad (\text{II.39})$$

$$n_0 \leq n,$$

there exists a family $(z_i^{m,n,N})_{i \in [1, N]}$ of N distinct points in E such that:

$$|f - p_{m,n,N}/q_{m,n,N}| < \varepsilon^n,$$

on $K \setminus E_{m,n}$ with $\text{cap}(E_{m,n}) \leq \delta$.

Conjecture II.4.1. *Let E and F be two compact sets in \mathbb{C} such that $0 \notin E$, $\text{cap}(F) = 0$ and $E \cap F = \emptyset$. Let $(z_i)_{i \in \mathbb{N}}$ be a family of distinct points in E . Let f be analytic in $\overline{\mathbb{C}} \setminus F$. Let $K \subset \mathbb{C}$ be a compact set, $\varepsilon > 0$, $\delta > 0$, $\mu > 1$, $\lambda \geq 1$. Then, there exists n_0 such that for all natural numbers m , n and N which satisfy:*

$$m + n + 1 \leq N \leq \mu n,$$

$$m/\lambda \leq n \leq \lambda m,$$

$$n_0 \leq n,$$

we have:

$$|f - p_{m,n,N}/q_{m,n,N}| < \varepsilon^n,$$

on $K \setminus E_{m,n}$ with $\text{cap}(E_{m,n}) \leq \delta$.

The sequel of this section is dedicated to the proof of Theorem II.4.2 and a discussion on Conjecture II.4.1.

II.4.1 Proof of Theorem II.4.2

First, we see that if f is a rational fraction, then for n and m large enough, the approximation error $|p_{m,n,N}/q_{m,n,N} - f|$ is uniformly equal to zero in $\mathbb{C} \setminus F$ hence the theorem is trivial in this case.

In the following, we assume that f is not a rational function. We can assume that the compact set K coincides with the disk $D(0, r)$ of center 0 and radius $r > 1$ chosen such that $E \subset D(0, r)$ and $F \subset D(0, r)$. Let $0 < \varepsilon < 1/3$ and $\delta \geq (2r\varepsilon)^{1/2}$. As $\text{cap}(F) = 0$, for all $\eta > 0$, there exists a natural number k and a polynomial h in \mathcal{P}_k^1 such that $F \subset D_\eta$ where:

$$D_\eta = \{z \in \mathbb{C}, |h(z)| < \eta^k\}. \quad (\text{II.40})$$

For the purpose of this proof, we choose:

$$\eta = \frac{\varepsilon^{2(1+\lambda)} \rho^\mu}{(3r)^\lambda \mathfrak{C}} \leq \varepsilon,$$

where $2\rho = \text{dist}(E, F)$ and $\mathfrak{C} = \mathfrak{C}(r, \mu, \lambda)$ is defined following the relation (II.46) in Section II.4.1.b. Let $n > k$ and $\ell \in \mathbb{N}^*$ such that $n - k < k\ell \leq n$. Let Γ be a cycle in D_η surrounding F . The situation is summarized on Figure II.18 where F is represented by

This will allow us simplify Equation (II.41) in order to express the approximation error $|f - p_{m,n,N}/q_{m,n,N}|$. Then, we study the boundedness of a_z which allows us to geometrically bound the approximation error and conclude.

II.4.1.a Definition of the polynomial a_z

For $z \in \mathbb{C}$, let a_z be a polynomial in $\mathcal{P}_{N-n-m-1}$ such that there exist polynomials χ_z and ψ_z in \mathcal{P}_n and \mathcal{P}_{m-1} respectively that satisfy for all $i \in \llbracket 1, N \rrbracket$:

$$h^\ell(z_i)a_z(z_i) = \overline{[\chi_z(z_i) - f(z_i)\psi_z(z_i)]\Pi'_N(z_i)}(z_i - z). \quad (\text{II.43})$$

For all $z \in \mathbb{C}$, we express the polynomials a_z , χ_z and ψ_z as:

$$\begin{aligned} a_z(\xi) &= \sum_{t=0}^{N-m-n-1} a_t(z)\xi^t, \\ \chi_z(\xi) &= \sum_{u=0}^n \chi_u(z)\xi^u, \\ \psi_z(\xi) &= \sum_{v=0}^{m-1} \psi_v(z)\xi^v, \end{aligned} \quad (\text{II.44})$$

where for all $t \in \llbracket 0, N-m-n-1 \rrbracket$, $u \in \llbracket 0, n \rrbracket$ and $v \in \llbracket 0, m-1 \rrbracket$, $z \mapsto a_t(z)$, $z \mapsto \chi_u(z)$ and $z \mapsto \psi_v(z)$ are complex valued functions. We shall show later that using an appropriate normalization, they actually are polynomials with respect to z .

The system of equations (II.43) can then be written as a homogeneous linear system of N equations which is given for all $i \in \llbracket 1, N \rrbracket$ by:

$$h^\ell(z_i) \sum_{t=0}^{N-m-n-1} a_t(z)z_i^t - \overline{\left[\sum_{u=0}^n \chi_u(z)z_i^u - f(z_i) \sum_{v=0}^{m-1} \psi_v(z)z_i^v \right]} \Pi'_N(z_i)(z_i - z) = 0.$$

As a system in the coefficients of the polynomials a_z , χ_z and ψ_z , it is a homogeneous linear system of N equations and $(N - m - n - 1 + 1) + (n + 1) + (m - 1 + 1) = N + 1$ unknowns so there exists a non trivial vector space of solutions. We seek a solution that has the property:

$$\forall z \in \mathbb{C}, a_z(z) = \Pi_N(z). \quad (\text{II.45})$$

The existence and uniqueness of such a polynomial a_z is ensured if the following determinant is non-zero:

$$D = \det \left[\underbrace{z_i^j h^\ell(z_i)}_{j=0, \dots, N-n-m-2} \mid \underbrace{\overline{z_i^j \Pi'_N(z_i)}}_{j=0, \dots, n} \mid \underbrace{\overline{z_i^j \Pi'_N(z_i) f(z_i)}}_{j=0, \dots, m-1} \right].$$

We show in Proposition II.4.4 in Section II.4.3 that this determinant is non-zero for almost every $(z_i)_{i \in \llbracket 1, N \rrbracket}$ in \mathbb{C}^N and we choose such a sequence $(z_i)_{i \in \llbracket 1, N \rrbracket} \in [D(0, r)]^N$. Hence a_z , χ_z and ψ_z uniquely exist and solve the system:

$$\left[\underbrace{z_i^j h^\ell(z_i)}_{j=0, \dots, N-n-m-1} \mid \underbrace{0}_{j=0, \dots, n} \mid \underbrace{\overline{z_i^j \Pi'_N(z_i) f(z_i)}(z_i - z)}_{j=0, \dots, m-1} \right] \begin{bmatrix} A_z \\ X_z \\ \Psi_z \end{bmatrix} = \begin{bmatrix} 0 \\ \vdots \\ 0 \\ a_z(z) \end{bmatrix},$$

where $A_z \in \mathbb{C}^{N-m-n-1}$, $X_z \in \mathbb{C}^n$ and $\Psi_z \in \mathbb{C}^{m-1}$ are the vectors of the coefficients of a_z , χ_z and ψ_z . By applying Cramer's rule to this system and simplifying, we get that for all $t \in \llbracket 0, N-m-n-1 \rrbracket$:

$$a_t(z) = \frac{1}{D} \det \left[\underbrace{z_i^j h^\ell(z_i)}_{j=0, \dots, N-n-m-1, j \neq t} \mid \underbrace{-\bar{z}_i^j \Pi'_N(z_i)(z_i - z)}_{j=0, \dots, n} \mid \underbrace{\bar{z}_i^j \Pi'_N(z_i) \overline{f(z_i)}(z_i - z)}_{j=0, \dots, m-1} \right].$$

Hence, by using Equation (II.44), we see that the polynomial a_z is given by:

$$a_z(\xi) = \frac{1}{D} \det \left[\underbrace{z_i^j h^\ell(z_i)}_{j=0, \dots, N-n-m-1} \mid \underbrace{\xi^j}_{j=0, \dots, n} \mid \underbrace{-\bar{z}_i^j \Pi'_N(z_i)(z_i - z)}_{j=0, \dots, n} \mid \underbrace{\bar{z}_i^j \Pi'_N(z_i) \overline{f(z_i)}(z_i - z)}_{j=0, \dots, m-1} \right],$$

and by combining the columns and expand the determinant of the numerator along its last row, we find:

$$a_z(\xi) = \frac{1}{D} \det \left[\underbrace{z_i^j h^\ell(z_i)(\xi - z_i)}_{j=0, \dots, N-n-m-2} \mid \underbrace{\bar{z}_i^j \Pi'_N(z_i)(z - z_i)}_{j=0, \dots, n} \mid \underbrace{\bar{z}_i^j \Pi'_N(z_i) \overline{f(z_i)}(z - z_i)}_{j=0, \dots, m-1} \right].$$

Remark 10. Because of Equation (II.37), we see that a_z will satisfy Equation (II.42) as it satisfies the system (II.43).

II.4.1.b Upper bound of the polynomial \mathbf{a}_z

By expanding $a_z(\xi)$ and ordering its terms along the power degrees in z and ξ , we have:

$$a_z(\xi) = \sum_{t=0}^{N-m-n-1} \sum_{u=0}^{n+1} \sum_{v=0}^m (-1)^{N-t-u-v} A_{t,u,v} \xi^t z^{u+v},$$

where for all $t \in \llbracket 0, N-m-n-1 \rrbracket$, $u \in \llbracket 0, n+1 \rrbracket$ and $v \in \llbracket 0, m \rrbracket$:

$$A_{t,u,v} = \frac{1}{D} \det \left[\underbrace{z_i^j h^\ell(z_i)}_{j=0, \dots, N-n-m-1, j \neq t} \mid \underbrace{\bar{z}_i^j \Pi'_N(z_i)}_{j=0, \dots, n+1, j \neq u} \mid \underbrace{\bar{z}_i^j \Pi'_N(z_i) \overline{f(z_i)}}_{j=0, \dots, m, j \neq v} \right].$$

Let $t \in \llbracket 0, N-m-n-1 \rrbracket$, $u \in \llbracket 0, n+1 \rrbracket$ and $v \in \llbracket 0, m \rrbracket$. Let us estimate $A_{t,u,v}$. First, we see that $A_{N-m-n-1, n+1, m} = 1$. Let us now consider $(t, u, v) \neq (N-m-n-1, n+1, m)$. Let us consider points $(z_i)_{i \in \llbracket 1, N \rrbracket}$ of the form:

$$\forall i \in \llbracket 1, N \rrbracket, z_i = \sigma \omega_i,$$

where $\sigma \in \mathbb{R}_+$ and $(\omega_i)_{i \in \llbracket 1, N \rrbracket}$ are points in $C(0, 1)$. We study the limit of $A_{t,u,v}$ when σ goes to 0. We define the equivalence at $x \in \overline{\mathbb{R}}$ of two functions J_1 and J_2 by:

$$J_1 \underset{x}{\sim} J_2 \iff J_1(z) = J_2(z) \left(1 + o(1) \right) \text{ as } z \rightarrow x.$$

We see that:

$$A_{t,u,v} \underset{\sigma \rightarrow 0}{\sim} \sigma^{N-t-u-v} \frac{\det \left[\begin{array}{c|c|c} \overbrace{\omega_i^j}^{j=0, \dots, N-n-m-1, j \neq t} & \overbrace{\overline{\omega}_i^j \pi'_N(\omega_i)}^{j=0, \dots, n+1, j \neq u} & \overbrace{\overline{\omega}_i^j \pi'_N(\omega_i) f(z_i)}^{j=0, \dots, m, j \neq v} \\ \hline \underbrace{\omega_i^j}_{j=0, \dots, N-n-m-2} & \underbrace{\overline{\omega}_i^j \pi'_N(\omega_i)}_{j=0, \dots, n} & \underbrace{\overline{\omega}_i^j \pi'_N(\omega_i) f(z_i)}_{j=0, \dots, m-1} \end{array} \right]}{\det \left[\begin{array}{c|c|c} \overbrace{\omega_i^j}^{j=0, \dots, N-n-m-1, j \neq t} & \overbrace{\overline{\omega}_i^j \pi'_N(\omega_i)}^{j=0, \dots, n+1, j \neq u} & \overbrace{\overline{\omega}_i^j \pi'_N(\omega_i) f(z_i)}^{j=0, \dots, m, j \neq v} \\ \hline \underbrace{\omega_i^j}_{j=0, \dots, N-n-m-2} & \underbrace{\overline{\omega}_i^j \pi'_N(\omega_i)}_{j=0, \dots, n} & \underbrace{\overline{\omega}_i^j \pi'_N(\omega_i) f(z_i)}_{j=0, \dots, m-1} \end{array} \right]},$$

where for all $i \in \llbracket 1, N \rrbracket$:

$$\pi'_N(\omega_i) = \prod_{j=1, j \neq i}^N (\omega_i - \omega_j).$$

As the quotient on the right-hand side is bounded, we find:

$$\lim_{\sigma \rightarrow 0} A_{t,v,u}(\sigma \omega_1, \dots, \sigma \omega_N) = 0.$$

Hence, as $A_{t,v,u}$ is a continuous function of the $(z_i)_{i \in \llbracket 1, N \rrbracket}$ in a neighborhood of 0, for all m, n and N in \mathbb{N} with $N \geq m + n + 1$, there exists $(z_i^{m,n,N})_{i \in \llbracket 1, N \rrbracket} \in [D(0, r)]^N$ such that for all $t \in \llbracket 0, N - m - n - 1 \rrbracket$, $u \in \llbracket 0, n + 1 \rrbracket$ and $v \in \llbracket 0, m \rrbracket$:

$$|A_{t,v,u}| \leq 1.$$

Hence, doing this choice for the $(z_i)_{i \in \llbracket 1, N \rrbracket}$, we have, for all $\xi \in D(0, r)$ and $z \in D(0, r)$:

$$\begin{aligned} |a_z(\xi)| &\leq \sum_{t=0}^{N-m-n-1} \sum_{u=0}^{n+1} \sum_{v=0}^m |\xi|^t |z|^{u+v} \\ &\leq \left(\sum_{t=0}^{N-m-n-1} r^t \right) \times \left(\sum_{u=0}^{n+1} r^u \right) \times \left(\sum_{v=0}^m r^v \right) \\ &\leq \frac{1}{(1-r)^3} (1 - r^{N-m-n}) (1 - r^{n+2}) (1 - r^{m+1}) \\ &\leq \mathfrak{C}^n, \end{aligned} \tag{II.46}$$

where $\mathfrak{C} = \mathfrak{C}(r, \mu, \lambda) \in \mathbb{R}_+^*$ is independent of m, n and N because of the assumptions (II.38) and (II.39).

II.4.1.c Upper bound of the error

By applying the formula (II.41) with $\hat{a} = a_z$ for $z \in \mathbb{C} \setminus D_\eta$ and using Equation (II.42), we find:

$$\frac{h^\ell(z)(p_{m,n,N} - q_{m,n,N}f)(z)a_z(z)}{\Pi_N(z)} = -\frac{1}{2\pi i} \int_\Gamma \frac{h^\ell(\xi)q_{m,n,N}(\xi)f(\xi)a_z(\xi)}{\Pi_N(\xi)(\xi - z)} d\xi. \tag{II.47}$$

Using Equation (II.47), we can estimate the error for all $z \in \mathbb{C} \setminus D_\eta$:

$$\left| \frac{p_{m,n,N}}{q_{m,n,N}} - f \right| (z) \leq C_0 \sup_{\xi \in \Gamma} \left| \frac{h^\ell(\xi)}{h^\ell(z)} \right| \sup_{\xi \in \Gamma} \left| \frac{a_z(\xi)}{a_z(z)} \right| \sup_{\xi \in \Gamma} \left| \frac{q_{m,n,N}(\xi)}{q_{m,n,N}(z)} \right| \sup_{\xi \in \Gamma} \left| \frac{\Pi_N(z)}{\Pi_N(\xi)} \right|,$$

where $C_0 = C_0(\eta, \Gamma, f)$ is independent of n . We find an upper bound of the right hand side by:

- $\sup_{\xi \in \Gamma} |h^\ell(\xi)| \leq \eta^{k\ell} < \eta^{n-k}$ because of the definition (II.40) and as $n - k < k\ell$,
- by choosing η small enough, we can assume that for all $\xi \in \Gamma$ and all $i \leq N$, $|\xi - z_i| > \rho$. Hence, we have the upper bound: $\sup_{\xi \in \Gamma} \left| \frac{1}{\Pi_N(\xi)} \right| \leq \left(\frac{1}{\rho} \right)^N$,
- using Lemma B.0.3: $\sup_{\xi \in \Gamma} \left| \frac{q_{m,n,N}(\xi)}{q_{m,n,N}(z)} \right| \leq \frac{(3r)^m}{|q^*(z)|}$ where q^* is a monic polynomial of degree $m^* \leq m$,
- for all $z \in \mathbb{C}$, $\frac{a_z(z)}{\Pi_N(z)} = 1$ because of the normalization (II.45),
- $h^\ell q^* \in \mathcal{P}_{2m}$ is a monic polynomial so, by definition (B.1) of the capacity, $|h^\ell q^*| \geq \varepsilon^{2m}$ on $D(0, r) \setminus \Phi$ where Φ is a set of capacity bounded by ε ,
- using Equation (II.46), we have $\sup_{\xi \in \Gamma} |a_z(\xi)| \leq \mathfrak{C}^n$.

Thus, for all $z \in D(0, r) \setminus E_{m,n}$ with $E_{m,n} = D_\eta \cup \Phi$:

$$\left| \frac{p_{m,n,N}}{q_{m,n,N}} - f \right| (z) \leq C_0 \mathfrak{C}^n \eta^{n-k} \frac{(3r)^m}{\varepsilon^{2m}} \frac{1}{\rho^N}.$$

Using our choice of η and the linear growth of N with n , we get for $n > n_0(\varepsilon)$:

$$\left| \frac{p_{m,n,N}}{q_{m,n,N}} - f \right| (z) < \varepsilon^n,$$

for all $z \in D(0, r) \setminus E_{m,n}$.

Using Lemma B.0.1 with $\alpha = \varepsilon$ and $d = 2$, the exceptional set has a capacity:

$$\text{cap}(E_{m,n}) \leq \varepsilon^{1/2} (2r)^{1/2} = (2r\varepsilon)^{1/2} \leq \delta,$$

which concludes our proof. The case $m \leq n$ can be handled similarly by changing the definition of ℓ .

Remark 11. If $\delta < (2r\varepsilon)^{1/2}$, we can apply the proof with $\varepsilon_0 = \frac{\delta^2}{2r} \geq \varepsilon$ hence get to the conclusion.

Remark 12. The present construction of the $(z_i^{m,n,N})_{i \in \llbracket 1, N \rrbracket}$ does not provide control on their localization. For each $(m, n, N) \in \mathbb{N}^3$, they belong to a neighborhood of 0 which may depend on those natural numbers. Hence we cannot prevent that they all converge to 0. In this sense, this theorem is linked to Theorem II.3.2 in which all the $(z_i)_{i \in \llbracket 1, N \rrbracket}$ are chosen at 0.

II.4.2 Study of Conjecture II.4.1

In the proof of Theorem II.4.2, this dependency is only needed to get Equation (II.46). Hence, if we can find another way to upper bound $|a_z(\xi)|$ geometrically with n without this dependency, the proof of Theorem II.4.2 will directly translate to a proof of Conjecture II.4.1. In order to study the growth of a_z , we consider the following parameters:

- $f : x \mapsto \exp(1/x)$ and $F = \{0\}$,
- $m = n$, $N = m + 2n + 1$, and $N \leq N_{max} = 40$,

- $E = C(0, 1)$ and $\forall t \in \llbracket 1, N_{max} \rrbracket$, $z_t = \exp\left(2\pi i \frac{t-1}{N_{max}}\right)$,
- $\Gamma = C(0, 1/2)$, $k = 3$ and $h : x \mapsto x^k$, $r = 2$ (i.e. $K = D(0, 2)$).

On Figure II.19, we plot $\sup_{z \in D(0,r), \xi \in \Gamma} |a_z(\xi)|$ with respect to n with the parameters described above. As we can see on Figure II.19, the quantity $\sup_{z \in D(0,r), \xi \in \Gamma} |a_z(\xi)|$ has a geometrical growth (linear in logarithmic scale) even with a fixed collection of points $(z_i)_{i \in \llbracket 1, N \rrbracket}$. Hence, it seems that the extra assumption on the points variability that is present in Theorem II.4.2 may not needed.

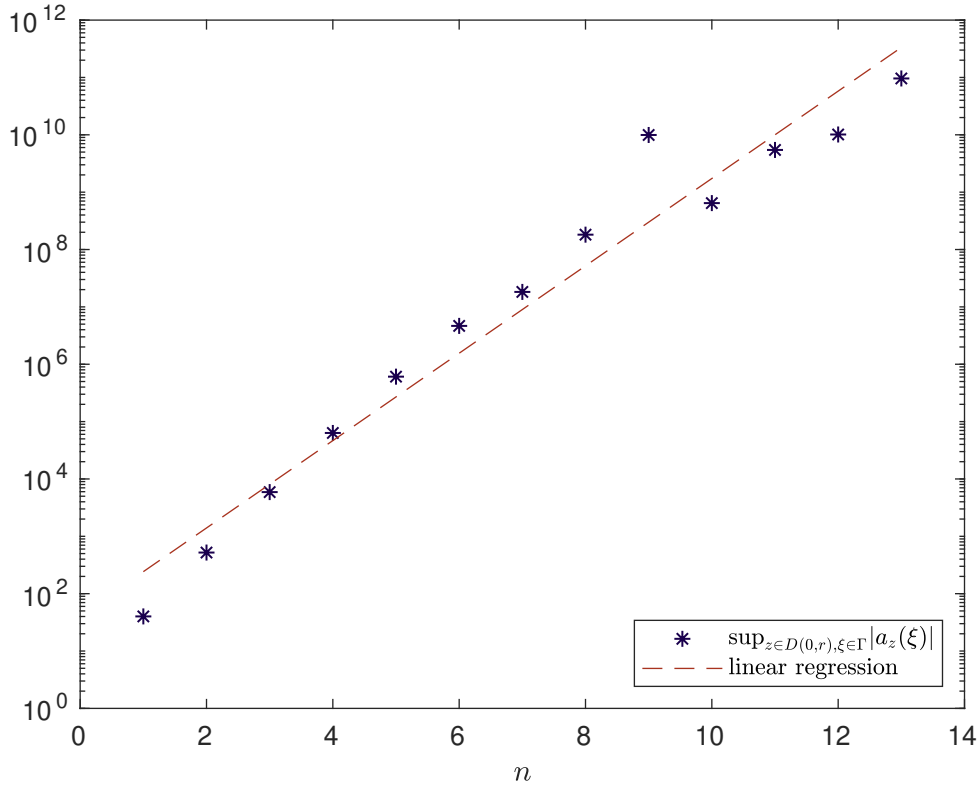


Figure II.19: Plot of $\sup_{z \in D(0,r), \xi \in \Gamma} |a_z(\xi)|$ (blue) and its linear regression (red) in logarithmic scale.

II.4.3 Non-zero determinant

Our goal in this section is to study the nullity of the following determinant:

$$D = D(z_1, \dots, z_N) = \det \left[\begin{array}{c|c|c} \underbrace{z_i^j h^\ell(z_i)}_{j=0, \dots, N-n-m-2} & \underbrace{\overline{z_i^j} \Pi'_N(z_i)}_{j=0, \dots, n} & \underbrace{\overline{z_i^j} \Pi'_N(z_i) \overline{f(z_i)}}_{j=0, \dots, m-1} \end{array} \right].$$

Lemma II.4.3. *If $f = p/q$ is a rational function with $p \in \mathcal{P}_n$ and $q \in \mathcal{P}_{m-1}$, then D is null for all $(z_1, \dots, z_N) \in \mathbb{C}^N$.*

Proof. Let $f = p/q$ where $p = \sum_{j=0}^n p_j X^j \in \mathcal{P}_n$ and $q = \sum_{j=0}^{m-1} q_j X^j \in \mathcal{P}_{m-1}$. Obviously, $q(z_i) \neq 0$ for all $i \in \llbracket 1, N \rrbracket$ as f is analytic in E . Let $(B_j)_j$ and $(C_j)_j$ be respectively the

columns of the second and third block of D . Then, we see that for all $i \in \llbracket 1, N \rrbracket$:

$$\left(\sum_{j=0}^n p_j B_j - \sum_{j=0}^{m-1} q_j C_j \right)_i = \Pi'_N(z_i) \overline{\left(p(z_i) - q(z_i) \frac{p(z_i)}{q(z_i)} \right)} = 0.$$

Hence, D is uniformly zero. \square

Proposition II.4.4. *Let f be an analytic function outside a compact set E with $\text{cap}(E) = 0$. If f is not a rational function, then D is non-zero almost everywhere in \mathbb{C}^N .*

Proof. The real and imaginary parts of D are analytic functions of (z_1, \dots, z_N) so either D is uniformly null or it is non-zero almost everywhere. To show that apart from the rational situation, D is not uniformly null, we study its behavior when the $(z_i)_i$ sequentially tends to $+\infty$ on the real line ($(z_i)_{i \in \llbracket 1, N \rrbracket} \in \mathbb{R}^N$). In this scope, we define a sequence $(D_t)_{t \in \mathbb{N}}$ by $D_0 = D$ and for all $t \geq 1$, D_t is computed from D_{t-1} and is independent of $z_{N-t+1} \in \mathbb{R}$. The construction of this sequence is performed such that D_N is the dominant coefficient of $D(r, r^2, \dots, r^N)$ when $r \rightarrow +\infty$. Hence if D_N is non-zero we can conclude that D is non-zero almost everywhere. We will see that for $t \geq 1$, D_t is of the form:

$$D_t = \mathfrak{d}_t(z_1, \dots, z_{N-t}) \det \left[\underbrace{z_i^j h^\ell(z_i) \overline{\mathfrak{g}_t(z_i)}}_{j=0, \dots, a_t} \mid \underbrace{z_i^j \Pi'_{N-t}(z_i)}_{j=0, \dots, b_t} \mid \underbrace{z_i^j \Pi'_{N-t}(z_i) \overline{\mathfrak{f}_t(z_i)}}_{j=0, \dots, c_t} \right], \quad (\text{II.48})$$

where the subscript i goes from 1 to $N - t$ and indexes the rows,

- $a_t \in \mathbb{N}$, $b_t \in \mathbb{N}$ and $c_t \in \mathbb{N}$ with $a_t + b_t + c_t + 3 = N - t$
- $\mathfrak{d}_t : \mathbb{C}^{N-t} \rightarrow \mathbb{C}$, $\mathfrak{f}_t : \mathbb{C} \rightarrow \mathbb{C}$ and $\mathfrak{g}_t : \mathbb{C} \rightarrow \mathbb{C}$ are such that:

$$\begin{aligned} \mathfrak{d}_t(z_1, \dots, z_{N-t}) &\underset{+\infty}{\sim} d_t(z_1, \dots, z_{N-t-1}) z_{N-t}^{\delta_t}, & \delta_t \in \mathbb{Z}, d_t : \mathbb{C}^{N-t-1} \rightarrow \mathbb{C}, d_t \neq 0, \\ \mathfrak{f}_t(z) &\underset{+\infty}{\sim} f_t z^{\varphi_t}, & \varphi_t \in \mathbb{Z}, f_t \in \mathbb{C}^*, \\ \mathfrak{g}_t(z) &\underset{+\infty}{\sim} g_t z^{\gamma_t}, & \gamma_t \in \mathbb{Z}, g_t \in \mathbb{C}^*. \end{aligned}$$

We can see that for $t = 0$, D_0 is of the form (II.48) with:

$$\begin{aligned} a_0 &= N - m - n - 2, \\ b_0 &= n, \\ c_0 &= m - 1, \\ \mathfrak{d}_0 &= 1, \\ \mathfrak{f}_0 &= f, \\ \mathfrak{g}_0 &= 1. \end{aligned} \quad (\text{II.49})$$

Let $t \in \mathbb{N}$. Let us describe the computation of D_{t+1} . By expanding the determinant in D_t on its last row, we see that in each of the three blocks, the columns are ordered in term

of magnitude with regards to z_{N-t} . Hence, we have:

$$D_t = \det \left[\underbrace{z_i^j h^\ell(z_i) \overline{\mathbf{g}_t(z_i)}}_{j=0, \dots, a_t-1} \mid \underbrace{z_i^j \Pi'_{N-t-1}(z_i)}_{j=0, \dots, b_t} \mid \underbrace{z_i^j \Pi'_{N-t-1}(z_i) \overline{\mathbf{f}_t(z_i)}}_{j=0, \dots, c_t} \right] \quad (\text{A})$$

$$\times d_t(z_1, \dots, z_{N-t-1}) \overline{\mathbf{g}_t} z_{N-t}^{N-t+\delta_t+\gamma_t+k\ell-1}$$

$$+ \det \left[\underbrace{z_i^j h^\ell(z_i) \overline{\mathbf{g}_t(z_i)}}_{j=0, \dots, a_t} \mid \underbrace{z_i^j \Pi'_{N-t-1}(z_i)}_{j=0, \dots, b_t-1} \mid \underbrace{z_i^j \Pi'_{N-t-1}(z_i) \overline{\mathbf{f}_t(z_i)}}_{j=0, \dots, c_t} \right] \quad (\text{B})$$

$$\times d_t(z_1, \dots, z_{N-t-1}) (-1)^{b_t} z_{N-t}^{N-t+\delta_t+2b_t+c_t}$$

$$+ \det \left[\underbrace{z_i^j h^\ell(z_i) \overline{\mathbf{g}_t(z_i)}}_{j=0, \dots, a_t} \mid \underbrace{z_i^j \Pi'_{N-t-1}(z_i)}_{j=0, \dots, b_t} \mid \underbrace{z_i^j \Pi'_{N-t-1}(z_i) \overline{\mathbf{f}_t(z_i)}}_{j=0, \dots, c_t-1} \right] \quad (\text{C})$$

$$\times d_t(z_1, \dots, z_{N-t-1}) \overline{\mathbf{f}_t} (-1)^{b_t+c_t+1} z_{N-t}^{N-t+\delta_t+b_t+2c_t+\varphi_t}$$

$$+ o \left(z_{N-t}^{\max(N-t+\delta_t+\gamma_t+k\ell-1, N-t+\delta_t+2b_t+c_t, N-t+\delta_t+b_t+2c_t+\varphi_t)} \right).$$

Then, we consider seven different cases depending which of the three terms (A), (B) and (C) is dominant with respect to z_{N-t} . These cases are as follows:

- **Case A:** the term (A) is dominant in z_{N-t} ,
- **Case B:** the term (B) is dominant in z_{N-t} ,
- **Case C:** the term (C) is dominant in z_{N-t} ,
- **Case A-B:** the terms (A) and (B) are of same degree in z_{N-t} and dominate the term (C),
- **Case A-C:** the terms (A) and (C) are of same degree in z_{N-t} and dominate the term (B),
- **Case B-C:** the terms (B) and (C) are of same degree in z_{N-t} and dominate the term (A),
- **Case A-B-C:** the three terms (A), (B) and (C) are of the same degree in z_{N-t} .

Table II.2 describes the conditions corresponding to each **Case**, Table II.4 describes the evolution of the degree of each term in each **Case** and Figure II.20 shows the possible transition of cases between t and $t+1$ for $t \in \llbracket 0, N-1 \rrbracket$. The proof goes as follows.

- We will see that, in each of these cases, D_{t+1} is of the form (II.48), with a column and a line less than D_t (see Table II.3).
- Hence, when applying this procedure, we eventually get to a situation in which two blocks are removed. At this stage, the remaining determinant can easily be computed as it is the determinant of the product of a diagonal matrix with a Vandermonde matrix. For example, when the first block is the only remaining one at $t = t_0 \leq N$:

$$D_{t_0} = \mathfrak{d}_{t_0} \det \begin{bmatrix} z_1^0 & \dots & z_1^{N-t_0-1} \\ \vdots & & \vdots \\ z_{N-t_0}^0 & \dots & z_{N-t_0}^{N-t_0-1} \end{bmatrix} \begin{bmatrix} h^\ell(z_1) \overline{\mathbf{g}_{t_0}(z_1)} & & 0 \\ & \ddots & \\ 0 & & h^\ell(z_{N-t_0}) \overline{\mathbf{g}_{t_0}(z_{N-t_0})} \end{bmatrix}.$$

Case A	$\gamma_t + kl - 1$	$>$	$2b_t + c_t$ $>$ $b_t + 2c_t + \varphi_t$
Case B	$2b_t + c_t$	$>$	$\gamma_t + kl - 1$ $>$ $b_t + 2c_t + \varphi_t$
Case C	$b_t + 2c_t + \varphi_t$	$>$	$\gamma_t + kl - 1$ $>$ $2b_t + c_t$
Case A-B	$\gamma_t + kl - 1$	$=$	$2b_t + c_t$ $>$ $b_t + 2c_t + \varphi_t$
Case A-C	$\gamma_t + kl - 1$	$>$	$2b_t + c_t$ $=$ $b_t + 2c_t + \varphi_t$
Case B-C	$2b_t + c_t$	$=$	$b_t + 2c_t + \varphi_t$ $>$ $\gamma_t + kl - 1$
Case A-B-C	$\gamma_t + kl - 1$	$=$	$2b_t + c_t$ $=$ $b_t + 2c_t + \varphi_t$

Table II.2: Conditions on γ_t , kl , φ_t , b_t and c_t to determine the **Case** at t .

- Hence, we see that D_N , which is the dominant coefficient D_N of $D(r, r^2, \dots, r^N)$ (and of $D_{t_0}(r, r^2, \dots, r^{N-t_0})$), can vanish only if $\mathfrak{d}_{t_0} \equiv 0$, $\mathfrak{g}_{t_0} \equiv 0$ or $\mathfrak{f}_{t_0} \equiv 0$ (when the third block is the only remaining one).
- The construction of these three functions implies that $\mathfrak{g}_{t_0} \neq 0$ and that \mathfrak{d}_{t_0} and \mathfrak{f}_{t_0} can be null only if there exist $t \in \llbracket 0, t_0 \rrbracket$ such that $\mathfrak{f}_t \equiv 0$ (see Equations (II.49), (II.50), (II.51), (II.52), (II.53), (II.54), (II.55), (II.56) and (II.57)). We will see below that the transformations performed on f in order to compute $(\mathfrak{f}_t)_t$ consist in removals of polynomial part and inversions (Equations (II.53) and (II.54)) hence $\mathfrak{f}_t \equiv 0$ is possible only if f was rational.
- This allows us to show that, as f is not rational, the dominant coefficient of $D(r, r^2, \dots, r^N)$ is not zero hence D is not uniformly zero so D is non-zero almost everywhere.

The rest of this section is devoted to the construction of D_{t+1} from D_t in every cases for $t \in \llbracket 0, N - 1 \rrbracket$.

	φ_{t+1}	a_{t+1}	b_{t+1}	c_{t+1}	γ_{t+1}
Case A	φ_t	$a_t - 1$	b_t	c_t	γ_t
Case B	φ_t	a_t	$b_t - 1$	c_t	γ_t
Case C	φ_t	a_t	b_t	$c_t - 1$	γ_t
Case A-B	φ_t	$a_t - 1$	b_t	c_t	γ_t
Case A-C	φ_t	$a_t - 1$	b_t	c_t	γ_t
Case B-C $d_t \geq 0$	$\varphi_t - 1$	a_t	$b_t - 1$	c_t	γ_t
Case B-C $d_t < 0$	$-\varphi_t - 1$	a_t	$c_t - 1$	b_t	$\gamma_t - \varphi_t$
Case A-B-C	φ_t	$a_t - 1$	b_t	c_t	γ_t

Table II.3: Changes in the various quantities of D_t from t to $t + 1$ for every cases.

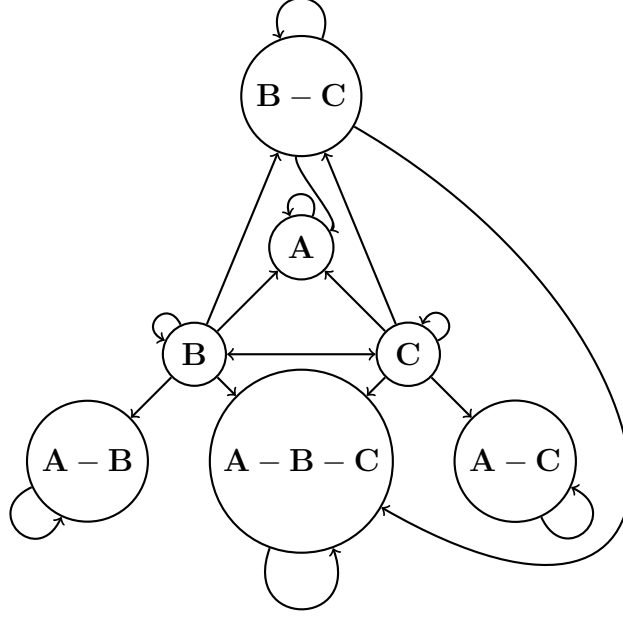


Figure II.20: Graph of the possible transitions between cases for D_t from t to $t+1$.

II.4.3.a Case A

We consider **Case A** hence the term (A) is dominant and we can write:

$$D_t = d_t(z_1, \dots, z_{N-t-1}) \overline{g_t} \det \left[\underbrace{z_i^j h^\ell(z_i) \overline{g_t(z_i)}}_{j=0, \dots, a_t-1} \mid \underbrace{z_i^j \Pi'_{N-t-1}(z_i)}_{j=0, \dots, b_t} \mid \underbrace{z_i^j \Pi'_{N-t-1}(z_i) \overline{f_t(z_i)}}_{j=0, \dots, c_t} \right] \\ \times z_{N-t}^{N-t+\delta_t+\gamma_t+k\ell-1} + o\left(z_{N-t}^{N-t+\delta_t+\gamma_t+k\ell-1}\right).$$

In this case, we define D_{t+1} as the dominant coefficient of D_t with respect to z_{N-t} . Hence, D_{t+1} is of the form (II.48) with:

$$\begin{aligned} a_{t+1} &= a_t - 1, \\ b_{t+1} &= b_t, \\ c_{t+1} &= c_t, \\ \mathfrak{d}_{t+1}(z_1, \dots, z_{N-t-1}) &= d_t(z_1, \dots, z_{N-t-1}) \overline{g_t}, \\ \mathfrak{f}_{t+1} &= \mathfrak{f}_t, \\ \mathfrak{g}_{t+1} &= \mathfrak{g}_t. \end{aligned} \tag{II.50}$$

II.4.3.b Case B

We consider **Case B** hence the term (B) is dominant and we can write:

$$D_t = \det \left[\underbrace{z_i^j h^\ell(z_i) \overline{g_t(z_i)}}_{j=0, \dots, a_t} \mid \underbrace{z_i^j \Pi'_{N-t-1}(z_i)}_{j=0, \dots, b_t-1} \mid \underbrace{z_i^j \Pi'_{N-t-1}(z_i) \overline{f_t(z_i)}}_{j=0, \dots, c_t} \right] \\ \times (-1)^{b_t} d_t(z_1, \dots, z_{N-t-1}) z_{N-t}^{N-t+\delta_t+2b_t+c_t} + o\left(z_{N-t}^{N-t+\delta_t+2b_t+c_t}\right).$$

	$\gamma_{t+1} + k\ell - 1$	$2b_{t+1} + c_{t+1}$	$b_{t+1} + 2c_{t+1} + \varphi_{t+1}$
Case A	$\gamma_t + k\ell - 1$	$2b_t + c_t$	$b_t + 2c_t + \varphi_t$
Case B	$\gamma_t + k\ell - 1$	$2b_t + c_t - 2$	$b_t + 2c_t + \varphi_t - 1$
Case C	$\gamma_t + k\ell - 1$	$2b_t + c_t - 1$	$b_t + 2c_t + \varphi_t - 2$
Case A-B	$\gamma_t + k\ell - 1$	$2b_t + c_t$	$b_t + 2c_t + \varphi_t$
Case A-C	$\gamma_t + k\ell - 1$	$2b_t + c_t$	$b_t + 2c_t + \varphi_t$
Case B-C $d_t \geq 0$	$\gamma_t + k\ell - 1$	$2b_t + c_t - 2$	$2b_t + c_t - 2$
Case B-C $d_t < 0$	$\gamma_t - \varphi_t + k\ell - 1$	$b_t + 2c_t - 2$	$b_t + 2c_t - 2$
Case A-B-C	$\gamma_t + k\ell - 1$	$2b_t + c_t$	$b_t + 2c_t + \varphi_t$

Table II.4: Changes in the degrees of the three dominant columns of D_t from t to $t + 1$ for every cases.

In this case, we define D_{t+1} as the dominant coefficient of D_t with respect to z_{N-t} . Hence, D_{t+1} is of the form (II.48) with:

$$\begin{aligned}
a_{t+1} &= a_t, \\
b_{t+1} &= b_t - 1, \\
c_{t+1} &= c_t, \\
\mathfrak{d}_{t+1}(z_1, \dots, z_{N-t-1}) &= (-1)^{b_t} d_t(z_1, \dots, z_{N-t-1}), \\
\mathfrak{f}_{t+1} &= \mathfrak{f}_t, \\
\mathfrak{g}_{t+1} &= \mathfrak{g}_t.
\end{aligned} \tag{II.51}$$

II.4.3.c Case C

We consider **Case C** hence the term (C) is dominant and we can write:

$$\begin{aligned}
D_t &= \det \left[\underbrace{z_i^j h^\ell(z_i) \overline{\mathfrak{g}_t(z_i)}}_{j=0, \dots, a_t} \mid \underbrace{z_i^j \Pi'_{N-t-1}(z_i)}_{j=0, \dots, b_t} \mid \underbrace{z_i^j \Pi'_{N-t-1}(z_i) \overline{\mathfrak{f}_t(z_i)}}_{j=0, \dots, c_t-1} \right] \\
&\times (-1)^{b_t+c_t+1} \overline{f_t} d_t(z_1, \dots, z_{N-t-1}) z_{N-t}^{N-t+\delta_t+b_t+2c_t+\varphi_t} + o\left(z_{N-t}^{N-t+\delta_t+b_t+2c_t+\varphi_t}\right).
\end{aligned}$$

In this case, we define D_{t+1} as the dominant coefficient of D_t with respect to z_{N-t} . Hence, D_{t+1} is of the form (II.48) with:

$$\begin{aligned}
a_{t+1} &= a_t, \\
b_{t+1} &= b_t, \\
c_{t+1} &= c_t - 1, \\
\mathfrak{d}_{t+1}(z_1, \dots, z_{N-t-1}) &= (-1)^{b_t+c_t+1} d_t(z_1, \dots, z_{N-t-1}) \overline{f_t}, \\
\mathfrak{f}_{t+1} &= \mathfrak{f}_t, \\
\mathfrak{g}_{t+1} &= \mathfrak{g}_t.
\end{aligned} \tag{II.52}$$

II.4.3.d Case B-C

The operations done for the **Case B-C** assume that $\varphi_t \geq 0$. If $\varphi_t < 0$, we change the configuration of D_t so that φ_t is positive in this new configuration:

$$\begin{aligned}
D_t &= \det \left[\underbrace{z_i^j h^\ell(z_i) \overline{\mathfrak{g}_t(z_i)}}_{j=0, \dots, a_t} \mid \underbrace{z_i^j \Pi'_{N-t}(z_i)}_{j=0, \dots, b_t} \mid \underbrace{z_i^j \Pi'_{N-t}(z_i) \overline{\mathfrak{f}_t(z_i)}}_{j=0, \dots, c_t} \right] \times \mathfrak{d}_t(z_1, \dots, z_{N-t}) \\
&= \det \left[\underbrace{z_i^j h^\ell(z_i) \frac{\overline{\mathfrak{g}_t(z_i)}}{\mathfrak{f}_t(z_i)}}_{j=0, \dots, a_t} \mid \underbrace{z_i^j \Pi'_{N-t}(z_i) \frac{1}{\mathfrak{f}_t(z_i)}}_{j=0, \dots, b_t} \mid \underbrace{z_i^j \Pi'_{N-t}(z_i)}_{j=0, \dots, c_t} \right] \\
&\quad \times \left(\prod_{u=1}^{N-t} \overline{\mathfrak{f}_t(z_u)} \right) \mathfrak{d}_t(z_1, \dots, z_{N-t}) \\
&= \det \left[\underbrace{z_i^j h^\ell(z_i) \frac{\overline{\mathfrak{g}_t(z_i)}}{\mathfrak{f}_t(z_i)}}_{j=0, \dots, a_t} \mid \underbrace{z_i^j \Pi'_{N-t}(z_i)}_{j=0, \dots, c_t} \mid \underbrace{z_i^j \Pi'_{N-t}(z_i) \frac{1}{\mathfrak{f}_t(z_i)}}_{j=0, \dots, b_t} \right] \\
&\quad \times (-1)^{(b_t+1)(b_t+c_t+1)} \left(\prod_{u=1}^{N-t} \overline{\mathfrak{f}_t(z_u)} \right) \mathfrak{d}_t(z_1, \dots, z_{N-t}).
\end{aligned}$$

Hence, D_t can be written in the same form with $\varphi_t > 0$ with:

$$\begin{aligned}
a_t^{\mathcal{B}} &= a_t^{\mathcal{A}}, \\
b_t^{\mathcal{B}} &= c_t^{\mathcal{A}}, \\
c_t^{\mathcal{B}} &= b_t^{\mathcal{A}}, \\
\mathfrak{d}_t^{\mathcal{B}}(z_1, \dots, z_{N-t}) &= (-1)^{(b_t^{\mathcal{A}}+1)(c_t^{\mathcal{A}}+1)+1} \mathfrak{d}_t^{\mathcal{A}}(z_1, \dots, z_{N-t}) \left(\prod_{u=1}^{N-t} \overline{\mathfrak{f}_t^{\mathcal{A}}(z_u)} \right), \quad (\text{II.53}) \\
\mathfrak{f}_t^{\mathcal{B}} &= \frac{1}{\mathfrak{f}_t^{\mathcal{A}}}, \\
\mathfrak{g}_t^{\mathcal{B}} &= \frac{\mathfrak{g}_t^{\mathcal{A}}}{\mathfrak{f}_t^{\mathcal{A}}},
\end{aligned}$$

where the superscript \mathcal{A} and \mathcal{B} distinguish the previous form with $\varphi_t < 0$ from the new form with $\varphi_t \geq 0$. One can see that this operation could be done as $\mathfrak{f}_t \neq 0$. Indeed if $\mathfrak{f}_t \equiv 0$, the term (C) is negligible with respect to (A) and it contradicts **Case B-C**.

This allows to get $\varphi_t > 0$, hence to continue the construction of this sequence. We consider **Case B-C** hence the terms (B) and (C) are dominant and we can write:

$$\begin{aligned}
D_t &= \left(\det \left[\underbrace{z_i^j h^\ell(z_i) \overline{\mathfrak{g}_t(z_i)}}_{j=0, \dots, a_t} \mid \underbrace{z_i^j \Pi'_{N-t-1}(z_i)}_{j=0, \dots, b_t-1} \mid \underbrace{z_i^j \Pi'_{N-t-1}(z_i) \overline{\mathfrak{f}_t(z_i)}}_{j=0, \dots, c_t} \right] \right. \\
&\quad \left. + \det \left[\underbrace{z_i^j h^\ell(z_i) \overline{\mathfrak{g}_t(z_i)}}_{j=0, \dots, a_t} \mid \underbrace{z_i^j \Pi'_{N-t-1}(z_i)}_{j=0, \dots, b_t} \mid \underbrace{z_i^j \Pi'_{N-t-1}(z_i) \overline{\mathfrak{f}_t(z_i)}}_{j=0, \dots, c_t-1} \right] \overline{f_t}(-1)^{c_t+1} \right) \\
&\quad \times d_t(z_1, \dots, z_{N-t-1}) (-1)^{b_t} z_{N-t}^{N-t+\delta_t+b_t+2c_t+\varphi_t} + o\left(z_{N-t}^{N-t+\delta_t+b_t+2c_t+\varphi_t}\right) \\
&= \det \left[\underbrace{z_i^j h^\ell(z_i) \overline{\mathfrak{g}_t(z_i)}}_{j=0, \dots, a_t} \mid \underbrace{z_i^j \Pi'_{N-t-1}(z_i)}_{j=0, \dots, b_t-1} \mid \underbrace{z_i^j \Pi'_{N-t-1}(z_i) (\overline{\mathfrak{f}_t(z_i)} - f_t z_i^{\varphi_t})}_{j=0, \dots, c_t} \right] \\
&\quad \times d_t(z_1, \dots, z_{N-t-1}) (-1)^{b_t} z_{N-t}^{N-t+\delta_t+b_t+2c_t+\varphi_t} + o\left(z_{N-t}^{N-t+\delta_t+b_t+2c_t+\varphi_t}\right).
\end{aligned}$$

In this case, we define D_{t+1} as the dominant coefficient of D_t with respect to z_{N-t} . Hence, D_{t+1} is of the form (II.48) with:

$$\begin{aligned}
a_{t+1} &= a_t, \\
b_{t+1} &= b_t - 1, \\
c_{t+1} &= c_t, \\
\mathfrak{d}_{t+1}(z_1, \dots, z_{N-t-1}) &= d_t(z_1, \dots, z_{N-t-1}) (-1)^{b_t}, \\
\mathfrak{f}_{t+1}(z) &= \mathfrak{f}_t(z) - f_t z^{\varphi_t}, \\
\mathfrak{g}_{t+1} &= \mathfrak{g}_t.
\end{aligned} \tag{II.54}$$

II.4.3.e Case A-B

We consider **Case A-B** hence the terms (A) and (B) are dominant and we can write:

$$\begin{aligned}
D_t &= \left(\det \left[\underbrace{z_i^j h^\ell(z_i) \overline{\mathfrak{g}_t(z_i)}}_{j=0, \dots, a_t-1} \mid \underbrace{z_i^j \Pi'_{N-t-1}(z_i)}_{j=0, \dots, b_t-1} \mid \overline{g_t z_i^{b_t} \Pi'_{N-t-1}(z_i)} \mid \underbrace{z_i^j \Pi'_{N-t-1}(z_i) \overline{\mathfrak{f}_t(z_i)}}_{j=0, \dots, c_t} \right] \right. \\
&\quad \left. - \det \left[\underbrace{z_i^j h^\ell(z_i) \overline{\mathfrak{g}_t(z_i)}}_{j=0, \dots, a_t-1} \mid \underbrace{z_i^j \Pi'_{N-t-1}(z_i)}_{j=0, \dots, b_t-1} \mid \underbrace{z_i^{a_t} h^\ell(z_i) \overline{\mathfrak{g}_t(z_i)}}_{j=0, \dots, b_t-1} \mid \underbrace{z_i^j \Pi'_{N-t-1}(z_i) \overline{\mathfrak{f}_t(z_i)}}_{j=0, \dots, c_t} \right] \right) \\
&\quad \times d_t(z_1, \dots, z_{N-t-1}) z_{N-t}^{N-t+\delta_t+\gamma_t+k\ell-1} + o\left(z_{N-t}^{N-t+\delta_t+\gamma_t+k\ell-1}\right).
\end{aligned}$$

In this case, we define D_{t+1} as the dominant coefficient of D_t with respect to z_{N-t} after keeping only the second determinant. Indeed, this column dominates the other as a function of the $(z_i)_i$ for all $i \in \llbracket 1, N-t \rrbracket$. Hence, D_{t+1} is of the form (II.48) with:

$$\begin{aligned}
a_{t+1} &= a_t - 1, \\
b_{t+1} &= b_t, \\
c_{t+1} &= c_t, \\
\mathfrak{d}_{t+1}(z_1, \dots, z_{N-t-1}) &= d_t(z_1, \dots, z_{N-t-1}) \overline{g_t}, \\
\mathfrak{f}_{t+1} &= \mathfrak{f}_t, \\
\mathfrak{g}_{t+1} &= \mathfrak{g}_t.
\end{aligned} \tag{II.55}$$

II.4.3.f Case A-C

We consider **Case A-C** hence the terms (A) and (C) are dominant and we can write:

$$\begin{aligned}
D_t = & \left(\det \left[\underbrace{z_i^j h^\ell(z_i) \overline{\mathfrak{g}_t(z_i)}}_{j=0, \dots, a_t-1} \mid \underbrace{z_i^j \Pi'_{N-t-1}(z_i)}_{j=0, \dots, b_t} \mid \underbrace{z_i^j \Pi'_{N-t-1}(z_i) \overline{\mathfrak{f}_t(z_i)}}_{j=0, \dots, c_t-1} \mid \overline{z_i^{c_t} \Pi'_{N-t-1}(z_i) \mathfrak{f}_t(z_i)} \right] \right. \\
& + \det \left[\underbrace{z_i^j h^\ell(z_i) \overline{\mathfrak{g}_t(z_i)}}_{j=0, \dots, a_t-1} \mid \underbrace{z_i^j \Pi'_{N-t-1}(z_i)}_{j=0, \dots, b_t} \mid \underbrace{z_i^j \Pi'_{N-t-1}(z_i) \overline{\mathfrak{f}_t(z_i)}}_{j=0, \dots, c_t-1} \mid \left. \frac{\overline{\mathfrak{f}_t}}{\mathfrak{g}_t} z_i^{a_t} h^\ell(z_i) \overline{\mathfrak{g}_t(z_i)} \right] \right) \\
& \times \overline{\mathfrak{g}_t} d_t(z_1, \dots, z_{N-t-1}) z_{N-t}^{N-t+\delta_t+\gamma_t+k\ell-1} + o(z_{N-t}^{N-t+\delta_t+\gamma_t+k\ell-1}).
\end{aligned}$$

In this case, we define D_{t+1} as the dominant coefficient of D_t with respect to z_{N-t} after only keeping the second determinant. Indeed, this column dominate the other as a function of the $(z_i)_i$ for all $i \in \llbracket 1, N-t \rrbracket$. Hence, D_{t+1} is of the form (II.48) with:

$$\begin{aligned}
a_{t+1} &= a_t - 1, \\
b_{t+1} &= b_t, \\
c_{t+1} &= c_t, \\
\mathfrak{d}_{t+1}(z_1, \dots, z_{N-t-1}) &= d_t(z_1, \dots, z_{N-t-1}) \overline{\mathfrak{g}_t}, \\
\mathfrak{f}_{t+1} &= \mathfrak{f}_t, \\
\mathfrak{g}_{t+1} &= \mathfrak{g}_t.
\end{aligned} \tag{II.56}$$

II.4.3.g Case A-B-C

We consider **Case A-B-C** hence all the terms (A), (B) and (C) are dominant and we can write:

$$\begin{aligned}
D_t = & \left(\det \left[\underbrace{z_i^j h^\ell(z_i) \overline{\mathfrak{g}_t(z_i)}}_{j=0, \dots, a_t-1} \mid \underbrace{z_i^j \Pi'_{N-t-1}(z_i)}_{j=0, \dots, b_t} \mid \underbrace{z_i^j \Pi'_{N-t-1}(z_i) \overline{\mathfrak{f}_t(z_i)}}_{j=0, \dots, c_t} \right] \times \overline{\mathfrak{g}_t} \right. \\
& + \det \left[\underbrace{z_i^j h^\ell(z_i) \overline{\mathfrak{g}_t(z_i)}}_{j=0, \dots, a_t} \mid \underbrace{z_i^j \Pi'_{N-t-1}(z_i)}_{j=0, \dots, b_t-1} \mid \underbrace{z_i^j \Pi'_{N-t-1}(z_i) \overline{\mathfrak{f}_t(z_i)}}_{j=0, \dots, c_t} \right] \times (-1)^{b_t} \\
& + \det \left[\underbrace{z_i^j h^\ell(z_i) \overline{\mathfrak{g}_t(z_i)}}_{j=0, \dots, a_t} \mid \underbrace{z_i^j \Pi'_{N-t-1}(z_i)}_{j=0, \dots, b_t} \mid \underbrace{z_i^j \Pi'_{N-t-1}(z_i) \overline{\mathfrak{f}_t(z_i)}}_{j=0, \dots, c_t-1} \right] \times \overline{\mathfrak{f}_t} (-1)^{b_t+c_t+1} \left. \right) \\
& \times d_t(z_1, \dots, z_{N-t-1}) z_{N-t}^{N-t+\delta_t+\gamma_t+k\ell-1} + o\left(z_{N-t}^{N-t+\delta_t+\gamma_t+k\ell-1}\right).
\end{aligned}$$

In this case, we define D_{t+1} as the dominant coefficient of D_t with respect to z_{N-t} after keeping only the second determinant. Indeed, its extra column dominate the others as a function of the $(z_i)_i$ for all $i \in \llbracket 1, N-t \rrbracket$. Hence, D_{t+1} is of the form (II.48) with:

$$\begin{aligned}
a_{t+1} &= a_t - 1, \\
b_{t+1} &= b_t, \\
c_{t+1} &= c_t, \\
\mathfrak{d}_{t+1}(z_1, \dots, z_{N-t-1}) &= d_t(z_1, \dots, z_{N-t-1}) \overline{\mathfrak{g}_t}, \\
\mathfrak{f}_{t+1} &= \mathfrak{f}_t, \\
\mathfrak{g}_{t+1} &= \mathfrak{g}_t.
\end{aligned} \tag{II.57}$$

□

II.5 Conclusion

In this section, we have studied the rational approximation of the scattered field created by an object when illuminated with a plane wave.

We first studied the high-frequency behavior of the field when the object is a metallic sphere and observed numerically the validity of extending data using this kind of approximation in order to perform a rational approximation using the vector-fitting algorithm. Applying this technique to other obstacle geometries (not spherical) for which we do not have explicit formulae for the high-frequency behavior is still an issue to explore.

We also proposed and studied two least-squares generalizations of Padé approximation: the least-squares Padé approximation at 0 and the least-square multipoint Padé approximation.

For the first approximation process, we established a generalized version of the celebrated Nuttall-Pommerenke theorem, while we showed a weaker result for the second one and we discussed a stronger conjecture. These results justify the use of these approximants for pole recovery of the field, because of Proposition II.1.3 which describes links between poles and zeros of these approximants and those of the approximated meromorphic function. Conjecture II.4.1 is unproven and there is a possibility that it needs extra assumptions on the points as for polynomial approximation [31].

For a deeper introduction to Clifford algebras, see [40]. Let $Cl_{0,3}(\mathbb{R})$ be the unital associative algebra generated on \mathbb{R} by (e_1, e_2, e_3) with the relations:

$$\forall (i, j) \in \{1, 2, 3\}^2, e_i \odot e_j = \begin{cases} -\mathbf{1} & i = j, \\ -e_j \odot e_i & i \neq j, \end{cases}$$

where we denote by \odot the product in this algebra and $\mathbf{1}$ is the multiplicative identity of the algebra. $Cl_{0,3}(\mathbb{R})$ is a 8-dimensional \mathbb{R} -vector space with the canonical base: $(\mathbf{1}, e_1, e_2, e_3, e_1 \odot e_2, e_2 \odot e_3, e_3 \odot e_1, e_1 \odot e_2 \odot e_3)$. Elements of $\text{span}(e_1, e_2, e_3)$ are called vectors and are identified with their \mathbb{R}^3 counterpart. The $\mathbf{1}$ coordinate of an element of $Cl_{0,3}(\mathbb{R})$ is called its real part and expressed with the usual symbol Re . The set $Cl_{0,3}(\mathbb{R})$ is a normed vector space when endowed with the Euclidean norm $|\cdot|$.

For $\Omega \subset \mathbb{R}^3$ an open set, a function $f \in L^1_{loc}(\Omega, Cl_{0,3}(\mathbb{R}))$ is said to be left Clifford analytic if $D \odot f = 0$ where $D = \sum_{j=1}^3 e_j \frac{\partial}{\partial x_j}$ is the Dirac operator. Such functions actually belong to $C^\infty(\Omega, Cl_{0,3}(\mathbb{R}))$. Vector-valued left Clifford analytic functions are actually gradient of harmonic functions. Hence, the prototype of such function is, for all $x \in \mathbb{R}^3$:

$$\forall z \in \mathbb{R}^3 \setminus \{x\}, f_x(z) = \frac{x - z}{|x - z|^3},$$

which is left Clifford analytic in $\mathbb{R}^3 \setminus \{x\}$. [41, Eq. 1.9].

Left Clifford analytic functions admit a Cauchy formula (see [41, Thm 1.8]). It states that for all V bounded, 3-dimensional, Lipschitz open domain in Ω , all $f \in L^1_{loc}(V, Cl_{0,3}(\mathbb{R}))$ left Clifford analytic and all $x \in \mathbb{R}^3$:

$$\frac{1}{4\pi} \int_{\partial V} \frac{x - z}{|x - z|^3} \odot \nu(z) \odot f(z) d\sigma(z) = \begin{cases} f(x) & x \in V, \\ 0 & x \notin \bar{V}, \end{cases} \quad (\text{A.1})$$

where $\nu(z)$ is the unitary outward vector normal to ∂V at z . This formula can be extended to unbounded domains for specific classes of functions as in Lemma A.0.1 which is proven bellow.

Lemma A.0.1. For all $x \in \mathbb{R}^3$ and all $f \in L^1_{loc}(\mathbb{R}^3, \mathcal{C}\ell_{0,3}(\mathbb{R}))$ left Clifford analytic such that there exists $\varphi : \mathbb{R}^+ \rightarrow \mathbb{R}^+$ which converges to 0 at $+\infty$ and:

$$|f(z)| \leq \varphi(|z|),$$

the Cauchy formula (A.1) holds true on \mathbb{R}^3_- :

$$\frac{1}{4\pi} \int_{\Pi} \frac{x-z}{|x-z|^3} \odot e_3 \odot f(z) d\sigma(z) = \begin{cases} f(x) & x \in \mathbb{R}^3_-, \\ 0 & x \in \mathbb{R}^3_+. \end{cases}$$

Proof. Let $r > |x|$, $\mathbb{D}_r \subset \Pi$ the disk of radius r and center $0_{\mathbb{R}^3}$ and $\mathbb{S}_r^- \subset \mathbb{R}^3_-$ the lower half-sphere of radius r and center $0_{\mathbb{R}^3}$. By applying the Cauchy formula (A.1) to f in the half-ball of boundary $\mathbb{S}_r^- \cup \mathbb{D}_r$, we get for $r > |x|$:

$$\int_{\mathbb{D}_r \cup \mathbb{S}_r^-} \frac{x-z}{|x-z|^3} \odot \nu(z) \odot f(z) d\sigma(z) = \begin{cases} f(x) & x \in \mathbb{R}^3_-, \\ 0 & x \in \mathbb{R}^3_+. \end{cases}$$

Let $\Lambda : z \mapsto \frac{x-z}{|x-z|^3} \odot \nu(z) \odot f(z)$. Clearly:

$$\begin{aligned} \lim_{r \rightarrow \infty} \int_{\mathbb{D}_r} \Lambda(z) d\sigma(z) &= \int_{\Pi} \Lambda(z) d\sigma(z) \\ &= \int_{\Pi} \frac{x-z}{|x-z|^3} \odot e_3 \odot f(z) d\sigma(z). \end{aligned}$$

Furthermore, by change of variable and for $r > |x|$:

$$\begin{aligned} \left| \int_{\mathbb{S}_r^-} \Lambda(z) d\sigma(z) \right| &= \left| \int_{\mathbb{S}_1^-} \frac{\frac{x_0}{r} - y}{\left| \frac{x_0}{r} - y \right|^3} \odot y \odot f(ry) d\sigma(y) \right| \\ &\leq \int_{\mathbb{S}_1^-} \left| \frac{\frac{x_0}{r} - y}{\left| \frac{x_0}{r} - y \right|^3} \odot y \odot f(ry) \right| d\sigma(y) \\ &\leq \int_{\mathbb{S}_1^-} \left| \frac{\frac{x_0}{r} - y}{\left| \frac{x_0}{r} - y \right|^3} \right| |f(ry)| d\sigma(y) \\ &\leq \varphi(r) \int_{\mathbb{S}_1^-} \frac{1}{\left| \frac{x_0}{r} - y \right|^2} d\sigma(y), \end{aligned} \tag{A.2}$$

using the property [40, Thm 5.16] that for all $x \in \mathcal{C}\ell_{0,3}(\mathbb{R})$ and $y \in \mathbb{R}^3$ identified with its corresponding vector in $\mathcal{C}\ell_{0,3}(\mathbb{R})$:

$$|x \odot y| = |x||y|.$$

As the integral on the right-hand side of Equation (A.2) is bounded, we see that:

$$\lim_{r \rightarrow \infty} \int_{\mathbb{S}_r^-} \Lambda(z) d\sigma(z) = 0.$$

This establishes Lemma A.0.1. □

The work done in Chapter II uses an important concept of potential theory in the complex plane which is the logarithmic capacity of sets. This appendix gives definitions and important properties of this capacity and an insight on this concept. For a more complete introduction to potential theory, see [42].

For all $m \in \mathbb{N}$, let \mathcal{P}_m be the set of complex polynomials of degree less or equal to m , \mathcal{P}_m^1 be the set of monic polynomials of degree m and \mathcal{P}_m^0 polynomials of degree less or equal to m which have value 1 at 0:

$$\begin{aligned}\mathcal{P}_m &= \left\{ \sum_{k=0}^m a_k X^k, \forall k \in \llbracket 0, m \rrbracket : a_k \in \mathbb{C} \right\}, \\ \mathcal{P}_m^1 &= \left\{ X^m + \sum_{k=0}^{m-1} a_k X^k, \forall k \in \llbracket 0, m-1 \rrbracket : a_k \in \mathbb{C} \right\}, \\ \mathcal{P}_m^0 &= \left\{ 1 + \sum_{k=1}^m a_k X^k, \forall k \in \llbracket 1, m \rrbracket : a_k \in \mathbb{C} \right\}.\end{aligned}$$

For a compact set $E \subset \mathbb{C}$, we define its capacity by:

$$\text{cap}(E) = \sup_{\mu \in P(E)} \exp \left(\iint \log(|x-y|) d\mu(x) d\mu(y) \right),$$

where $P(E)$ is the set of all Borel probability measures on \mathbb{C} whose support is a compact subset of E . For the purpose of this work, we consider another definition of the capacity which is the transfinite diameter:

$$\text{cap}(E) = \lim_{k \rightarrow \infty} \inf_{h \in \mathcal{P}_k^1} \max_{z \in E} |h(z)|^{1/k}. \quad (\text{B.1})$$

These two definitions are equivalent [42, Cor. 5.5.5]. Furthermore, let us express some properties of the capacity:

- For any compact measurable set E :

$$\text{meas}(E) \leq \pi \text{cap}(E)^2. \quad (\text{B.2})$$

- Countable sets have capacity 0.
- If $E \subset \mathbb{C}$ contains a connected subset then:

$$\text{cap}(E) > 0.$$

- For all $r > 0$:

$$\text{cap}(D(0, r)) = \text{cap}(C(0, r)) = r. \quad (\text{B.3})$$

where $C(0, r)$ and $D(0, r)$ are respectively the circle and disk of center 0 and radius r in \mathbb{C} .

From Equation (B.3), we see that measurable sets $E \subset \mathbb{C}$ that are negligible for the Lebesgue measure ($\text{meas}(E) = 0$) are not necessarily negligible for the capacity ($\text{cap}(E) = 0$) but the opposite is true because of the property (B.2). Hence, the capacity is a finer tool to measure the size of small sets.

In Sections II.3 and II.4 we will need several lemmas which are given below.

Lemma B.0.1. *Let $d \in \mathbb{N}$, $\alpha > 0$, and $(A_i)_{i \in \llbracket 1, d \rrbracket}$ a sequence of Borel subsets of \mathbb{C} such that for all $i \in \llbracket 1, d \rrbracket$:*

$$\text{cap}(A_i) \leq \alpha,$$

then, for $A = \bigcup_{i=1}^d A_i$:

$$\text{cap}(A) \leq \alpha^{1/d} \text{diam}(A)^{1-1/d}. \quad (\text{B.4})$$

Proof. By applying [42, Thm 5.1.4] to $A = \bigcup_{i=1}^d A_i$, we have:

$$\begin{aligned} \frac{1}{\log(\text{diam}(A)/\text{cap}(A))} &\leq \sum_{i=1}^d \frac{1}{\log(\text{diam}(A)/\text{cap}(A_i))} \\ &\leq \frac{d}{\log(\text{diam}(A)/\alpha)}, \end{aligned}$$

which naturally leads to the inequation (B.4). \square

Lemma B.0.2. [29, Lem.]. *Let $r > 0$ and $m \in \mathbb{N}$ be given and let g be a polynomial in \mathcal{P}_m such that:*

$$\max_{z \in C(0, r)} |g(z)| \geq 1.$$

Let $0 < \varepsilon < \frac{1}{3}$ and $B = \{z \in D(0, r), |g(z)| \leq \varepsilon^m\}$. Then $\text{cap}(B) \leq 3r\varepsilon$.

Lemma B.0.3. [30, Lem. 2]. *Let $r > 0$ and $m \in \mathbb{N}$ be given and let g be a polynomial in \mathcal{P}_m^1 . Then there exist m^* in $\llbracket 0, m \rrbracket$ and a polynomial g^* in $\mathcal{P}_{m^*}^1$ such that for all $z \in D(0, r)$:*

$$\max_{\xi \in D(0, r)} \frac{|g(\xi)|}{|g(z)|} \leq \frac{(3r)^m}{|g^*(z)|}.$$

Definition B.0.1. Let f be a complex function. A sequence $(g_n)_{n \in \mathbb{N}}$ of functions is said to converge in capacity to f if for all compact $K \subset \mathbb{C}$, $\varepsilon > 0$ and $\delta > 0$, there exists $n_0 \in \mathbb{N}$ such that for all $n \geq n_0$:

$$|g_n - f| < \varepsilon^n,$$

in $K \setminus E_n$ where $\text{cap}(E_n) < \delta$.

Figures

I.1	Setting of this study in the half-space ($\Omega = \mathbb{R}_-^3$).	16
I.2	Setting of this study in the spherical case ($\Omega = \mathbb{B}$).	17
I.3	Schematic geometry in the half-space case.	28
I.4	Schematic geometry in the spherical case.	28
I.5	Locations of the critical points of the criterion (I.9).	36
I.6	Criteria on the horizontal square $[-4, 4]^2 \times \{-1\}$	38
I.7	Squared norms of the gradients of the criteria on the horizontal square $[-4, 4]^2 \times \{-1\}$	39
I.8	Criteria on the vertical line $\{0\} \times \{0\} \times [-5, 0]$	39
I.9	Criteria on the horizontal disk containing x_0	40
I.10	Squared norms of the gradients of the criteria on the horizontal disk containing x_0	40
I.11	Criteria on the vertical line $\{0\} \times \{0\} \times [-1, 1]$	41
I.12	Criterion \tilde{I}_Π on the horizontal square $[-10, 10]^2 \times \{-1\}$. The stars indicate the locations of the critical points: x_{c0} (blue), $x_{c1}(x_{03})$ and $x_{c2}(x_{03})$ (red) and $x_{c3}(x_{03})$ and $x_{c4}(x_{03})$ (green).	42
I.13	Criterion \tilde{I}_Π on the horizontal disk $x_{c3} + (D(0, 1) \times \{0\})$ and on the vertical line $\{x_{c3} + tu_z, t \in [-1, 1]\}$	42
I.14	Criterion \tilde{I}_Π on the horizontal disk $x_{c4} + (D(0, 1) \times \{0\})$ and on the vertical line $\{x_{c4} + tu_z, t \in [-1, 1]\}$	43
I.15	Criterion \tilde{I}_Π on the horizontal disk $x_{c1}(x_{03}/2) + (D(0, 1) \times \{0\})$ and on the vertical line $\{x_{c1}(x_{03}/2) + tu_z, t \in [-3/2, 1/2]\}$	43
I.16	Criterion \tilde{I}_Π on the horizontal disk $x_{c1}(x_{03}) + (D(0, 1) \times \{0\})$ and on the vertical line $\{x_{c1}(x_{03}) + tu_z, t \in [-1, 1]\}$	43
I.17	Criterion \tilde{I}_Π on the horizontal disk $x_{c1}(3x_{03}/2) + (D(0, 1) \times \{0\})$ and on the vertical line $\{x_{c1}(3x_{03}/2) + tu_z, t \in [-1/2, 3/2]\}$	44
II.1	Geometric situation of the scattering of an incident wave on an object.	46
II.2	Poles of E_{sc} for a metallic sphere of radius $a = 1$	48
II.3	Poles and zeros of f and its approximant g_n different compact sets. Red crosses are poles of g_n , blue circles are zeroes of g_n and the black star is a double pole of f	51

II.4	Geometrical representation of the path Γ in the resolution of the eikonal equation.	54
II.5	Distinction between the lit region (in white) and the shadow region (in gray) for a spheroid.	55
II.6	Schema of the reflection of an electromagnetic wave on a metallic sphere.	55
II.7	Schematic illustration of ray paths from the scattering of a metallic sphere.	56
II.8	Geometric description of the surfaces W_1 and W_2 used in the resolution of the transport equation.	57
II.9	Comparison between Mie (blue) series and the first Luneberg-Kline term A_0 (red) with $a = 0.15/2$ m, at a distance $r = 1$ m at a frequency $f = 5$ GHz for all $\theta \in [0, 2\pi]$	59
II.10	Schematic representation of the curves C (red), C_- (dashed blue), C_+ (dashed black) and C_-^S (dashed red).	60
II.11	Comparison between the compensated Mie series $P(\rho) \exp(2i\rho)$ (in red) and the first optic term A_0 (in blue).	62
II.12	Comparison between the compensated Mie series $P(\rho) \exp(2i\rho) - A_0$ (in red) and the second optic term $A_1/(ik)$ (in blue).	63
II.13	Comparison between the compensated Mie serie $P(\rho) \exp(2i\rho) - A_0 - A_1/(ik)$ (in red) and the first creeping term (in blue).	63
II.14	Exact poles (red) and reconstructed poles (blue) using 500 frequencies uniformly distributed from 0 to 5 GHz.	64
II.15	Exact poles (red) and reconstructed poles (blue) using 500 frequencies uniformly distributed from 0 to 5 GHz and extended to 10 GHz with the Luneberg-Kline approximation.	65
II.16	Exact poles (red) and reconstructed poles (blue) using 500 frequencies uniformly distributed from 0 to 5 GHz and extended to 10 GHz with the complete approximation.	65
II.17	Scheme of the geometrical setting of the different sets and points considered in the proof of Theorem II.3.2.	73
II.18	Scheme of the geometrical setting of the different sets and points considered in the proof of Theorem II.4.2.	77
II.19	Plot of $\sup_{z \in D(0,r), \xi \in \Gamma} a_z(\xi)$ (blue) and its linear regression (red) in logarithmic scale.	82
II.20	Graph of the possible transitions between cases for D_t from t to $t + 1$	86

Tables

II.1	Error made in the approximation with respectively one, two and three terms of the optics part and two terms of the optics part and one term of the creeping wave part at frequency 5 GHz for $a = 0.15/2$ m and $r = 1$ m.	61
II.2	Conditions on γ_t , $k\ell$, φ_t , b_t and c_t to determine the Case at t	85
II.3	Changes in the various quantities of D_t from t to $t + 1$ for every cases.	85
II.4	Changes in the degrees of the three dominant columns of D_t from t to $t + 1$ for every cases.	87

LIST OF SYMBOLS

- $\text{Arg min}_\Omega J$ Arguments of the minimum of a function J in the set Ω .
- $0_{\mathbb{R}^n}$ Null vector of \mathbb{R}^n .
- $C(0, r)$ Circle of center 0 and radius r in \mathbb{C} .
- $D(0, r)$ Disk of center 0 and radius r in \mathbb{C} .
- \mathbb{R}_-^3 Lower half-space in \mathbb{R}^3 .
- \mathbb{R}_+^3 Upper half-space in \mathbb{R}^3 .
- Π Horizontal plane in \mathbb{R}^3 passing through $0_{\mathbb{R}^3}$.
- \mathbb{S} Sphere of center $0_{\mathbb{R}^3}$ and radius 1.
- \mathbb{B} Open ball of center $0_{\mathbb{R}^3}$ and radius 1.
- \mathbb{S}_a Sphere of center $0_{\mathbb{R}^3}$ and radius a .
- \mathbb{B}_a Open ball of center $0_{\mathbb{R}^3}$ and radius a .
- x^+ Symmetric of $x \in \mathbb{R}^3$ with respect to Π .
- Ω^c Complement of a set Ω in \mathbb{R}^n .
- $\bar{\Omega}$ Closure of a set Ω .
- ∇u Gradient of a function u .
- Δu Laplacian of a function u .
- ΔH Laplacian of a field H .
- $\nabla \cdot H$ Divergence of a field H .

$\nabla \times H$...	Curl of a field H .
$L^2(\Omega)$...	Set of square integrable functions on a set Ω .
$\mathcal{D}(\mathbb{R}^n)$...	Set of infinitely differentiable functions with compact support in \mathbb{R}^n .
$\mathcal{D}'(\mathbb{R}^n)$...	Set of distributions on \mathbb{R}^n .
$\mathcal{M}(\mathbb{R}^n)$...	Set of measures on \mathbb{R}^n .
δ_x	...	Dirac mass at $x \in \mathbb{R}^n$.
$\text{Cl}_{0,3}(\mathbb{R})$...	Clifford algebra of dimension 8.
$\mathbf{1}$...	Multiplicative identity of the algebra $\text{Cl}_{0,3}(\mathbb{R})$.
\odot	...	Product of the algebra $\text{Cl}_{0,3}(\mathbb{R})$.
$\text{Re}(x)$...	Real part of $x \in \text{Cl}_{0,3}(\mathbb{R})$.
\mathcal{P}_m	...	Set of polynomials of degree less than m .
\mathcal{P}_m^1	...	Set of monic polynomials of degree m .
\mathcal{P}_m^0	...	Set of polynomials of degree m with constant coefficient 1.
$\text{cap}(E)$...	Capacity of a compact set E .
$\text{diam}(A)$...	Diameter of a set A .
$\text{surf}(W)$...	Area of a surface $W \subset \mathbb{R}^3$.
$\ell^\Gamma(A, B)$...	Length of a curve Γ between points A and B .
I_d	...	Identity matrix of size 3×3 .
$\text{tr}(M)$...	Trace of a matrix M .
$\det(M)$...	Determinant of a matrix M .
\hat{J}_ν	...	Spherical Bessel function of the second kind of parameter $\nu \in \mathbb{C}$.
$\hat{H}_\nu^{(2)}$...	Spherical Hankel function of the second kind of parameter $\nu \in \mathbb{C}$.
P_n^1	...	Associated Legendre function of order $(1, n)$.
Ai	...	Airy function.

- [1] P. Asensio and J. Leblond, “Critical points for least-squares estimation of dipolar sources in inverse problems for Poisson equation.” Accepted for publication in *Computational Methods and Function Theory*, 2023.
- [2] P. Asensio, J.-M. Badier, J. Leblond, J.-P. Marmorat, and M. Nemaire, “A layer potential approach to inverse problems in brain imaging.” Accepted for publication in *Journal of Inverse and Ill-posed Problems*, 2023.
- [3] P. Asensio, L. Baratchart, and J. Leblond, “A Nuttall-Pommerenke theorem for least-square rational approximant of analytic functions.” Working paper, 2023.
- [4] M. Clerc, J. Leblond, J.-P. Marmorat, and T. Papadopoulo, “Source localization using rational approximation on plane sections,” *Inverse Problems*, vol. 28, no. 5, p. 055018, 2012.
- [5] L. Baratchart, D. P. Hardin, E. A. Lima, E. B. Saff, and B. P. Weiss, “Characterizing kernels of operators related to thin-plate magnetizations via generalizations of Hodge decompositions,” *Inverse Problems*, vol. 29, no. 1, p. 015004, 2012.
- [6] J. D. Jackson, *Classical Electrodynamics*. New York, NY: Wiley, 3rd ed. ed., 1999.
- [7] A. E. Badia and T. Ha-Duong, “An inverse source problem in potential analysis,” *Inverse Problems*, vol. 16, no. 3, pp. 651–663, 2000.
- [8] M. Nemaire, *Problèmes inverses de potentiel et applications à l’électromagnétique quasi-statique*. PhD thesis, IMB - Institut de Mathématiques de Bordeaux, 2023.
- [9] S. Axler, P. Bourdon, and W. Ramey, *Harmonic Function Theory*. Springer New York, 1992.
- [10] L. Baratchart, A. Abda, F. Ben Hassen, and J. Leblond, “Recovery of pointwise sources or small inclusions in 2D domains and rational approximation,” *Inverse Problems*, vol. 21, pp. 51–74, 2005.
- [11] J. Sarvas, “Basic mathematical and electromagnetic concepts of the biomagnetic inverse problem,” *Physics in Medicine and Biology*, vol. 32, pp. 11–22, jan 1987.
- [12] R. Dautray and J.-L. Lions, *Mathematical analysis and numerical methods for science and technology*, vol. 1-2. New York, NY: Springer Science & Business Media, 2012.

- [13] F. W. J. Olver, , D. W. Lozier, R. F. Boisvert, and C. W. Clark, *The NIST Handbook of Mathematical Functions*. New York, NY: Cambridge Univ. Press, 2010.
- [14] C. Yacoub, “On the Dunkl version of monogenic polynomials,” *Advances in Applied Clifford Algebras*, vol. 21, no. 4, pp. 839–847, 2011.
- [15] Y. Zaky, *Decomposition of the scattered field into singularities for object classification using artificial intelligence algorithms*. Theses, Université Côte d’Azur, Mar. 2022.
- [16] Y. Zaky, N. Fortino, J.-Y. Dauvignac, F. Seyfert, M. Olivi, and L. Baratchart, “Comparison of SEM methods for poles estimation from scattered field by canonical objects,” in *2020 IEEE Radar Conference (RadarConf20)*, pp. 1–6, 2020.
- [17] B. Gustavsen and A. Semlyen, “Rational approximation of frequency domain responses by vector fitting,” *IEEE Transactions on Power Delivery*, vol. 14, no. 3, pp. 1052–1061, 1999.
- [18] B. Gustavsen, “Improving the pole relocating properties of vector fitting,” *IEEE Transactions on Power Delivery*, vol. 21, no. 3, pp. 1587–1592, 2006.
- [19] D. Deschrijver, M. Mrozowski, T. Dhaene, and D. De Zutter, “Macromodeling of multiport systems using a fast implementation of the vector fitting method,” *IEEE Microwave and Wireless Components Letters*, vol. 18, no. 6, pp. 383–385, 2008.
- [20] P. Stefanov, “Scattering and Inverse Scattering in \mathbb{R}^n ,” 2018.
- [21] R. F. Harrington, *Time-Harmonic Electromagnetic Fields*. IEEE-Press, 2001.
- [22] H. Padé, “Sur la représentation approchée d’une fonction par des fractions rationnelles,” *Annales scientifiques de l’École Normale Supérieure*, vol. 3e série, 9, pp. 3–93, 1892.
- [23] M. Olivi, F. Seyfert, and J.-P. Marmorat, “Identification of microwave filters by analytic and rational h2 approximation,” *Automatica*, vol. 49, no. 2, pp. 317–325, 2013.
- [24] L. Baratchart, M. Cardelli, and M. Olivi, “Identification and rational l2 approximation a gradient algorithm,” *Automatica*, vol. 27, no. 2, pp. 413–417, 1991.
- [25] L. Baratchart, M. Olivi, and F. Seyfert, “Boundary Nevanlinna-Pick interpolation with prescribed peak points. Application to impedance matching,” *SIAM Journal on Mathematical Analysis*, 2017.
- [26] Y. Nakatsukasa, O. Sète, and L. N. Trefethen, “The AAA algorithm for rational approximation,” *SIAM Journal on Scientific Computing*, vol. 40, pp. A1494–A1522, jan 2018.
- [27] G. A. Baker and P. Graves-Morris, *Padé Approximants*. Encyclopedia of Mathematics and its Applications, Cambridge University Press, 2 ed., 1996.
- [28] J. Nuttall, “The convergence of Padé approximants of meromorphic functions,” *Journal of Mathematical Analysis and Applications*, vol. 31, no. 1, pp. 147–153, 1970.
- [29] C. Pommerenke, “Padé approximants and convergence in capacity,” *Journal of Mathematical Analysis and Applications*, vol. 41, no. 3, pp. 775–780, 1973.

- [30] H. Wallin, “Potential theory and approximation of analytic functions by rational interpolation,” in *Complex Analysis Joensuu 1978* (I. Laine, O. Lehto, and T. Sorvali, eds.), (Berlin, Heidelberg), pp. 434–450, Springer Berlin Heidelberg, 1979.
- [31] J.-P. Calvi and N. Levenberg, “Uniform approximation by discrete least squares polynomials,” *Journal of Approximation Theory*, vol. 152, no. 1, pp. 82–100, 2008.
- [32] W. Rudin, *Real and Complex Analysis*. McGraw-Hill series in higher mathematics, McGraw-Hill, 1966.
- [33] D. Bouche, F. Molinet, and R. Mittra, *Asymptotic Methods in Electromagnetics*. Springer Berlin Heidelberg, 1997.
- [34] M. Baker, “Alhazen’s problem,” *American Journal of Mathematics*, vol. 4, no. 1, pp. 327–331, 1881.
- [35] C. A. Valagiannopoulos, “An overview of the watson transformation presented through a simple example,” *Progress In Electromagnetics Research*, vol. 75, pp. 137–152, 2007.
- [36] T. Senior, “Analytical and numerical studies of the back scattering behavior of spheres,” tech. rep., The University of Michigan, 02 1965.
- [37] W. Lee, T. K. Sarkar, H. Moon, and M. Salazar-Palma, “Computation of the natural poles of an object in the frequency domain using the cauchy method,” *IEEE Antennas and Wireless Propagation Letters*, vol. 11, pp. 1137–1140, 2012.
- [38] R. Salem, *Algebraic Numbers and Fourier Analysis*. Heath mathematical monographs, Heath, 1963.
- [39] R. Engelking, *General Topology*. Sigma series in pure mathematics, Heldermann, 1989.
- [40] J. Gilbert and M. Murray, *Clifford Algebras and Dirac Operators in Harmonic Analysis*. Cambridge Studies in Advanced Mathematics, Cambridge: Cambridge University Press, 1991.
- [41] M. Mitrea, *Clifford Wavelets, Singular Integrals, and Hardy Spaces*. Berlin: Springer Berlin Heidelberg, 1994.
- [42] T. Ransford, *Potential Theory in the Complex Plane*, ch. 5. London Mathematical Society Student Texts, Cambridge University Press, 1995.